ELECTROCHEMICAL ATOMIC LAYER DEPOSITION (E-ALD) OF PT AND PTRU NANOFILM

By

NAGARAJAN JAYARAJU

(Under the Direction of John L. Stickney)

ABSTRACT

Electrochemical atomic layer deposition (E-ALD) has been developed in this research group to grow monometallic and bimetallic nanofilms. E-ALD is an electrochemical analog of atomic layer epitaxy (ALE) and atomic layer deposition (ALD), all of which are based on growth of material an atomic layer at a time. Under potential deposition (UPD) is a thermodynamic process, where one element forms an atomic layer on to the other. A less noble metal (Sacrificial metal) is deposited at UPD and is then exchanged with more noble metal at open circuit potential (OCP). This process is referred to as surface limited redox replacement reaction (SLRR). E-ALD promotes two-dimensional growth, resulting in better control of composition and structure than conventional electrodeposition method. The present study investigates E-ALD using UPD and SLRR cycles to form metal nanofilms on Au on glass substrates. Pb and Cu were explored as the sacrificial metal. Pt, Ru, PtRu and Ru modified Pt nanofilms were deposited using a labview program. Pt and Pt based alloys are of interest as a electrode materials in fuel cells.

Electrodeposits were formed in an automated flow cell system consisting of pumps, valve, electrochemical cell and a potentiostat; all controlled using a labview program. The nanofilms were deposited and characterized by cyclic voltammetry in sulfuric acid. The catalytic activity of the nanofilms was studied by CO adsorption and electrooxidation. Current and open

circuit potentials were monitored simultaneously as a function of time. The atomic proportions were determined from electron probe microanalysis (EPMA).

INDEX WORDS:
Fuel Cell, Electrodeposition, E-ALD, UPD, Cyclic Voltammetry, EPMA, .

ELECTROCHEMICAL ATOMIC LAYER DEPOSITION (E-ALD) OF PT AND PTRU NANOFILM

By

NAGARAJAN JAYARAJU

B.Tech, Madurai Kamaraj University, India, 2000

M.S, University of Georgia, 2006

A Dissertation Submitted to the Graduate Faculty of the University of Georgia in Partial Fulfillment of the Requirements for the Degree

DOCTOR OF PHILOSOPHY

ATHENS, GEORGIA

2010

ELECTROCHEMICAL ATOMIC LAYER DEPOSITION (E-ALD) OF PT AND PTRU NANOFILM

By

NAGARAJAN JAYARAJU

Major Professor: John L. Stickney

Committee: I. Jonathan Amster
Marcus D. Lay

Electronic Version Approved:

Maureen Grasso
Dean of the Graduate School
The University of Georgia
December 2010

DEDICATION

I would like to dedicate my PhD to my parents, Mr. C. Jayaraju and Mrs. Jothi. Without your unconditional love, support and guidance, I could have not reached this position. I would like to thank you from the bottom of my heart. Thank you for your words of advice and the importance of education, hard work you instilled on me. I would like to thank my wife Subashini for her support. I would like to thank my sisters, Rajakumari, Kalaiselvi and my brother Mahendiran, for being there all the time. I would also like to thank my brother-in law Rajendiran and Venkatachalam for their support. You have always been a source of encouragement for me.

ACKNOWLEDGEMENTS

I would like to express my sincere gratitude to my research advisor, Professor John L. Stickney, for his advice and encouragement during my PhD study. He has not only been a good teacher, but more than that, he has been a father like figure for me. I have learnt a lot from being a good scientist to being a good person. Also, I would like to thank Professors I. Jonathan Amster and Marcus D. Lay for serving on my advisory committee and guiding me through my research.

I would like to thank Dr. Youn-Guen Kim for all his advice and support. I would also like to thank the past and present members of Professor Stickney's group for their friendship and memorable times.

At last, I would like to thank all my friends for their help and support.

TABLE OF CONTENTS

Page

ACKNOWLEDGEMENTS..... v

LIST OF TABLES..... viii

LIST OF FIGURES..... ix

CHAPTER

1 INTRODUCTION..... 1

Experimental..... 5

References..... 7

2 ELECTROCHEMICAL ATOMIC LAYER DEPOSITION (E-ALD) OF PT NANOFILMS..... 15

Abstract..... 16

Introduction..... 17

Experimental..... 20

Results and Discussion..... 21

Conclusion..... 30

Acknowledgements..... 31

References..... 32

3 PTRU NANOFILM FORMATION BY ELECTROCHEMICAL ATOMIC LAYER DEPOSITION (E-ALD)..... 55

Abstract..... 56

Introduction..... 58

Experimental..... 61

Results and Discussion..... 63

Conclusion..... 72

Acknowledgements..... 73

References..... 74

4 RU MODIFIED PT NANOFILM FORMATION BY ELECTROCHEMICAL ATOMIC LAYER DEPOSITION (E-ALD) AND THEIR CATALYTIC ACTIVITY TOWARDS CO ELECTROOXIDATION..... 96

Abstract..... 97

Introduction..... 98

Experimental..... 101

Results and Discussion..... 102

Conclusion..... 108

Acknowledgements..... 109

References..... 110

5 CO OXIDATION STUDIES ON PT NANOFILM PREPARED BY ELECTROCHEMICAL ATOMIC LAYER DEPOSITION (E-ALD)..... 135

Abstract..... 136

Introduction..... 137

Experimental..... 139

Results and Discussion..... 141

Conclusion..... 144

Acknowledgements..... 145

References..... 146

6 CONCLUSION AND FUTURE STUDIES... 165

LIST OF TABLES

Page

Table 1. Summary of the onset potentials and peak potentials of CO Electrooxidation for electrodes prepared by E-ALD..... 94

LIST OF FIGURES

Page

Figure 2.1. Electrochemical ALD cycle cartoon for Pt film deposition on Au substrates……38

Figure 2.2. Time-Potential-Current graph illustrating one Pt ALD cycle. Cu is deposited at +100mV and is replaced by Pt^{+2} ions at open circuit……..39

Figure 2.3. Cu deposition charge as a function of Pt deposition cycles using Pt^{+2} and Pt^{+4}…….....40

Figure 2.4. Cyclic Voltammogram for Pb UPD on Au in 1mM $Pb(ClO_4)_2$ in 0.5M $NaClO_4$; Scan rate 10mV/s…….41

Figure 2.5. Time-Current- Potential graph illustrating one Pt ALD cycle. Pb is deposited at -400mV and is replaced by $PtCl_4^{2-}$ ions at open circuit……..42

Figure 2.6. Pb coverage as a function of deposition cycles……...43

Figure 2.7. Cyclic voltammetry of 25 cycles Pt film immediately after deposition in 0.5M H_2SO_4; Scan rate: 10mV/s. Pt was deposited using $PtCl_4^{2-}$ ions…….44

Figure 2.8. Cyclic voltammetry of 25 cycles Pt film in 0.5M H_2SO_4 by scanning between 1.400V and -0.160V; Scan rate: 10mV/s. Pt was deposited using $PtCl_4^{2-}$ ions……...45

Figure 2.9. Cyclic voltammetry of (A) 5 cycles (B) 10 cycles (C) 15 cycles and (D) 20 cycles Pt film in 0.5M H_2SO_4 by scanning between 1.400V and -0.160V; Scan rate: 10mV/s. Pt was deposited using $PtCl_4^{2-}$ ions……..46

Figure 2.10.Surface area (ML vs. Au) of Pt film calculated from Pt oxide reduction charge and Hydrogen adsorption and desorption charge. Pt was deposited using $PtCl_4^{2-}$ ions……..47

Figure 2.11.Three CVs of a 25 cycle Pt deposit in 0.5M H_2SO_4. The positive limit of Scan 1 and scan 3 was +1200mV while scan 2 was +1400mV. Scan rate:10mV/s……48

Figure 2.12.The CV of a clean Au substrate in 0.5M H_2SO_4 with a positive limit of +1200mV. Scan rate: 10mV/s……....49

Figure 2.13.Four different 25 cycle Pt films deposited with different stop potential. Surface area (ML vs. Au) of 25 cycle Pt film calculated from Pt oxide reduction charge and Hydrogen adsorption and desorption charge in 0.5M H_2SO_4. Pt was deposited using $PtCl_4^{2-}$ ions……....50

Figure 2.14.Atomic % for Pt film deposited using Pt(II) and Pt(IV) as a function of stop potentials……51

Figure 2.15.Four different 25 cycle Pt films deposited with different stop potential. Surface area (ML vs. Au) of 25 cycle Pt film calculated from Pt oxide reduction charge and Hydrogen adsorption and desorption charge in 0.5M H_2SO_4. Pt was deposited using $PtCl_6^{2-}$ ions……...52

Figure 2.16.(A)Time-Current- Potential graph illustrating one Pt ALD cycle for charging current, Hydrogen evolution, reduction of adsorbed $PtCl_6^{2-}$ species and Pb UPD at -400mV. (B) Pb is deposited at -400mV and is replaced by $PtCl_4^{2-}$ ions at open circuit……....53

Figure 2.17.STM image of 25 cycle Pt film deposited on template-stripped Au using $PtCl_6^{2-}$ precursor ions……..54

Figure 3.1. Cartoon representation for the formation of PtRu nanofilm by E-ALD and SLRR……....83

Figure 3.2. Cyclic voltammogram of Au electrode in 1mM $Pb(ClO_4)_2$ in 0.5M $NaClO_4$; pH~ 4.5; Scan rate: 10mVs^{-1}……84

Figure 3.3. Graph of Current-Time-Potential plot for one PtRu E-ALD cycle…….85

Figure 3.4. (A) Coverage for Pb UPD during Pt and Ru deposition and (B) Maximum coverage for Pt and Ru calculated from reaction stoichiometry…….....86

Figure 3.5. Cyclic voltammogram of PtRu electrode (A) 70/30 Pt/Ru (B) 82/18 Pt/Ru and (C) 50/50 Pt/Ru in 0.5M H_2SO_4; Scan rate: 10mVs^{-1}……...87

Figure 3.6. Cartoon scheme of sputtered (70/30 Pt/Ru) and E-ALD prepared PtRu (70/30Pt/Ru, 82/18 Pt/Ru and 50/50 Pt/Ru) nanofilm electrodes……88

Figure 3.7. CO stripping voltammetry on PtRu electrode (70/30 Pt/Ru) in 0.5M H_2SO_4 with first (A), second (B) and third (C) continuous CO adsorption and oxidation cycles. Scan rate: 10mVs^{-1}. (—) stripping of CO in the first positive going sweep; (----) second positive going sweep during each cycle…….89

Figure 3.8. CO stripping voltammetry on various PtRu alloy electrodes in 0.5M H_2SO_4. Scan rate: 10mVs^{-1}……......90

Figure 3.9. Cartoon scheme of various electrodes prepared by E-ALD……91

Figure 3.10.CO stripping voltammetry on Pure Pt, Pure Ru, 50/50 Pt/Ru alloy, Ru-modified Pt and Pt-modified Ru electrodes in 0.5M H_2SO_4 . Scan rate: 10mVs^{-1}……..92

Figure 3.11.Stability test performed on 50/50 Pt/Ru alloy by subjecting to 20 continuous CO adsorption and stripping voltammetry in 0.5M H_2SO_4 . Scan rate: 10mVs^{-1}……..93

Figure 3.12.CO stripping voltammetry on 50/50 Pt/Ru (Base alloy) electrode with

various surface ending layers in 0.5M H_2SO_4. Scan rate: 10mVs^{-1}……94

Figure 4.1. Cartoon representation of A) Pt E-ALD cycle and B) Ru E-ALD cycle……..119

Figure 4.2. Cyclic voltammogram of Au in 1mM $Pb(ClO_4)_2$ with 0.5M $NaClO_4$; pH~ 4.5; Scan rate: 10mVs^{-1}……120

Figure 4.3. Time-Current-Potential graph for: A) one Pt E-ALD cycle and B) one Ru E-ALD cycle……....121

Figure 4.4. Cyclic voltammetry (0.5M H_2SO_4, 10mVs^{-1}) for CO stripping on 0.16ML Ru modified Pt electrode……..122

Figure 4.5. (▲) Points represent the Pb coverage and (■) represents the maximum Ru coverage possible from reaction stoichiometry at the corresponding Pb deposition potentials used for modifying the Pt surface……...123

Figure 4.6. CO oxidation curves on the Pt electrode modified with 0.16ML, 0.20ML, 0.35ML, 0.39ML and 0.83 ML Ru in 0.5M H_2SO_4; Scan rate: 10mVs^{-1}……124

Figure 4.7. CV of a clean Pt electrode in 0.5M H_2SO_4; Scan rate: 10mVs^{-1}……...125

Figure 4.8. CO oxidation on the Pt electrode modified with 0.35ML Ru in 0.5M H_2SO_4; Scan rate: 10mVs^{-1}. (---) Represents Ru on contaminated Pt nanofilm and (—) represents Ru on cleaned Pt nanofilm electrode……...126

Figure 4.9. CO stripping voltammogram (0.5M H_2SO_4, 10mVs^{-1}) on the Pt surface modified with 0.31ML Ru……127

Figure 4.10.(▲) Points represent Pb coverage and (■) represents the maximum Ru coverage possible from reaction stoichiometry as a function of deposition cycles……128

Figure 4.11.CO oxidation curves obtained after each cycle Ru deposition on the same

Pt electrode (0.5M H_2SO_4, 10mVs^{-1})……......129

Figure 4.12.Cumulative Pb coverage (▲) and maximum Ru coverage (■) as a function of deposition cycles……...130

Figure 4.13.Three continuous CO stripping curves on the Pt electrode modified with 1.07 ML Ru (0.5M H_2SO_4, 10mVs^{-1})……...131

Figure 4.14.Twelve continuous CO stripping curves on the Pt electrode modified with 0.35 ML Ru (0.5M H_2SO_4, 10mVs^{-1})……...132

Figure 4.15.Twelve continuous CO stripping curves on the Pt electrode modified with 0.75 ML Ru (0.5M H_2SO_4, 10mVs^{-1})……...133

Figure 4.16.Twelve continuous CO stripping curves on the Pt electrode modified with 1.34 ML Ru (0.5M H_2SO_4, 10mVs^{-1})……...134

Figure 5.1. Cartoon representation for the formation of Pt nanofilm by E-ALD and SLRR…..152

Figure 5.2. Cyclic voltammogram of Au in 1mM $Pb(ClO_4)_2$ in 0.5M $NaClO_4$; pH~ 4.5; Scan rate: 10mVs^{-1} ……153

Figure 5.3. Graph of Current – Time – Potential plot for one Pt E-ALD cycle…….....154

Figure 5.4. Cyclic voltammogram of Pt in 0.5M H_2SO_4 between 400mV and 50mV; Scan rate: 10mVs^{-1}…….155

Figure 5.5. Cyclic voltammogram of Pt in 0.5M H_2SO_4 between 1600mV and 50mV; Scan rate: 10mVs^{-1}…….156

Figure 5.6. Cyclic voltammogram of Pt in 0.5M H_2SO_4 between 410mV and 50mV; Scan rate: 10mVs^{-1}…….157

Figure 5.7. Graph of Current – Time – Potential plot for one Pt E-ALD cycle. After Pt deposition the potential was switched between 1200mV and 400mV in blank

to clean the surface off the contaminants……..158

Figure 5.8. Cyclic voltammogram of Pt in 0.5M H_2SO_4; Scan rate: 10mVs^{-1}……159

Figure 5.9. Chronoamperometric oxidation of adsorbed CO on the Pt nanofilm at 750mV…...160

Figure 5.10.CO stripping voltammetry of Pt in 0.5M H_2SO_4; Scan rate: 10mVs^{-1}…….161

Figure 5.11.CO stripping voltammetry of Pt in 0.5M H_2SO_4; Scan rate: 10mVs^{-1}…….162

Figure 5.12.Cyclic voltammogram of Pt in 0.5M H_2SO_4; Scan rate: 10mVs^{-1}……...163

CHAPTER 1

INTRODUCTION

Fuels cells are an electrochemical device that converts chemical energy in to electrical energy [1]. Fuel cells combine hydrogen and oxygen to produce electricity and water. Hydrogen is fed into the anode compartment of the fuel cell. Air provides the oxygen and enters the fuel cell at the cathode compartment. The anode and cathode compartments are separated by a Nafion membrane to avoid mixing of the fuel. Hydrogen is oxidized at the anode into protons and electrons. The electrons travel through the external circuit to the load and returns to the cathode while the protons diffuse through the membrane to the cathode compartment. The reduction of oxygen to water takes place at the cathode. The Proton Exchange Membrane Fuel Cells (PEMFCs) fuel cells are the most promising fuel cells and show excellent performance when fed with hydrogen. However, production, storage and use of hydrogen are a major limitation for its commercial purpose. Further, its performance is severely affected by poisoning species such as Carbon monoxide (CO) present in trace amounts in the hydrogen fuel [2].

Another important fuel cell is the Direct Methanol Fuel Cell (DMFC), which uses methanol as the fuel instead of hydrogen. Methanol has higher energy density and can be fed with dilute aqueous solution of methanol in water. Methanol is also easy to store and transport, making it a suitable fuel for fuel cells. The PEMFCs and DMFCs [3] are low and intermediate temperature fuel cells which can be operated between 30-150 °C. Fuel Cells are considered as environmentally friendly as they do not produce toxic by-products. However, they are not emission-free. They still produce carbon dioxide which is a green house gas.

Phosphoric acid fuel cells, Solid oxide fuel cells and molten carbonate fuel cells are the other major types of fuel cells. Fuel cells applications are classified into stationary and mobile applications. Stationary applications include heat and power systems for resident, industrial and commercial buildings. Mobile applications include transportation (cars, buses, etc) [4] and portable electronic devices (Laptops, cell phones…etc).

Pt and PtRu are used as cathode and anode material in fuel cells although there is other Pt based alloys under investigation. Pt showed higher activity for oxygen reduction reactions. Pt is a very expensive material and there is a need to make economical use of it. Pt can be deposited by various methods such as molecular beam epitaxy (MBE) [5-7], chemical vapor deposition (CVD) [8-9], physical vapor deposition (PVD) [10], metallorganic chemical vapor deposition (MOCVD) [11-13] and electrodeposition [14].

One of the major drawbacks of the DMFCs is the various intermediates (CO_{ads}, COH_{ads}, HCO_{ads}, and HCOOads) [15] that are formed during the oxidation of methanol to CO_2. It has been shown that some Pt alloys such as PtRu, PtCo, PtSn, PtMo, PtRuCo and PtRuNiZr [16-22] can help to oxidize adsorbed CO, and thus decrease the overpotential observed while running a fuel cell. PtRu alloy have shown higher catalytic activity and cell performance among the catalysts currently available and are frequently used as an anode material in direct methanol fuel cells (DMFC) due to its increased CO tolerance [23] [24] [25-30]. The presence of a second alloying element, in addition to platinum, facilitated the removal of adsorbed intermediates from the catalyst surface [31-32]. The higher catalytic activity of PtRu alloy and the increased CO tolerance can be explained due to a ligand effect (electronic effect) or the bifunctional mechanism. In the ligand effect [33-35], the addition of Ru increases CO tolerance via electronic interactions, causing a reduction in CO-Pt bond strength. In the bifunctional mechanism [30-31,

36-37], it is proposed that Ru adsorbs oxygenated surface species by dissociation of water at lower potentials for CO oxidation to CO_2.

The majority of methods for the preparation of PtRu alloys for electrocatalysts involve thermal decomposition of precursors [38-39], spray pyrolysis[40-41], sol-gel technology[42], ionic liquids[43-44], chemical deposition[45-46] and electrodeposition[35, 47-51]. Electrodeposition provides simple, cost effective, low temperature processes for growing thin films.

Atomic layer deposition (ALD) is a methodology for the formation of conformal nanofilms, based on the use of surface limited reactions and deposition of an atomic layer at a time. The electrochemical form of ALD (E-ALD) was invented in this group and was initially referred to as electrochemical atomic layer epitaxy (EC-ALE). Most electrochemical surface limited reactions are referred to as underpotential deposition (UPD) {Kolb, 1978 #297;Adzic, 1984 #414;Gewirth, 1997 #200;Herrero, 2001 #2412;Magnussen, 2002 #2894}. UPD is a thermodynamic process, where one element deposits on a second, due to the free energy of formation of a surface compound or alloy. UPD involves the formation of an atomic layer of one element on a second at a potential prior to (under) that needed to deposit the element on itself. An atomic layer refers to a deposit which is only one atom thick. The corresponding coverage is not specified, it cannot be more than one atom thick, but the surface density is not specified. Coverage is described in terms of monolayers (ML), where a ML is one adsorbate atom for every substrate atom. In the present report, the Au on glass substrates are approximated as Au(111) single crystal surfaces, for the purpose of determining coverage. One ML corresponds to $1.35X10^{15}$ atoms/cm^2, or 217 μC/cm^2, for a one electron process, per surface atom.

E-ALD of metal, or elemental, nanofilms was not possible until recently, with the development of monolayer restricted galvanic displacement (MRGD) by Brankovic, Wang and Adzic [52-53]. MRGD has also been referred to as surface limited redox replacement reactions (SLRR). It involves the electrodeposition of an atomic layer of a sacrificial metal by UPD, and its subsequent replacement by open circuit potential (OCP) exposure to a solution containing precursor ions to a more noble element. The replacement reaction should be limited by the amount of the sacrificial element, generally a monolayer or less. Depositions of single monolayers of Pt and Pd were some of the first examples of SLRR [52-53]. Atomic level control was revealed, by scanning tunneling microscopy (STM) in the formation of a Pt atomic layer. Those deposits were formed using Cu UPD as the sacrificial layer, which was subsequently exchanged for Pt in a solution containing $PtCl_6^{2-}$ ions. Studies of noble metal deposition by galvanic displacement have been extended by Vasilic and Dimitrov [54-56], Mroek and Weaver [57] and Kim and Stickney [58-60]. The author's group has studied the use of SLRR as a cycle for E-ALD formation of Cu [61], Ru [62] and Pt [58], on gold substrates.

IN the present study monometallic Pt nanofilm and bimetallic PtRu nanofilm alloys were formed using E-ALD and SLRR cycles. For Pt deposition, both Cu and Pb UPD were investigated as sacrificial layers, while both Pt(II) and Pt(IV) precursors were used to exchange for the sacrificial layers. For PtRu nanofilm deposition, Pb was used as the sacrificial metal while the precursors were Pt (IV) and Ru(III). The films were then characterized by cyclic voltammetry (CV). The catalytic activity towards CO electrooxidation was studied by CO stripping voltammetry. PtRu nanofilms showed higher catalytic activity compared to pure Pt and pure Ru electrodes. The compositions were determined by Electron probe microanalysis (EPMA).

Experimental

The electrodeposition of the nanofilms were carried out in an automated electrochemical flow cell system (Electrochemcal ALD L.C) consisting of peristaltic pumps, Teflon solenoid valves, an electrochemical flow cell and a potentiostat. The flow cell system was controlled using a program based on LABVIEW (National Instruments). A gold wire embedded in the Plexiglas flow cell was used as the auxiliary electrode. An Ag/AgCl (3M NaCl) (Bioanalytical systems, Inc., West Lafayette, IN) electrode was used as the reference electrode. The flow cell ($4X1X0.1cm^3$) consisted of a planar substrate held away from the counter electrode by a 1mm thick silicone rubber gasket. The deposition area was $3.77cm^2$. Solution flow rate of 9ml/min were used during the deposition process.

Solutions used were 1mM $Pb(ClO_4)_2$, 2mM CuSO4, 0.1mM $RuCl_3$, 0.1mM K_2PtCl_4 and 0.1mM H_2PtCl_6. The Pb solutions were made with 0.5M $NaClO_4$ (pH 4.5). The Cu solutions were made with 50 mM H_2SO_4 (pH 1.5). The Ru solutions were made with 50 mM HCl (pH 1.5), and the Pt solutions with 50 mM $HClO_4$ (pH 1.3). The blank solution was 0.5M $NaClO_4$ (pH 4.5). CVs were performed in 0.5M H_2SO_4. All solutions were prepared using water from a nanopure water filtration system (Barnstead, Dubuque, IA) (18MΩ) attached to the house DI water system. Chemicals were obtained from Sigma-Aldrich or Alfa Aesar. Solutions bottles were contained inside a Plexiglas box, and deaerated by bubbling with dry nitrogen.

The substrates were Au on glass, formed by initial deposition of a 5 nm Ti adhesion layer, then 300 nm of Au. The Au was vapor deposited with the substrate at 280^o C, and then the deposits were annealed at 400^o C for 12 hours, producing a prominent (111) growth habit. The Au substrates were cleaned in nitric acid for 2 minutes and then by electrochemical cycling between 1.600V and 0.010V in 0.5M sulfuric acid, at 10mV/s, prior to deposition.

The deposition conditions for the formation of Pt nanofilms using Pt(II) and Pt(IV) precursors was discussed in Chapter 2. In this chapter i will talk about the experiments performed to deposit Pt by surface limited redox replacement (SLRR) using Cu and Pb as the sacrificial metal. Also I will discuss about the difference in the behavior of Pt(II) precursor compared to Pt(IV) precursor in the deposition of Pt nanofilm. In Chapter 3, I will discuss about the electrodeposition of PtRu alloy electrodes by E-ALD. I will describe the experiments done to prepare superlattice of PtRu nanoalloy as well as the methods to develop materials of varying compositions. The electrodes prepared are characterized by cyclic voltammetry and the catalytic activities are studied by CO adsorption and oxidation studies. The catalytic activity of the alloy electrodes are then compared to Pt, Ru and modified electrodes. In Chapter 4, most of the work is focused on modifying the electrode surfaces with different adatom and studying their catalytic activity towards CO electrooxidation. Ru-modified Pt electrodes and Pt-modified Ru electrodes were prepared and the enhancement in the CO electooxidation potential were compared to pure Pt, pure Ru and PtRu alloy electrodes. Chapter 5 talks about the various studies carried out to clean the Pt electrodes prepared by E-ALD without oxidizing the surface. CO were adsorbed from solution on to the Pt electrodes immediately after deposition to prevent the surface from contamination and the clean surface can be degenerated by oxidizing the CO.

References

1. Carrette, L., K.A. Friedrich, and U. Stimming, *Fuel cells: Principles, types, fuels, and applications.* ChemPhysChem, 2000. **1**: p. 162-193.
2. Wee, J.-H. and K.-Y. Lee, *Overview of the development of CO-tolerant anode electrocatalysts for proton-exchange membrane fuel cells.* Journal of Power Sources, 2006. **157**(1): p. 128-135.
3. Kamarudin, S.K., et al., *Overview on the challenges and developments of micro-direct methanol fuel cells (DMFC).* Journal of Power Sources, 2007. **163**(2): p. 743-754.
4. Shukla, A.K., M.K. Ravikumar, and K.S. Gandhi, *Direct methanol fuel cells for vehicular applications.* Journal of Solid State Electrochemistry, 1998. **2**(2): p. 117-122.
5. Nishikawa, K., M. Yamamoto, and T. Kingetsu, *Dependence of electrical resistivity on surface topography of MBE-grown Pt film.* Applied Surface Science, 1997. **113-114**: p. 412-416.
6. Kato, T., et al., *Magnetic anisotropy of MBE grown MnPt3 and CrPt3 ordered alloy films.* Journal of Magnetism and Magnetic Materials, 2004. **272-276**(Part 2): p. 778-779.
7. Makarov, D., et al., *Growth of Pt thin films on WSe2.* Surface Science, 2007. **601**(9): p. 2032-2037.
8. Garcia, J.R.V. and T. Goto, *Chemical Vapor Deposition of Iridium, Platinum, Rhodium and Palladium.* MATERIALS TRANSACTIONS, 2003. **44**(9): p. 1717-1728.
9. Huang, S.-F., et al., *Preparation of Pt-Ru Alloyed Thin Films Using a Single-Source CVD Precursor.* Chemical Vapor Deposition, 2003. **9**(3): p. 157-161.

10. Mattox, D.M., *Physical Sputtering and Sputter Deposition (Sputtering)*, in *Handbook of Physical Vapor Deposition (PVD) Processing (Second Edition)*. 2010, William Andrew Publishing: Boston. p. 237-286.

11. Kwon, J.-H. and S.-G. Yoon, *Preparation of Pt thin films deposited by metalorganic chemical vapor deposition for ferroelectric thin films.* Thin Solid Films, 1997. **303**(1-2): p. 136-142.

12. Valet, O., et al., *Study of platinum thin films deposited by MOCVD as electrodes for oxide applications.* Microelectronic Engineering, 2002. **64**(1-4): p. 457-463.

13. Goswami, J., et al., *MOCVD of Platinum Films from (CH3)3CH3CpPt and Pt(acac)2: Nanostructure, Conformality, and Electrical Resistivity.* Chemical Vapor Deposition, 2003. **9**(4): p. 213-220.

14. Lu, G. and G. Zangari, *Electrodeposition of Platinum on Highly Oriented Pyrolytic Graphite. Part I: Electrochemical Characterization.* The Journal of Physical Chemistry B, 2005. **109**(16): p. 7998-8007.

15. Léger, J.M., *Mechanistic aspects of methanol oxidation on platinum-based electrocatalysts.* Journal of Applied Electrochemistry, 2001. **31**(7): p. 767-771.

16. Igarashi, H., et al., *CO Tolerance of Pt alloy electrocatalysts for polymer electrolyte fuel cells and the detoxification mechanism.* Physical Chemistry Chemical Physics, 2001. **3**(3): p. 306-314.

17. Petrii, O.A., *Pt-Ru electrocatalysts for fuel cells: a representative review.* Journal of Solid State Electrochemistry, 2008. **12**(5): p. 609-642.

18. Hayden, B.E., M.E. Rendall, and O. South, *Electro-oxidation of Carbon Monoxide on Well-Ordered Pt(111)/Sn Surface Alloys.* Journal of the American Chemical Society, 2003. **125**(25): p. 7738-7742.

19. Samjeské, G., et al., *CO and methanol oxidation at Pt-electrodes modified by Mo.* Electrochimica Acta, 2002. **47**(22-23): p. 3681-3692.

20. Hsieh, Y.-C., et al., *Displacement Reaction in Pulse Current Deposition of PtRu for Methanol Electro-Oxidation.* Journal of the Electrochemical Society, 2009. **156**(6): p. B735-B742.

21. Strasser, P., et al., *High Throughput Experimental and Theoretical Predictive Screening of Materials − A Comparative Study of Search Strategies for New Fuel Cell Anode Catalysts.* The Journal of Physical Chemistry B, 2003. **107**(40): p. 11013-11021.

22. Whitacre, J.F., T. Valdez, and S.R. Narayanan, *Investigation of Direct Methanol Fuel Cell Electrocatalysts Using a Robust Combinatorial Technique.* Journal of the Electrochemical Society, 2005. **152**(9): p. A1780-A1789.

23. Zhang, J., *PEM Fuel Cell Electrocatalysts and Catalyst Layers*. 2008: Springer London.

24. Cha, H.-C., C.-Y. Chen, and J.-Y. Shiu, *Investigation on the durability of direct methanol fuel cells.* Journal of Power Sources, 2009. **192**(2): p. 451-456.

25. Liu, H., et al., *A review of anode catalysis in the direct methanol fuel cell.* Journal of Power Sources, 2006. **155**(2): p. 95-110.

26. Kabbabi, A., et al., *In situ FTIRS study of the electrocatalytic oxidation of carbon monoxide and methanol at platinum-ruthenium bulk alloy electrodes.* Journal of Electroanalytical Chemistry, 1998. **444**(1): p. 41-53.

27. Gasteiger, H.A., N.M. Markovic, and P.N. Ross, *H2 and CO electrooxidation on well-characterized Pt, Ru, and Pt-Ru.2. Rotating disk electrode studies of CO/H2 mixtures at 62[thinsp][compfn]C.* J. Phys. Chem., 1995. **99**: p. 16757-16767.

28. Gasteiger, H.A., et al., *Electro-oxidation of small organic molecules on well-characterized Pt---Ru alloys.* Electrochimica Acta, 1994. **39**(11-12): p. 1825-1832.

29. Hoster, H., et al., *Pt-Ru model catalysts for anodic methanol oxidation: Influence of structure and composition on the reactivity.* Physical Chemistry Chemical Physics, 2001. **3**(3): p. 337-346.

30. Ianniello, R., et al., *CO adsorption and oxidation on Pt and Pt---Ru alloys: dependence on substrate composition.* Electrochimica Acta, 1994. **39**(11-12): p. 1863-1869.

31. Watanabe, M. and S. Motoo, *Electrocatalysis by ad-atoms: Part II. Enhancement of the oxidation of methanol on platinum by ruthenium ad-atoms.* Journal of Electroanalytical Chemistry, 1975. **60**(3): p. 267-273.

32. Watanabe, M. and S. Motoo, *Electrocatalysis by ad-atoms: Part III. Enhancement of the oxidation of carbon monoxide on platinum by ruthenium ad-atoms.* Journal of Electroanalytical Chemistry, 1975. **60**(3): p. 275-283.

33. Krausa, M. and W. Vielstich, *Study of the electrocatalytic influence of Pt/Ru and Ru on the oxidation of residues of small organic molecules.* Journal of Electroanalytical Chemistry, 1994. **379**(1-2): p. 307-314.

34. Tong, et al., *An NMR Investigation of CO Tolerance in a Pt/Ru Fuel Cell Catalyst.* Journal of the American Chemical Society, 2001. **124**(3): p. 468-473.

35. Sasaki, K. and R.R. Adzic, *Monolayer-Level Ru- and NbO[sub 2]-Supported Platinum Electrocatalysts for Methanol Oxidation.* Journal of the Electrochemical Society, 2008. **155**(2): p. B180-B186.

36. Gasteiger, H.A., et al., *Carbon monoxide electrooxidation on well-characterized platinum-ruthenium alloys.* The Journal of Physical Chemistry, 1994. **98**(2): p. 617-625.

37. Gasteiger, H.A., et al., *Methanol electrooxidation on well-characterized platinum-ruthenium bulk alloys.* The Journal of Physical Chemistry, 1993. **97**(46): p. 12020-12029.

38. Sivakumar, P., R. Ishak, and V. Tricoli, *Novel Pt-Ru nanoparticles formed by vapour deposition as efficient electrocatalyst for methanol oxidation: Part I. Preparation and physical characterization.* Electrochimica Acta, 2005. **50**(16-17): p. 3312-3319.

39. Sivakumar, P. and V. Tricoli, *Novel Pt-Ru nanoparticles formed by vapour deposition as efficient electrocatalyst for methanol oxidation: Part II. Electrocatalytic activity.* Electrochimica Acta, 2006. **51**(7): p. 1235-1243.

40. Xue, X., et al., *Physical and Electrochemical Characterizations of PtRu/C Catalysts by Spray Pyrolysis for Electrocatalytic Oxidation of Methanol.* Journal of the Electrochemical Society, 2006. **153**(5): p. E79-E84.

41. Chakraborty, D., et al., *Mixed Phase Pt-Ru Catalyst for Direct Methanol Fuel Cell Anode by Flame Aerosol Synthesis.* Journal of the Electrochemical Society, 2005. **152**(12): p. A2357-A2363.

42. Kim, J.Y., et al., *A Sol-Gel-Based Approach to Synthesize High-Surface-Area Pt-Ru Catalysts as Anodes for DMFCs.* Journal of the Electrochemical Society, 2003. **150**(11): p. A1421-A1431.

43. Xue, X., et al., *Novel preparation method of Pt-Ru/C catalyst using imidazolium ionic liquid as solvent.* Electrochimica Acta, 2005. **50**(16-17): p. 3470-3478.

44. He, P., et al., *Electrodeposition of Platinum in Room-Temperature Ionic Liquids and Electrocatalytic Effect on Electro-oxidation of Methanol.* Journal of the Electrochemical Society, 2005. **152**(4): p. E146-E153.

45. Yan, S., et al., *Polyol synthesis of highly active PtRu/C catalyst with high metal loading.* Electrochimica Acta, 2006. **52**(4): p. 1692-1696.

46. Colmenares, L., et al., *Ethanol oxidation on novel, carbon supported Pt alloy catalysts--Model studies under defined diffusion conditions.* Electrochimica Acta, 2006. **52**(1): p. 221-233.

47. Rodríguez-Nieto, F.J., T.Y. Morante-Catacora, and C.R. Cabrera, *Sequential and simultaneous electrodeposition of Pt-Ru electrocatalysts on a HOPG substrate and the electro-oxidation of methanol in aqueous sulfuric acid.* Journal of Electroanalytical Chemistry, 2004. **571**(1): p. 15-26.

48. Coutanceau, C., et al., *Preparation of Pt–Ru bimetallic anodes by galvanostatic pulse electrodeposition: characterization and application to the direct methanol fuel cell.* Journal of Applied Electrochemistry, 2004. **34**(1): p. 61-66.

49. Gavrilov, A.N., et al., *Pt-Ru electrodeposited on gold from chloride electrolytes.* Electrochimica Acta, 2007. **52**(8): p. 2775-2784.

50. Cattaneo, C., et al., *Characterization of platinum-rutheniun electrodeposits using XRD, AES and XPS analysis.* Journal of Electroanalytical Chemistry, 1999. **461**(1-2): p. 32-39.

51. Mkwizu, T.S., M.K. Mathe, and I. Cukrowski, *Electrodeposition of Multilayered Bimetallic Nanoclusters of Ruthenium and Platinum via Surface-Limited*

Redox−Replacement Reactions for Electrocatalytic Applications. Langmuir, 2009. **26**(1): p. 570-580.

52. Brankovic, S.R., J.X. Wang, and R.R. Adzic, *Metal monolayer deposition by replacement of metal adlayers on electrode surfaces.* Surface Science, 2001. **474**(1-3): p. L173-L179.

53. Brankovic, S.R., J.X. Wang, and R.R. Adzic, *New methods of controlled monolayer-to-multilayer deposition of Pt for designing electrocatalysts at an atomic level.* Journal of the Serbian Chemical Society, 2001. **66**(11-12): p. 887-898.

54. Vasilic, R. and N. Dimitrov, *Epitaxial growth by monolayer-restricted galvanic displacement.* Electrochemical and Solid State Letters, 2005. **8**(11): p. C173-C176.

55. Vasilic, R., L.T. Viyannalage, and N. Dimitrov, *Epitaxial growth of Ag on Au(111) by galvanic displacement of Pb and Tl monolayers.* Journal of the Electrochemical Society, 2006. **153**(9): p. C648-C655.

56. Viyannalage, L.T., R. Vasilic, and N. Dimitrov, *Epitaxial growth of Cu on Au(111) and Ag(111) by surface limited redox replacement - An electrochemical and STM study.* Journal of Physical Chemistry C, 2007. **111**(10): p. 4036-4041.

57. Mrozek, M.F., Y. Xie, and M.J. Weaver, *Surface-Enhanced Raman Scattering on Uniform Platinum-Group Overlayers: Preparation by Redox Replacement of Underpotential-Deposited Metals on Gold.* Analytical Chemistry, 2001. **73**(24): p. 5953-5960.

58. Kim, Y.-G., et al., *Platinum Nanofilm Formation by EC-ALE via Redox Replacement of UPD Copper: Studies Using in-Situ Scanning Tunneling Microscopy.* The Journal of Physical Chemistry B, 2006. **110**(36): p. 17998-18006.

59. Kim, J.Y., Y.G. Kim, and J.L. Stickney, *Copper nanofilm formation by electrochemical atomic layer deposition - Ultrahigh-vacuum electrochemical and in situ STM studies.* Journal of the Electrochemical Society, 2007. **154**(4): p. D260-D266.

60. Kim, J.Y., Y.G. Kim, and J.L. Stickney, *Cu nanofilm formation by electrochemical atomic layer deposition (ALD) in the presence of chloride ions.* Journal of Electroanalytical Chemistry, 2008. **621**(2): p. 205-213.

61. Thambidurai, C., et al., *Copper Nanofilm Formation by Electrochemical ALD.* Journal of the Electrochemical Society, 2009. **156**(8): p. D261-D268.

62. Thambidurai, C., Y.-G. Kim, and J.L. Stickney, *Electrodeposition of Ru by atomic layer deposition (ALD).* Electrochimica Acta, 2008. **53**(21): p. 6157-6164.

CHAPTER 2

ELECTROCHEMICAL ATOMIC LAYER DEPOSITION (E-ALD) OF PT NANOFILMS[1]

[1]Jayaraju, N., et al. To be submitted to Journal of Electrochemical Society.

Abstract

This paper describes platinum nanofilm formation via the electrochemical form of atomic layer deposition (E-ALD). Atomic layer deposition (ALD) is the formation of materials an atomic layer at a time using surface limited reactions. E-ALD is the application of electrochemical surface limited reactions, such as underpotential deposition (UPD), to form nanofilms of materials using an ALD cycle. UPD is the electrodeposition of an atomic layer of one element on a second, at a potential prior to (under) that needed to deposit the element on itself. Surface limited redox replacement (SLRR) is where an atomic layer of a reactive metal is exchanged for one of a more noble metal. In the present study, SLRR was used to form Pt atomic layers in an ALD cycle. Both Cu and Pb UPD were used as sacrificial atomic layers for replacement with Pt. Deposits in this study were formed using 25 E-ALD cycles, were each cycle was intended to form one atomic layer. However, deposits formed using Cu or Pb UPD sacrificial layers, and Pt(II) and Pt(IV) precursors were investigated. Initial deposits contained an order of magnitude more Pt deposition then expected, and the surfaces roughened. Investigations revealed that excessively positive potentials achieved during exchange at open circuit were associated with the excess Pt deposition. It is proposed here that the anionic Pt precursors were adsorbed more strongly at high potentials, and thus more difficult to rinse from the cell. Those adsorbed precursors were then available for reduction as the negative potentials used for UPD of the sacrificial element, and thus contributed to the excessive growth of Pt. Increased rinsing of the Pt precursor solution, eliminated the excess Pt, and allowed layer by layer growth expected of an ALD process.

Keywords: Pt, E-ALD, UPD, ALD, SLRR, Fuel cell, EPMA, .

Introduction

Metal thin films can be grown by a variety of techniques, including: molecular beam epitaxy (MBE) [1-3], chemical vapor deposition (CVD) [4-5], physical vapor deposition (PVD) [6], metallorganic chemical vapor deposition (MOCVD) [7-9] and electrodeposition[10-14]. Electrodeposition is a simple, cost effective, low temperature process for the formation of metal films. However, Pt electrodeposition has proven difficult, generally resulting in complex 3-D growth, and surface roughening [15] [16]. It is thus desirable to develop better ways to control Pt thin film formation to facilitate the design and growth catalytic surfaces, for example, with known morphology, composition and structure.

One method for promoting layer by layer growth is atomic layer deposition (ALD) {George, 2010 #17619}. ALD describes a family of deposition methodologies where materials are formed an atomic layer at a time, using surface limited reactions. The electrochemical analog of ALD, E-ALD, was invented in this group [17-18], thought it was initially referred to as electrochemical atomic layer epitaxy (EC-ALE) for historical reasons{Suntola, 1977 #17749}. Most electrochemical surface limited reactions are referred to as underpotential deposition (UPD) [19-22]. UPD is the formation of an atomic layer of one element on a second at a potential prior to (under) that needed to deposit the element on itself. An atomic layer refers to a deposit which is only one atom thick, without specific reference to the coverage. Coverage is frequently described in terms of monolayers (ML), where a ML, in this report, corresponds to one adsorbate atom for every substrate surface atom. UPD is a thermodynamic phenomenon where one element deposits on a second, driven by the free energy of formation of a surface compound or alloy. Initial E-ALD studies focused on the formation of compounds, where one element was deposited on a second at an underpotential, and then vice-versa.

Direct electrodeposition of smooth, high quality films of some of the more noble elements has proven difficult. Pt, for instance, tends to form clusters because of its high cohesive energy [23], resulting in formation of "platinum black", a very high surface area form of metallic Pt. Because of platinum's importance as a catalyst, the electrochemical formation of Pt nano particles and films has been extensively studied. For example, electrodeposition of Pt nanoparticles on highly oriented pyrolytic graphite was achieved by Lu et al. [11]. Detailed studies have been performed of the electrodeposition of Pt on Au, and the formation of Pt nanoparticles [24-26]. Uosaki et al. [24] achieved quasi 2D layer by layer growth of platinum on Au(111), showed that nucleation of Pt starts mainly at defects, step edges for example, and resulted in some three-dimensional clusters on gold. Deposition of optimal 2D platinum nanofilms remains difficult to achieve.

E-ALD of metal (or elemental) nanofilms was felt by the authors to not be possible, until the development of monolayer restricted galvanic displacement (MRGD) by Brankovic, Wang and Adzic [27-28] and Weaver [29]. MRGD has also been referred to as surface limited redox replacement (SLRR), and will be referred to as such here. It involves the electrodeposition of an atomic layer of a sacrificial element by UPD. That layer is then replaced by exposure to a solution containing precursor ions of a more noble element, at open circuit potential (OCP). The replacement reaction is limited by the amount of the sacrificial element, generally less then a monolayer. Deposition of single monolayers of Pt and Pd were some of the first examples of elements formed using SLRR [27-28], where atomic level control was revealed by scanning tunneling microscopy (STM) of the resulting Pt atomic layers. The Pt was deposited by exchange of a Cu UPD sacrificial layer, using a solution of Pt^{+4} ions. Weaver et al. [29], attempted to grow a multilayer Pt nanofilm by repeating SLRR, using Cu UPD as the sacrificial atomic layer.

They repeatedly applied the SLRR, up to eight times, in the first example of E-ALD of Pt. Deposits were performed using both $PtCl_4^{2-}$ and $PtCl_6^{2-}$ precursors. It is expected that twice as much Pt would be formed if Pt(II) were used rather than Pt(IV), given that each Cu UPD layer is a finite source of electrons. However, examination of the voltammetry recorded by Weaver et al. suggests that more then twice as much Pt was produced using Pt(II) rather then Pt(IV). Dimitrov et al. [30] developed a very simple "one-pot" solution method for SLRR, based on pulsed deposition. Adzic et al. studied Pt monolayer deposition on metals and alloy carbon-supported nanoparticles [31] as well as bimetallic systems consisting of transition metal monolayers (Ir, Ru, Rh, Re, Pt and Os) over Au, Pd or Pt layers, for oxygen reduction in fuel cells [32]. The author's group has studied the use of SLRR cycles for E-ALD formation of Cu [33], Pt [34-35] and Ru [36] nanofilm on Au substrates, as well as PtRu structured alloys (in preparation).

The driving force for SLRR is the potential difference between the sacrificial and the depositing metals, which will vary as the reaction progresses, dropping the sacrificial element's coverage and increasing the depositing element's. Changes in the solution composition will be a factor as well. Noble metal atomic layers have been deposited using Cu[27] [37] [31] [38] [39], Ni[40], and Pb [41] [30] [33, 36] [42] as sacrificial atomic layers.

The present study investigates E-ALD using SLRR cycles to form Pt nanofilms on Au on glass substrates. An automated electrochemical flow deposition system (Electrochemical ALD L.C.) was used to form the deposits. Use of Pb and Cu UPD for the formation of sacrificial metal layers for the deposition of Pt was compared and contrasted. In addition, Pt^{+2} and Pt^{+4} were compared as Pt precursors for the exchange.

Experimental

Electrodeposits were formed using an automated electrochemical flow cell system (Electrochemical ALD L.C.), similar to those previously described [43-44]. The system consisted of peristaltic pumps, Teflon solenoid valves, an electrochemical flow cell, and a potentiostat, all controlled using a program based on Labview (National Instruments). A gold wire, embedded in the Plexiglas flow cell face, was used as the auxiliary electrode and an Ag/AgCl (3M NaCl) (Bioanalytical Systems, Inc., West Lafayette, IN) was used as the reference. The flow cell (4X1X0.1cm^3) consisted of a planar substrate held away from a counter electrode by a 1mm thick silicone rubber gasket. The deposition area was 3.77 cm^2, and a solution flow rate of 9 ml/min was used.

Solutions used included 2mM $CuSO_4$, 1mM $PbClO_4$, 0.1mM K_2PtCl_4, 0.1mM H_2PtCl_6, 0.5M H_2SO_4 and 0.5M $NaClO_4$. The Cu solution were made with 0.5 M H_2SO_4 (pH 1.5), while the Pb solutions were made with 0.5 M $NaClO_4$ (pH 4.5). The Pt solutions were made with 50 mM $HClO_4$ (pH 1.3). The 0.5M H_2SO_4 and 0.5M $NaClO_4$ were used as blank solutions. All solutions were prepared using water from a nanopure water filtration system (Barnstead, Dubuque, IA) (18Ω), attached to the house DI water system. Chemicals were obtained from sigma-Aldrich or Alfa Aesar. Solution bottles were contained inside a Plexiglas box and were deaerated by bubbling with dry nitrogen, prior to deposition.

The Pt films were generally formed using 25 E-ALD cycles, on Au on glass substrates. The glass slides, after etching in dilute HF, were initially coated with a 5 nm adhesion layer of titanium, and then 300 nm of Au. The substrates were held at 280°C during deposition, and then annealed at 400°C for 12 hours, producing a prominent (111) growth mode. The gold substrates were cleaned in nitric acid for 2 minutes and then repeatedly cycled between 1400 mV and -200

mV in 0.5M sulfuric acid prior to deposition, at 10 mV/s. The Au substrates were characterized using cyclic voltammetry, as were the resulting Pt deposits. Cyclic voltammetry was performed in 0.5 M H_2SO_4.

The deposits were initially inspected using a Jenavert metallo-graphic optical microscope, at 1000X. Electron probe microanalysis (EPMA) was run using a Joel 8600 wavelength dispersive scanning electron microprobe, for elemental analysis. STM experiments were performed using a Nanoscope III (Digital instruments, Santa Barbara, CA) equipped with W tips, electrochemically etched (15V ac in 1M KOH) from 0.25 mm wires.

Results and Discussions

Cu Sacrificial Atomic Layers

Initial Pt deposits were formed using Cu UPD as the sacrificial metal, and Figure 1 is a cartoon depicting the E-ALD cycle. A graph showing current and potential as a function of time for two E-ALD cycles is shown in Figure 2, where the solid line is the current-time trace and the dashed is potential-time (the dashes do not show up well). The cycle consisted Cu^{2+} ion solution introduction into the cell, for 20 s at 100 mV, to form Cu UPD. The auxiliary electrode was then disconnected, allowing the cell to go to open circuit potential (OCP), and the solution was switched to $PtCl_4^{-2}$ ions, for the exchange. The OCP shifted positively over the next 70 sec, stabilizing at 650 mV over 100 s. The resulting deposit contained less than 2% Cu. Pt nanofilms were formed by repeating this cycle 25 times.

The charge associated with Cu UPD was monitored from cycle to cycle, and plotted in Figure 3 (squares). That charge grew dramatically for the first 10 cycles, and then reached steady state. Charges in Figure 3 are displayed in terms of ML of Cu, rather than coulombs. The

charge for the first cycle was equivalent to 0.74 ML, and grew to 5.92 ML by the 25th cycle. It had been assumed by the authors that the Cu sacrificial layer coverage would remain constant from cycle to cycle, as it was based on UPD (Figure 3). That the surface area of the Pt deposit increased by an order of magnitude over the first 10 cycles, suggested a dramatic increase in deposit area: in surface roughness. Quantification of the peak for Pt oxide reduction, from CVs of the resulting Pt surfaces in sulfuric acid, suggested an area close to 16.6 ML/cm^2 after only 25 Pt E-ALD cycles.

A second 25 cycle Pt nanofilm was formed using Cu UPD, this time using a Pt(IV) ion ($PtCl_6^{-2}$). The charges for Cu UPD are plotted in Figure 3 as the triangles, displaying a slope half that for the first 25 cycle deposit, which is consistent with it taking twice as many cycles with the Pt(IV) species at four electrons per Pt atom, compared two electrons for the Pt(II) species. The Cu UPD coverage increased from 0.77ML in the 1st cycle to a 6.18 ML in the 25th cycle. The resulting deposit surface area, from the Pt oxide reduction peak of a CV in sulfuric acid of the resulting deposit, was 10.5 ML. Again, this suggests a dramatic increase in surface roughening during deposition, and that significantly more Pt was deposited each cycle then desired. EPMA showed 27.7% Pt for the 25 cycle deposit using the Pt(II) precursor and 12.1% Pt for the 25 cycle deposit using the Pt(IV) precursor, with less than 2% Cu. The rest of the signal was Au%, from the substrate. Deposition of twice as much Pt using the Pt(II) precursor, relative to the Pt(IV) precursor was expected, given half as many electrons were required per Pt atom. However, experience with EPMA and the formation of nanofilms using E-ALD cycles suggested that a Pt coverage for a 25 cycle deposit should be in the range of 2-4 %, rather then 12-28%. The quantification program used with the microprobe is based on the assumption that the material is a homogenous alloy, rather then layers, so the atomic % reported here only provide a

relative measure of the amounts deposited. These results with Cu suggest 5 to 10 times too much deposition resulted, helping to account for the excessive surface areas measured using Pt oxide reduction, and the high values for Cu UPD (Figure 3).

Pb UPD sacrificial atomic layers

Pb UPD sacrificial layers were initially investigated to see how a larger driving force would influence the resulting Pt deposits. The formal potential for Pb, in these studies, was -430 mV, while that for the Cu was closer to -30 mV. The E^o for Pt is listed as about +1 V (vs. Ag/AgCl). A window opening CV study for a Au substrate in the Pb^{2+} solution was performed to progressively more negative potentials (Figure 4). The scans all started at 300 mV and displayed a slowly increasing charge to lower potentials, with a peak at −200 mV, consistent with Pb UPD on a Au(111) electrode [45][66]. Bulk Pb deposition began near −430 mV, and stripped in a sharp oxidation peak at -400 mV, in the subsequent positive going scan. There was also a broad oxidation peak around −300 mV, corresponding to dealloying of Pb from the Au substrate [45]. Pb UPD stripping consisted of an oxidation feature at -150 mV, suggesting the presences of a couple of peaks. Based on the CVs in Figure 4, -400mV was selected for deposition of the sacrificial Pb atomic layers, which resulted in about 0.5 ML on both on Au and Pt. In most E-ALD cycle, atomic layers with coverages up to about a ML tend to result in good deposits. That the coverage was not 1 ML was not a problem, few UPD deposit result in 1 ML. However, experience with E-ALD in general has shown that less then 1 ML/cycle tends to result in deposits with good stoichiometry, structure and morphology, while more then a 1 ML/cycle tends to result in significant surface roughening and 3D growth [33].

Pt(II) Precursors

Twenty five Pt cycle nanofilms were formed using Pb UPD sacrificial atomic layers and the Pt(II) precursor solution ($PtCl_4^{2-}$). Figure 5 displays current-time and potential-time traces for two cycles. Figure 5 should be compared with Figure 2, where Cu UPD sacrificial layers were used, and the exchange was give 180 seconds, compared with the 10-15 seconds with the Pb UPD. An OCP replacement (exchange) time of 60 s was used by Adzic et al. [27] in their early study, though they were not repeating the cycle. Experience in this group has shown that the time needed for exchange can vary considerably from one system to the next, as exemplified by Pt[37] vs. Ru[36] vs. Cu[33].

For the deposits where Cu UPD was used for the sacrificial layer a set exchange time was applied (180 s). For the Pt deposits where Pb UPD was used, instead of a set time, cycles were programmed using a "stop potential". Previous E-ALD studies using Pb sacrificial layers suggested that above 0 mV there was essentially no Pb layer left on the surface, and the exchange was completed. Thus, in the present study using Pb, the control program was set to monitor the OCP during exchange, and to rinse the cell with blank when it reached 0 mV, referred to hear as the stop potential. Using a stop potential of 0 mV, the Pt precursor was rinsed from the cell with blank for 11 s. For the first 6 s the cell remained at OCP (generally continuing to rise), so that all Pt precursor ions were removed from the cell and would not be electrodeposited when a potential was applied. So, after 6 s of rinsing with blank at OCP, 5 more seconds of blank rinsing was performed at a controlled potential of 100 mV. It was assumed that any last traces of Pb would strip from the surface at 100 mV. The dashed curve in Figure 5 (the potential-time trace) shows the application of the stop potential step: 6 s flush once OCP = 0 mV has been reached, and a step to 100 mV and 5 s more flushing. Note, in Figure 5,

the OCP had exceeded 100 mV before the switch from OCP to 100 mV, so the potential actually dropped to 100 mV. Draw a line at 0 mV in figure 5, so you can see where we reach 0 V.

Figure 6 displays the Pb UPD coverages formed for every cycle in a 25 cycle deposit, and should be compared with Figure 3, where Cu UPD was used and no stop potential. In Figure 6 there was essentially no change from cycle to cycle for Pb UPD, about 0.54 ML, while in Figure 3, the Cu coverage increased dramatically over the first 10-15 cycles. This suggests that the surface area remained uniform when Pb UPD and the stop potential were used.

The resulting Pt nanofilms were characterized using CVs in 0.5 M sulfuric acid at a scan rate of 10 mV/s. Figure 7 is the first CV after deposition, and shows little of the expected hydrogen waves, suggesting contamination. Pt is notoriously difficult to keep clean {Hubbard, 1978 #659}, as it strongly adsorbs organic molecules containing nearly any functional group [46]. The best Pt CVs are run under extremely stringent conditions, using unstirred solutions in ultra clean Pyrex cells {Clavilier, 1980 #15019; Clavilier, 1992 #14970; 2004 #14948; Zolfaghari, 1997 #4873}. In the present studies, the electrochemical flow cell was constructed using Plexi Glass, and solution was flowed over the deposit surface for most of the cycle, so some contamination was expected. To decrease contamination, the cells could be made out of Pyrex glass and everything could be kept scrupulously clean. Alternatively, the Pt surface could be protected with a surfactant of some kind, something that can prevent contamination of the Pt surface while allowing the chemistry to continue. It is understood by practitioners of Pt single crystal electrochemistry that experimental times must be minimized to keep the Pt clean, so it is not anticipated that Pyrex cell and exhaustive cleaning will be sufficient to keep an unprotected Pt film clean during 25 E-ALD cycles. On the other hand, initial attempts at using surfactants such as I atoms and CO look promising [37, 47]. The first studies of Pt deposition using SLRR

by this group involved an atomic layer of I atoms to protect the surface [37]. More recently, some work using CO has been performed, and will be the subject of a subsequent report.

The deposit in Figure 7 was cleaned by cycling between 1400 mV and -160 mV and the steady state voltammetry in Figure 8 was obtained. A sequence of deposits formed with increasing numbers of cycles is displayed in Figure 9. The surface areas were determined using charges for the hydrogen waves and for Pt oxide reduction, for each deposit, and the results are shown in Figure 10. The coverages were based on the assumption that the surface resembled a Pt(111), and one electron was needed to deposit one hydrogen atom on each surface Pt atom, and two electrons were required for oxide reduction. Both measurements suggest an increase in surface area with the cycle #, though much less than observed for deposits formed using Cu UPD (Figure 3). Figure 10, like Figure 3, shows coverage increases for the first 15 cycles, and then a relative plateau. EPMA showed 2.7 atomic % Pt in the 25 cycle film, about what would be expected using a Pt(II) precursor, in contrast to the 27.8% reported for 25 cycle deposits using Cu UPD.

It is of note that the CVs in Figures 8 and 9 show oxide reduction peaks for both Pt (530 mV) and Au (1000 mV). The extent of the Au oxide reduction peak is evidently a function of the number of cycles performed, as it was for Weaver [29]. Those results raise the question of whether the oxide ratio is a measure of the ratio of metals on the surface? Ideally, for a ½ ML sacrificial layer of Pb each cycle, and 100% exchange efficiency for Pt(II), 12.5 monolayers of Pt should result, or a little over 2 nm. However, experience has shown that exchange is seldom 100%. In addition, if Pt(IV) were to be used, it would be closer to 1 nm. So the Pt deposits are thin. It is clear that some of the surface is contaminated (Figure 7). It is anticipated that no Pt would deposit on contaminated areas, so those areas would be even thinner.

The extent of the Au oxide reduction peak has been shown to also be a function of the positive scan potential limit (Figure 11). Figure 11 shows three CVs for a 25 cycle Pt deposit. The positive limit of the first cycle was 1200 mV and no Au oxide reduction at 1000 mV was evident. In the second cycle, the scan went to 1400 mV, and a significant Au oxide reduction peak at 1000 mV was evident. The third scan was again to 1200 mV, and again no Au oxide reduction was evident. Figure 12 a CV to 1200 mV of a clean Au electrode, and a significant Au reduction feature is evident. Figures 11 and 12 suggest that there was no Au present at the surface after 25 cycles, or a peak at 1000 mV for Au oxide reduction would have been present in scans to 1200 mV. On the other hand, that the 1000 mV reduction peak was present after scans to 1400 mV is consistent with surface roughening, known to occur with Pt during oxidation {Wagner, 1983 #14946; You, 1994 #15820; Itaya, 1990 #17940}. These results suggest that more than the top metallic monolayer is affected by oxidation to 1400 mV and some Au atoms near the surface become oxidized as well, possibly in the second or third layer, below the surface. Some may have been present near the surface because of contamination. Au is not easily contaminated, however, Pt is. When the surface was oxidized, the contamination would be removed, and the top few layers of metal would oxidize, including some shallow Au atoms.

Overall, comparing the surface areas and absolute coverages of Pt films formed using Pb and those formed using Cu, it appears there may have been more factors contributing to the a difference then just changing the element used to form the sacrificial layers. Other known differences include longer replacement times and higher OCP with the Cu studies: a set 180 s for the exchange, and OCP exceeding 650 mV by the end (Figure 2). While deposits made using Pb UPD and a stop potential of 0 mV (the dashed curve in Figure 5) resulting in maximum OCP of less then 200 mV.

To investigate the dependence of the deposit thickness on the OCP achieved during the exchange, and the length of time allowed for exchange, a deposit was made using Pb UPD, the Pt(II) precursor, and no stop potential step. Instead, the exchange was allowed to go for 60 s each cycle. The resulting Pt film was much thicker than where a 0 mV stop potential was used (19 % Pt by EPMA), suggesting the issue was not the use of Pb UPD instead of Cu, but more to do with use of higher potentials (570 mV was obtained), and possibly longer times.

To further investigate the importance of the exchange time and the maximum OCP, a sequence of deposits were formed using successively higher stop potentials (0, 100, 200 and 300 mV) in combination with the Pt(II) precursor. The resulting surface areas were plotted in Figure 13, as a function of the stop potential used. Use of 0 or 100 mV resulted in about 1.8 ML, while higher stop potentials produced significant increases. Figure 14 displays the corresponding Pt atomic % from EPMA, with both the Pt(II) and Pt(IV) precursors. Using 300 mV as a stop potential resulted in increased amounts of Pt deposited for both precursors, but with significantly higher coverages using Pt(II). No Pb was indicated to be present from EPMA, even when 0 mV was used as the stop potential. It does not appear that the presence of Pb was responsible for the increases in deposited Pt at higher potentials (Figure 14), as it has all been removed by 0 mV. The growth of thicker deposits at the higher potentials appears independent of the sacrificial element, as similar trends were observed using both Pb and Cu UPD sacrificial layers. Similar trends were observed using Pt(IV) precursors as well (Figure 14), though usually with lower coverages (Figure 15).

Initial thoughts in this group were that the sacrificial element or the Pt precursor oxidation state was a direct factor in the formation of the excessively thick and rough 25 cycle deposits. Given the above data, neither factor appeared controlling. The observations were that

the coverages increase the longer the deposit was left at OCP and/or the higher the OCP attained. The two are linked, in that longer times at OCP tended to result in higher potentials. If it were just the length of time, it would suggest that there is a reactant in solution that slowly reduces Pt onto the surface. It was thought that Pt(II) might result in disproportionation, where the same ion acts both as the oxidizing agent and a reducing agent, forming elemental Pt and Pt(IV). However, Pt(IV) also resulted in an increase in coverage with time, though not as dramatic as with Pt(II). If the thickness was a function of how high the OCP achieved was, it initially appeared counter intuitive from the point of view of reducing Pt onto the promote anion adsorption. Both Pt precursors were present in solution as anions: $PtCl_4^{2-}$ and PtCl62-. I think uosaki showed that there is an adsorbed layer of these pt precurors at positive potentials. Make sure you check to see what literature could have predicted this.

The cycle was designed to rinse the cell for 11 sec before the potential was set negative to deposit the sacrificial layer, which appeared to be sufficient to exchange solutions and remove weakly adsorbed species. The 11 second corresponds to flushing 3-4 volumes of blank through the cell. However, if a species was more strongly associated with the deposit, it might not have been rinsed from the cell in 11 s, and might be reduced when the potential was shifted negative to form the sacrificial layer (Figures 2 and 5). If that were the case, then the current passed during Pb UPD should show be in excess, which was the case when higher OCPs were achieved. The charge had four components: DL charging with the change in potential, hydrogen evolution on the Pt surface when Pb UPD was initiated, Pb UPD, and reduction of any adsorbed species. To try and separate the contributions, the controlled potential part of the cycle was split into two parts. Initially, when the potential was set at -400 mV and no Pb^{2+} was introduced, just blank. That allowed all charging current to pass and all adsorbed species to be reduced. After 10 s at -

400 mV the Pb^{2+} solution was introduced, and the charge for Pb UPD was determined separately (Figure 16A). Figure 16A clearly shows large currents when the potential is switched, where on a small fraction can be attributed to charging and hydrogen evolution. When the Pb^{2+} solution is then introduced, UPD is observed, and is barely noticeable on the same scale as the initial charge for reduction of the adsorbed species. To prove that the charge was due to reduction of an adsorbed species, the cycle was repeated with 60s rinse (Figure 16B), rather then 11s. The current was dramatically reduced, compared with Figure 16A, confirming that the extra charge was the result of adsorption of anionic precursors at high potentials, that were not sufficiently rinsed from the cell before controlled potential deposition of Cu or Pb UPD. The result was deposition of excess Pt, and roughening of the deposit surface.

Figure 17 displays 200nm and 100nm STM image of a 25 cycle Pt film formed using a Pt(IV) precursor did you use the right program to avoid excess Pt? , onto template stripped Au ref template stripped Au. The E-ALD cycle for Pt included a 0 mV stop potential how about the rinsing? . The STM image showed that Pt films were deposited with a mean roughness of about 1nm with a particle size of about 5-8nm. Does it need to be in the paper?

Conclusions

Initial studies of the deposition of Pt films by E-ALD have been reported. EPMA confirmed the formation of Pt films, and the absence of the sacrificial elements Cu or Pb. The SLRR were based on the exchange of Pt for a sacrificial atomic layer at open circuit. CVs of Pt deposits between +1400 mV and -160 mV were performed to clean the films, which showed the expected Pt features. In addition, a peak for Au oxide reduction was evident, even though the Au surface should have been covered with Pt. If the voltammetry was limited to potentials below 1200 mV,

no Au oxide reduction was evident, indicating that the Au was not the top layer, but was brought to the surface during oxidations up to 1400 mV.

Initial Pt deposits, formed using Cu or Pb UPD sacrificial layers, were an order of magnitude thicker then expected, for a 25 cycle E-ALD deposit. Reasons for the excess Pt were investigated, and appeared related to how positive the OCP drifted during the exchange step. To limit the OCP, a "stop potential" was used, where once the potential exceeded the stop potential, the Pt precursor was flushed from the cell, preventing further deposition. It was, however, found that insufficient rinsing was being used, as at positive potentials, anionic Pt precursors were adsorbed to the deposit, and survived the brief rinse applied. By increasing the rinse times, complete removal of the Pt precursor was achieved, preventing the build up of Pt in excess of that resulting from replacement of the sacrificial atomic layers.

Acknowledgments

Support from the National Science foundation, Division of Materials Research, and some initial support from the Bio Fuels program of the DOE is gratefully acknowledged.

References

1. Nishikawa, K., M. Yamamoto, and T. Kingetsu, *Dependence of electrical resistivity on surface topography of MBE-grown Pt film.* Applied Surface Science, 1997. **113-114**: p. 412-416.
2. Kato, T., et al., *Magnetic anisotropy of MBE grown MnPt3 and CrPt3 ordered alloy films.* Journal of Magnetism and Magnetic Materials, 2004. **272-276**(Part 2): p. 778-779.
3. Makarov, D., et al., *Growth of Pt thin films on WSe2.* Surface Science, 2007. **601**(9): p. 2032-2037.
4. Garcia, J.R.V. and T. Goto, *Chemical Vapor Deposition of Iridium, Platinum, Rhodium and Palladium.* MATERIALS TRANSACTIONS, 2003. **44**(9): p. 1717-1728.
5. Huang, S.-F., et al., *Preparation of Pt-Ru Alloyed Thin Films Using a Single-Source CVD Precursor.* Chemical Vapor Deposition, 2003. **9**(3): p. 157-161.
6. Mattox, D.M., *Physical Sputtering and Sputter Deposition (Sputtering),* in *Handbook of Physical Vapor Deposition (PVD) Processing (Second Edition)*. 2010, William Andrew Publishing: Boston. p. 237-286.
7. Kwon, J.-H. and S.-G. Yoon, *Preparation of Pt thin films deposited by metalorganic chemical vapor deposition for ferroelectric thin films.* Thin Solid Films, 1997. **303**(1-2): p. 136-142.
8. Valet, O., et al., *Study of platinum thin films deposited by MOCVD as electrodes for oxide applications.* Microelectronic Engineering, 2002. **64**(1-4): p. 457-463.
9. Goswami, J., et al., *MOCVD of Platinum Films from (CH3)3CH3CpPt and Pt(acac)2: Nanostructure, Conformality, and Electrical Resistivity.* Chemical Vapor Deposition, 2003. **9**(4): p. 213-220.

10. Duarte, M.M.E., et al., *Platinum particles electrodeposition on carbon substrates.* Electrochemistry Communications, 2006. **8**(1): p. 159-164.

11. Lu, G. and G. Zangari, *Electrodeposition of Platinum on Highly Oriented Pyrolytic Graphite. Part I: Electrochemical Characterization.* The Journal of Physical Chemistry B, 2005. **109**(16): p. 7998-8007.

12. Lu, G. and G. Zangari, *Electrodeposition of platinum nanoparticles on highly oriented pyrolitic graphite: Part II: Morphological characterization by atomic force microscopy.* Electrochimica Acta, 2006. **51**(12): p. 2531-2538.

13. Choi, K.H., H.S. Kim, and T.H. Lee, *Electrode fabrication for proton exchange membrane fuel cells by pulse electrodeposition.* Journal of Power Sources, 1998. **75**(2): p. 230-235.

14. Itaya, K., H. Takahashi, and I. Uchida, *Electrodeposition of Pt ultramicroparticles in Nafion films on glassy carbon electrodes.* Journal of Electroanalytical Chemistry, 1986. **208**(2): p. 373-382.

15. Saitou, M., *Electrochemical characterization of platinum black electrodeposited from electrolyte including lead acetate trihydrate.* Surface and Coatings Technology, 2006. **201**(6): p. 3611-3614.

16. Zhou, L., Y.F. Cheng, and M. Amrein, *Fabrication by electrolytic deposition of platinum black electrocatalyst for oxidation of ammonia in alkaline solution.* Journal of Power Sources, 2008. **177**(1): p. 50-55.

17. Gregory, B.W. and J.L. Stickney, *Electrochemical atomic layer epitaxy (ECALE).* Journal of Electroanalytical Chemistry, 1991. **300**(1-2): p. 543-561.

18. Gregory, B.W., D.W. Suggs, and J.L. Stickney, *Conditions for the deposition of cadmium telluride (CdTe) by electrochemical atomic layer epitaxy.* Journal of the Electrochemical Society, 1991. **138**(5): p. 1279-84.

19. Kolb, D.M., *Physical and Electrochemcial Properties of Metal Monolayers on Metallic Substrates*, in *Advances in Electrochemistry and Electrochemical Engineering*, H. Gerischer and C.W. Tobias, Editors. 1978, John Wiley: New York. p. 125.

20. Adzic, R.R., *Electrocatalytic Properties of the Surfaces Modified by Foreign Metal Ad Atoms*, in *Advances in Electrochemistry and Electrochemical Engineering*, H. Gerishcher and C.W. Tobias, Editors. 1984, Wiley-Interscience: New York. p. 159.

21. Gewirth, A.A. and B.K. Niece, *Electrochemical applications of in situ scanning probe microscopy.* Chemical Reviews, 1997. **97**(4): p. 1129-1162.

22. Herrero, E., L.J. Buller, and H.D. Abruna, *Underpotential Deposition at Single Crystal Surfaces of Au, Pt, Ag and Other Materials.* Chemical Reviews, 2001. **101**(7): p. 1897-1930.

23. Bauer, E. and J.H. van der Merwe, *Structure and growth of crystalline superlattices: From monolayer to superlattice.* Physical Review B, 1986. **33**(Copyright (C) 2009 The American Physical Society): p. 3657.

24. Uosaki, K., et al., *Electrochemical Epitaxial Growth of a Pt(111) Phase on an Au(111) Electrode.* The Journal of Physical Chemistry B, 1997. **101**(38): p. 7566-7572.

25. Waibel, H.F., et al., *Initial stages of Pt deposition on Au(111) and Au(100).* Electrochimica Acta, 2002. **47**(9): p. 1461-1467.

26. Nagahara, Y., et al., *In Situ Scanning Tunneling Microscopy Examination of Molecular Adlayers of Haloplatinate Complexes and Electrochemically Produced Platinum*

Nanoparticles on Au(111). The Journal of Physical Chemistry B, 2004. **108**(10): p. 3224-3230.

27. Brankovic, S.R., J.X. Wang, and R.R. Adzic, *Metal monolayer deposition by replacement of metal adlayers on electrode surfaces.* Surface Science, 2001. **474**(1-3): p. L173-L179.
28. Brankovic, S.R., J.X. Wang, and R.R. Adzic, *New methods of controlled monolayer-to-multilayer deposition of Pt for designing electrocatalysts at an atomic level.* Journal of the Serbian Chemical Society, 2001. **66**(11-12): p. 887-898.
29. Mrozek, M.F., Y. Xie, and M.J. Weaver, *Surface-Enhanced Raman Scattering on Uniform Platinum-Group Overlayers: Preparation by Redox Replacement of Underpotential-Deposited Metals on Gold.* Analytical Chemistry, 2001. **73**(24): p. 5953-5960.
30. Viyannalage, L.T., R. Vasilic, and N. Dimitrov, *Epitaxial growth of Cu on Au(111) and Ag(111) by surface limited redox replacement - An electrochemical and STM study.* Journal of Physical Chemistry C, 2007. **111**(10): p. 4036-4041.
31. Adzic, R.R., et al., *Platinum Monolayer Fuel Cell Electrocatalysts.* Topics in Catalysis, 2007. **46**(3/4): p. 249-262.
32. Zhou, W.P., et al., *Improving Electrocatalysts for O-2 Reduction by Fine-Tuning the Pt-Support Interaction: Pt Monolayer on the Surfaces of a Pd3Fe(111) Single-Crystal Alloy.* Journal of the American Chemical Society, 2009. **131**(35): p. 12755-12762.
33. Thambidurai, C., et al., *Copper Nanofilm Formation by Electrochemical ALD.* Journal of the Electrochemical Society, 2009. **156**(8): p. D261-D268.

34. Kim, J.Y., Y.G. Kim, and J.L. Stickney, *Copper nanofilm formation by electrochemical atomic layer deposition - Ultrahigh-vacuum electrochemical and in situ STM studies.* Journal of the Electrochemical Society, 2007. **154**(4): p. D260-D266.

35. Kim, J.Y., Y.G. Kim, and J.L. Stickney, *Cu nanofilm formation by electrochemical atomic layer deposition (ALD) in the presence of chloride ions.* Journal of Electroanalytical Chemistry, 2008. **621**(2): p. 205-213.

36. Thambidurai, C., Y.-G. Kim, and J.L. Stickney, *Electrodeposition of Ru by atomic layer deposition (ALD).* Electrochimica Acta, 2008. **53**(21): p. 6157-6164.

37. Kim, Y.-G., et al., *Platinum Nanofilm Formation by EC-ALE via Redox Replacement of UPD Copper: Studies Using in-Situ Scanning Tunneling Microscopy.* The Journal of Physical Chemistry B, 2006. **110**(36): p. 17998-18006.

38. Yu, Y.L., et al., *The study of Pt@Au electrocatalyst based on Cu underpotential deposition and Pt redox replacement.* Electrochimica Acta, 2009. **54**(11): p. 3092-3097.

39. Qu, D., C.W.J. Lee, and K. Uosaki, *Pt Nano-Layer Formation by Redox Replacement of Cu Adlayer on Au(111) Surface.* Bulletin of the Korean Chemical Society, 2009. **30**(12): p. 2875-2876.

40. Rettew, R.E., J.W. Guthrie, and F.M. Alamgir, *Layer-by-Layer Pt Growth on Polycrystalline Au: Surface-Limited Redox Replacement of Overpotentially Deposited Ni Monolayers.* Journal of the Electrochemical Society, 2009. **156**(11): p. D513-D516.

41. Vasilic, R., L.T. Viyannalage, and N. Dimitrov, *Epitaxial growth of Ag on Au(111) by galvanic displacement of Pb and Tl monolayers.* Journal of the Electrochemical Society, 2006. **153**(9): p. C648-C655.

42. Jayaraju, N., D. Vairavapandian, and J.L. Stickney, *Electrochemical Atomic Layer Deposition (ALD) of Pt Nanofilms.* In Prep, 2010.

43. Stickney, J.L., *Electrochemical Atomic Layer Epitaxy (EC-ALE): Nanoscale Control in the Electrodeposition of Compound Semiconductors*, in *Advances in Electrochemical Science and Engineering*, R.C. Alkire and D.M. Kolb, Editors. 2002, Wiley-VCH: Weinheim. p. 1-105.

44. Mathe, M.K., et al., *Formation of HgSe Thin Films Using Electrochemical Atomic Layer Epitaxy.* Journal of the Electrochemical Society, 2005. **152**(11): p. C751-C755.

45. Green, M.P., et al., *Insitu Scanning Tunneling Microscopy Studies of the Underpotential Deposition of Lead on Au(111).* Journal of Physical Chemistry, 1989. **93**(6): p. 2181-2184.

46. Stickney, J.L., et al., *A survey of factors influencing the stability of organic functional groups attached to platinum electrodes.* JEC, 1981. **125**: p. 73.

47. Strbac, S., et al., *In situ STM imaging of spontaneously deposited ruthenium on Au(111).* Surface Science, 2002. **517**(1-3): p. 207-218.

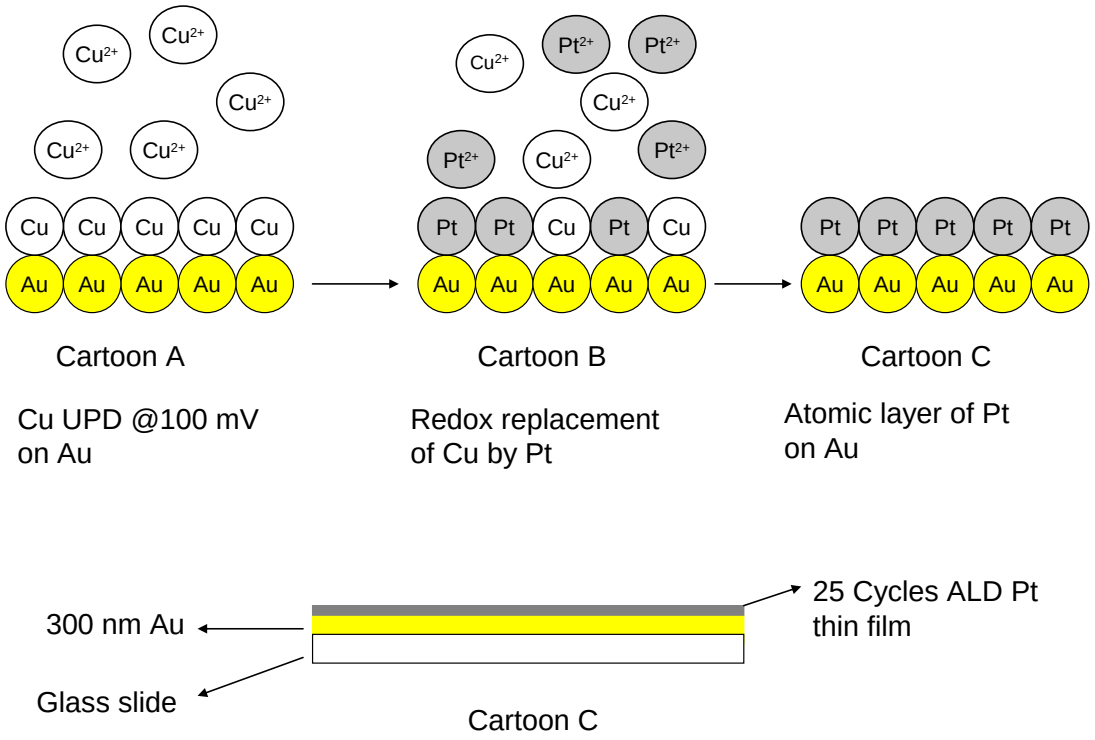

Figure 2.1 Electrochemical ALD cycle cartoon for Pt film deposition on Au substrates.

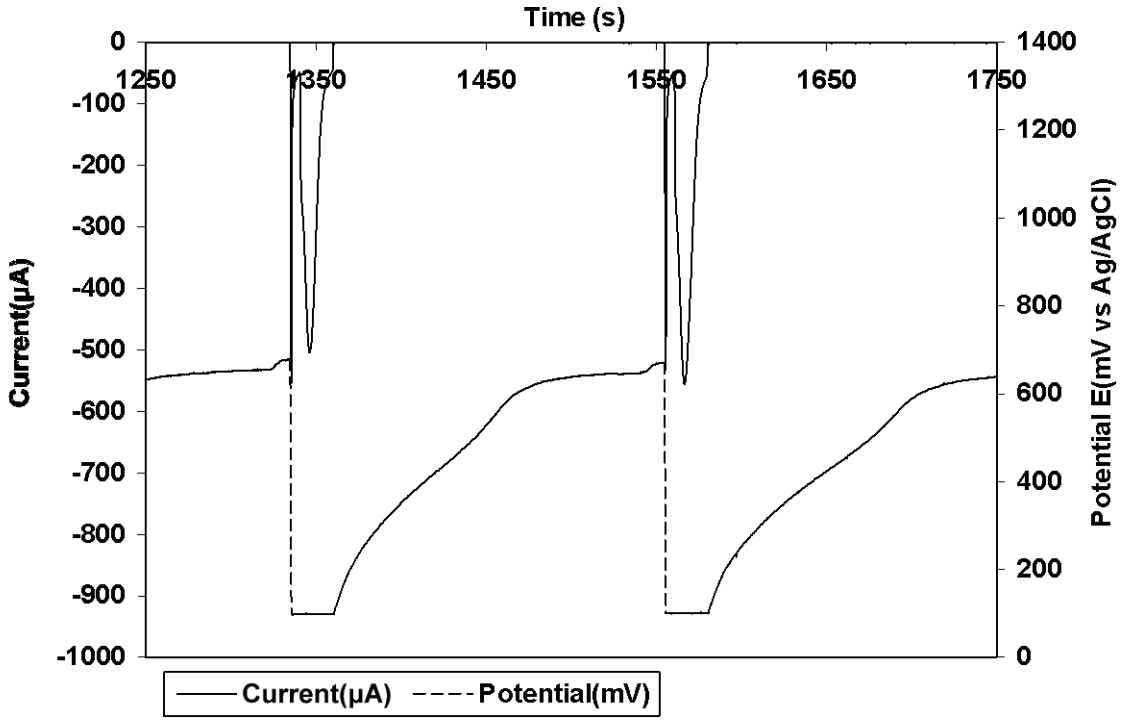

Figure 2.2: Time-Potential-Current graph illustrating one Pt ALD cycle. Cu is deposited at +100mV and is replaced by Pt^{+2} ions at open circuit.

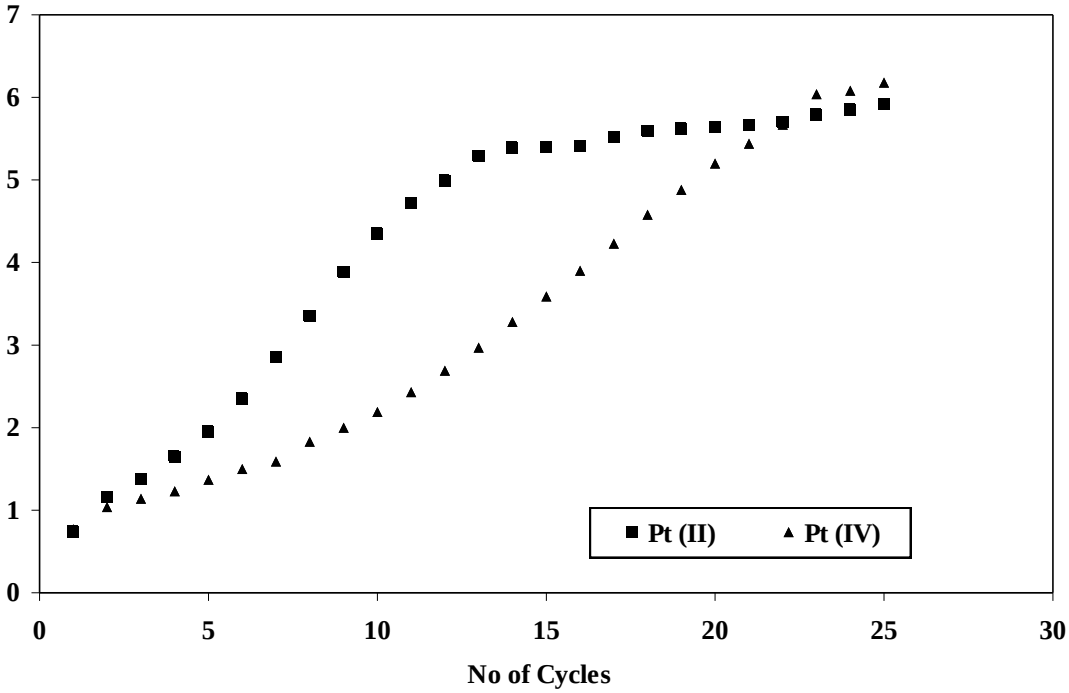

Figure 2.3 Cu deposition charge as a function of Pt deposition cycles using Pt^{+2} and Pt^{+4}.

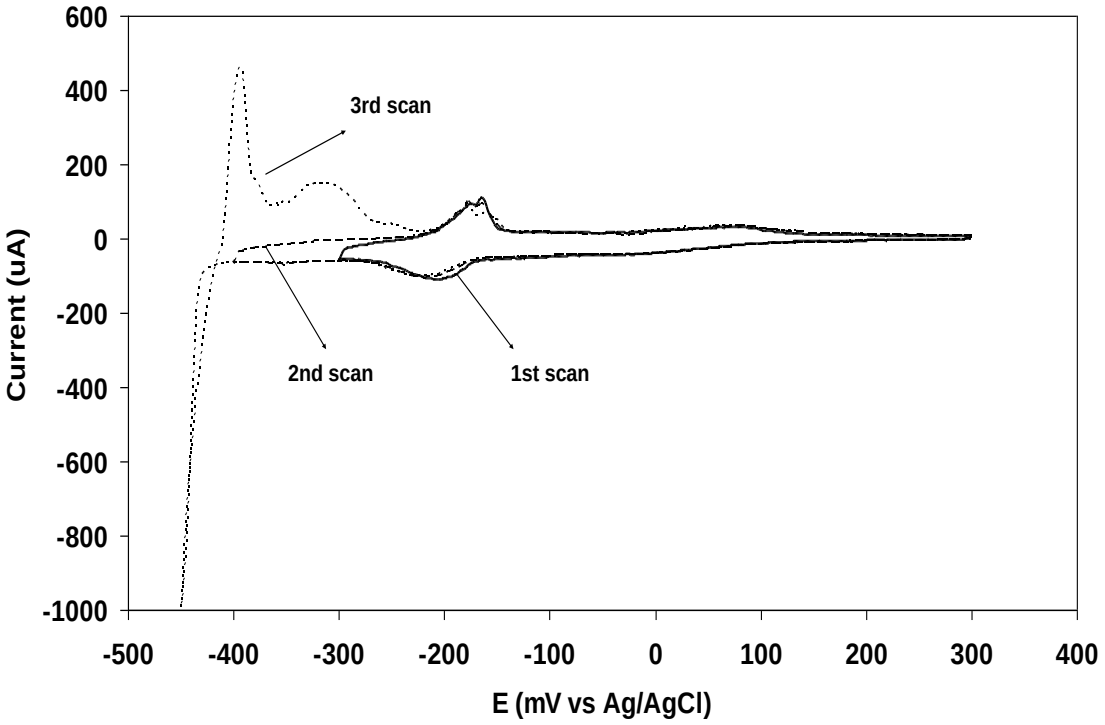

Figure 2.4. Cyclic Voltammogram for Pb UPD on Au in 1mM $Pb(ClO_4)_2$ in 0.5M $NaClO_4$; Scan rate 10mV/s.

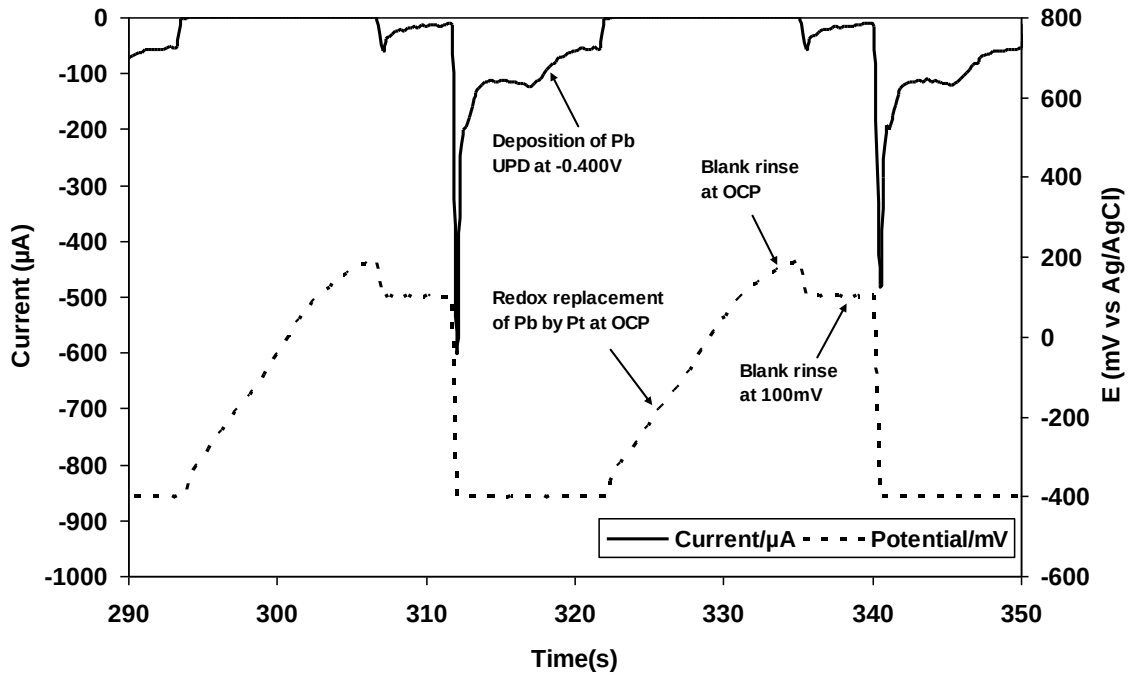

Figure 2.5. Time-Current- Potential graph illustrating one Pt ALD cycle. Pb is deposited at -400mV and is replaced by $PtCl_4^{2-}$ ions at open circuit.

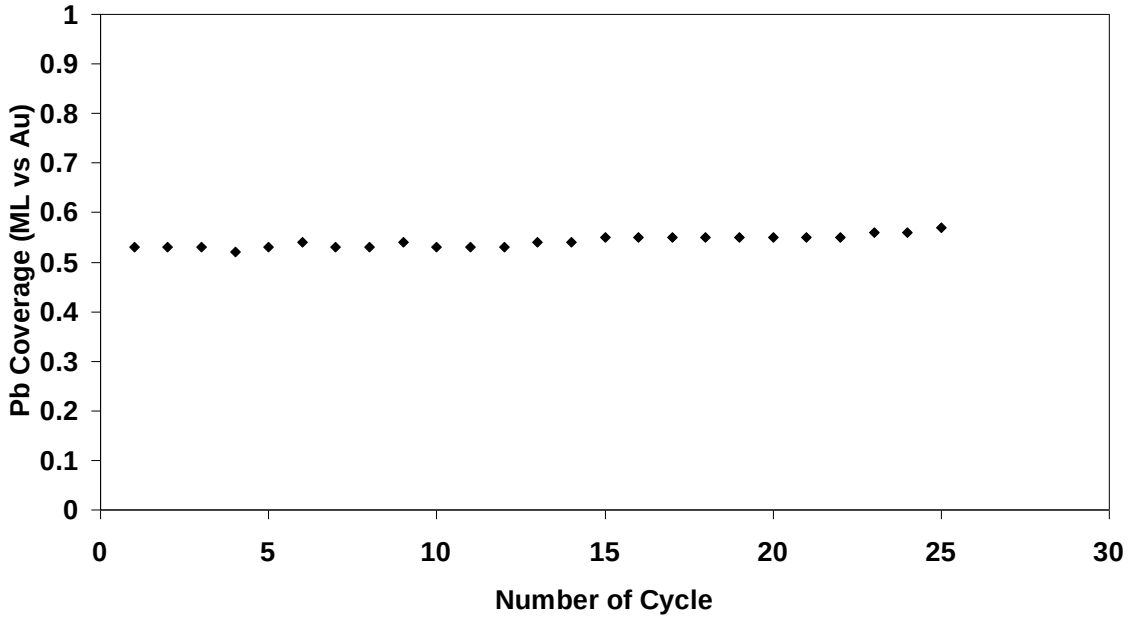

Figure 2.6. Pb coverage as a function of deposition cycles.

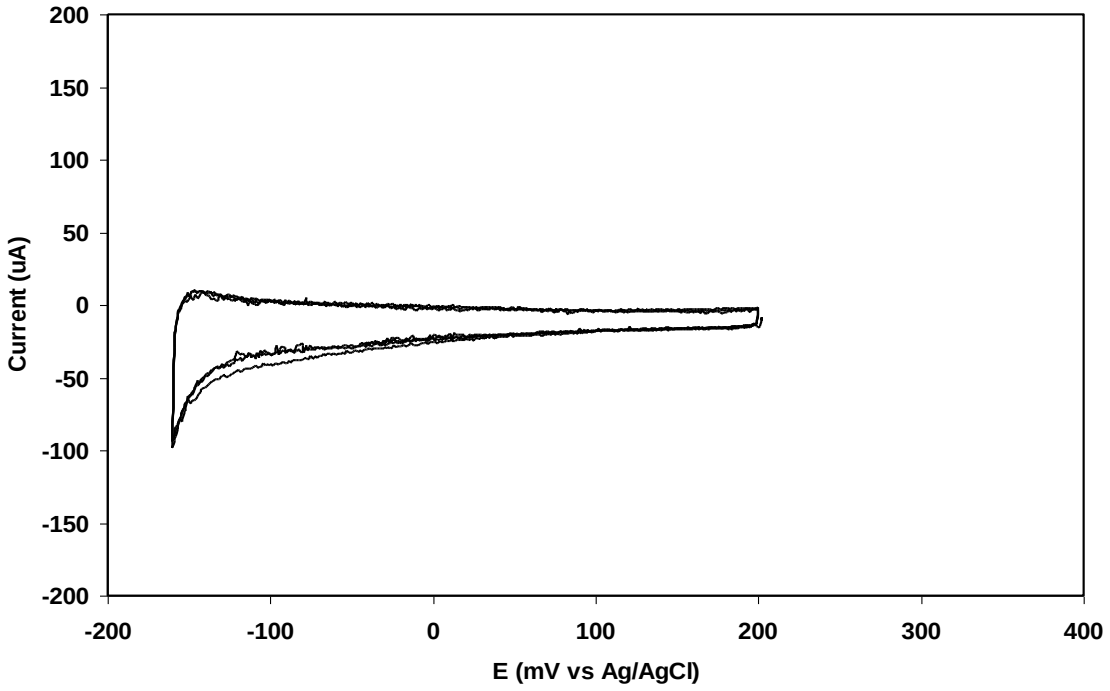

Figure 2.7. Cyclic voltammetry of 25 cycles Pt film immediately after deposition in 0.5M H_2SO_4; Scan rate: 10mV/s. Pt was deposited using $PtCl_4^{2-}$ ions.

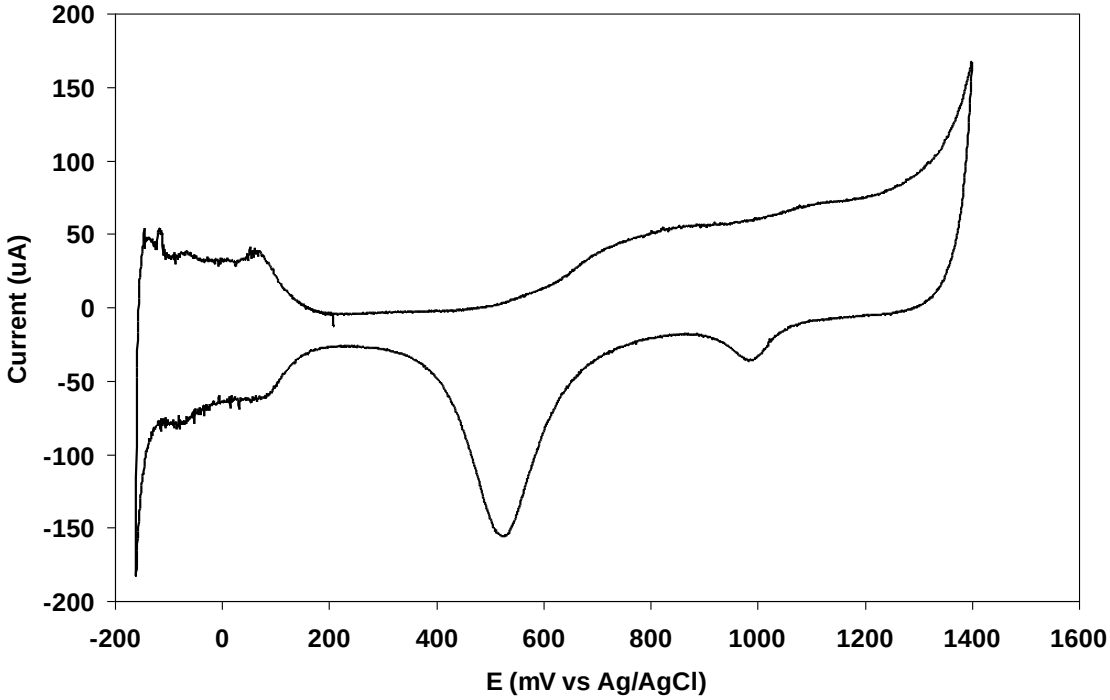

Figure 2.8. Cyclic voltammetry of 25 cycles Pt film in 0.5M H_2SO_4 by scanning between 1.400V and -0.160V; Scan rate: 10mV/s. Pt was deposited using $PtCl_4^{2-}$ ions.

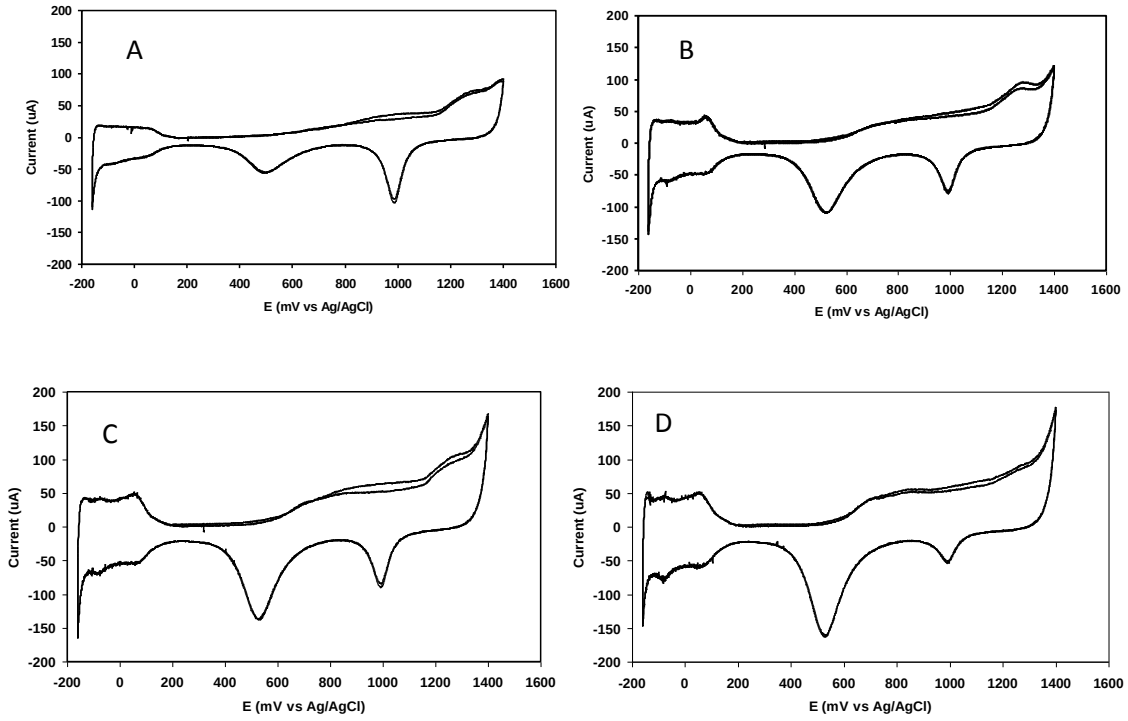

Figure 2.9. Cyclic voltammetry of (A) 5 cycles (B) 10 cycles (C) 15 cycles and (D) 20 cycles Pt film in 0.5M H_2SO_4 by scanning between 1.400V and -0.160V; Scan rate: 10mV/s. Pt was deposited using $PtCl_4^{2-}$ ions.

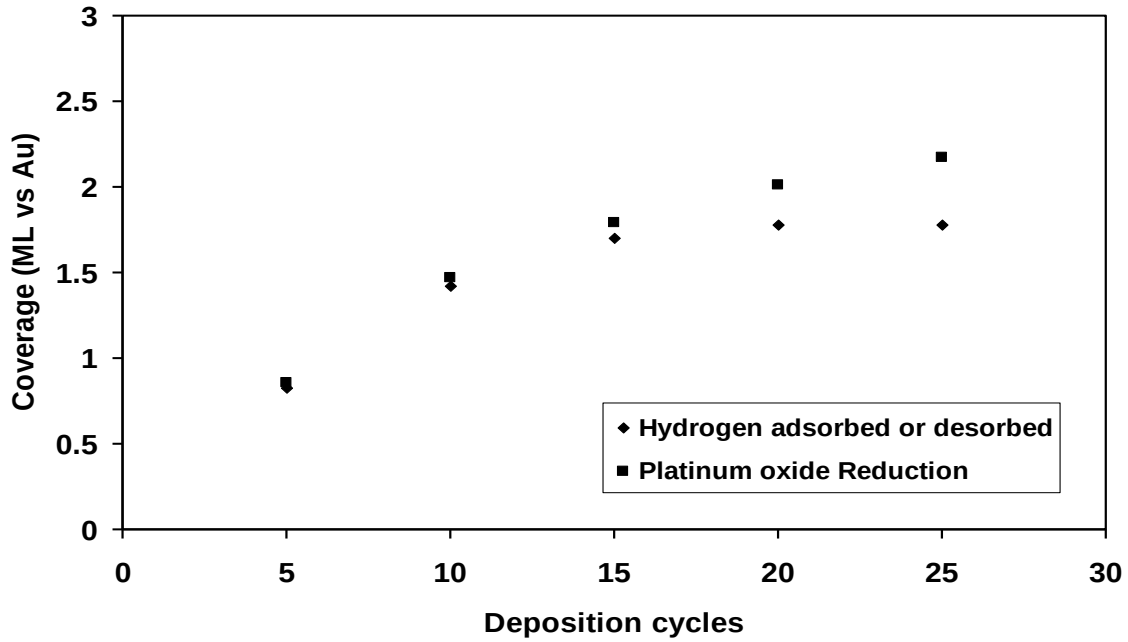

Figure 2.10. Surface area (ML vs. Au) of Pt film calculated from Pt oxide reduction charge and Hydrogen adsorption and desorption charge. Pt was deposited using $PtCl_4^{2-}$ ions.

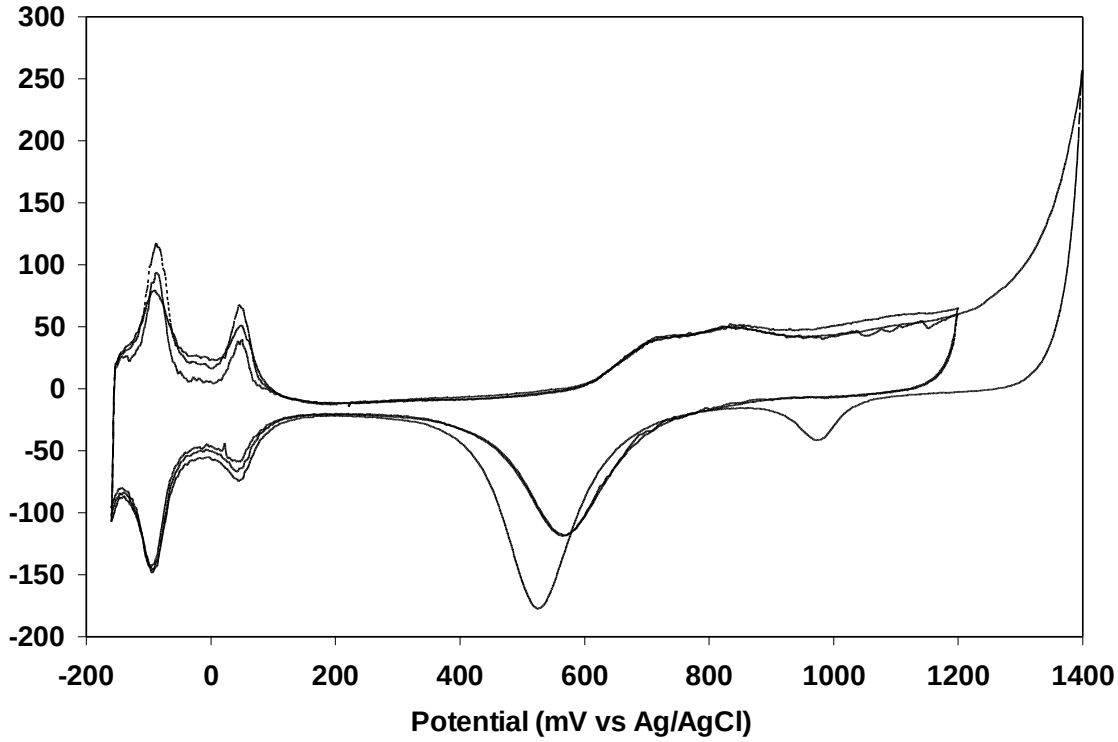

Figure 2.11. Three CVs of a 25 cycle Pt deposit in 0.5M H_2SO_4. The positive limit of Scan 1 and scan 3 was +1200mV while scan 2 was +1400mV. Scan rate: 10mV/s.

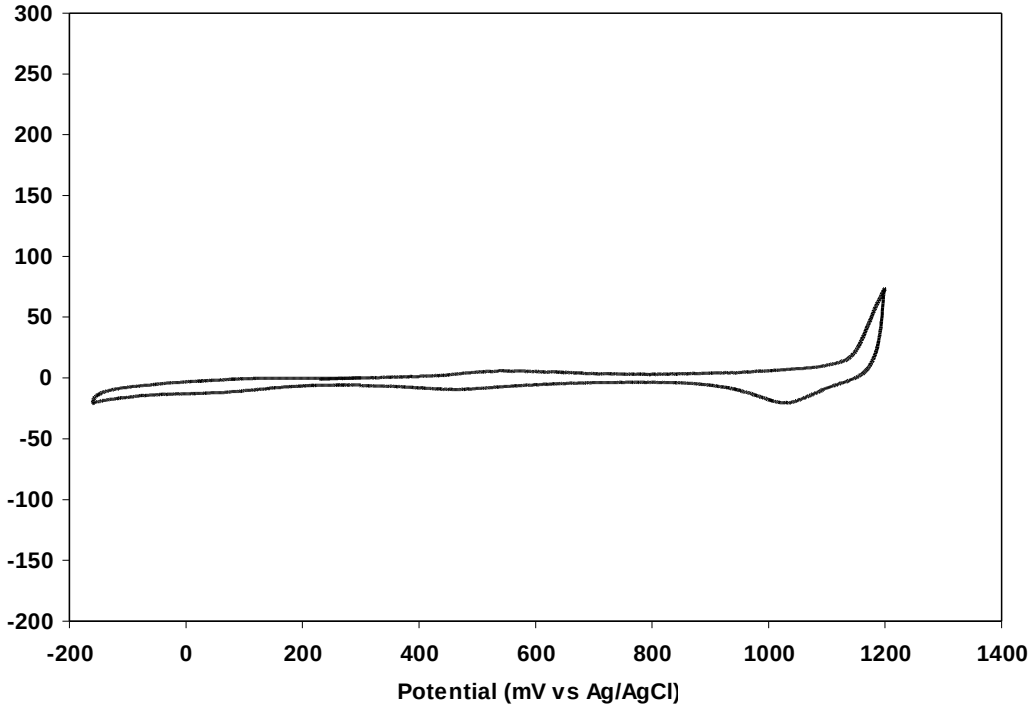

Figure 2.12. The CV of a clean Au substrate in 0.5M H_2SO_4 with a positive limit of +1200mV. Scan rate: 10mV/s.

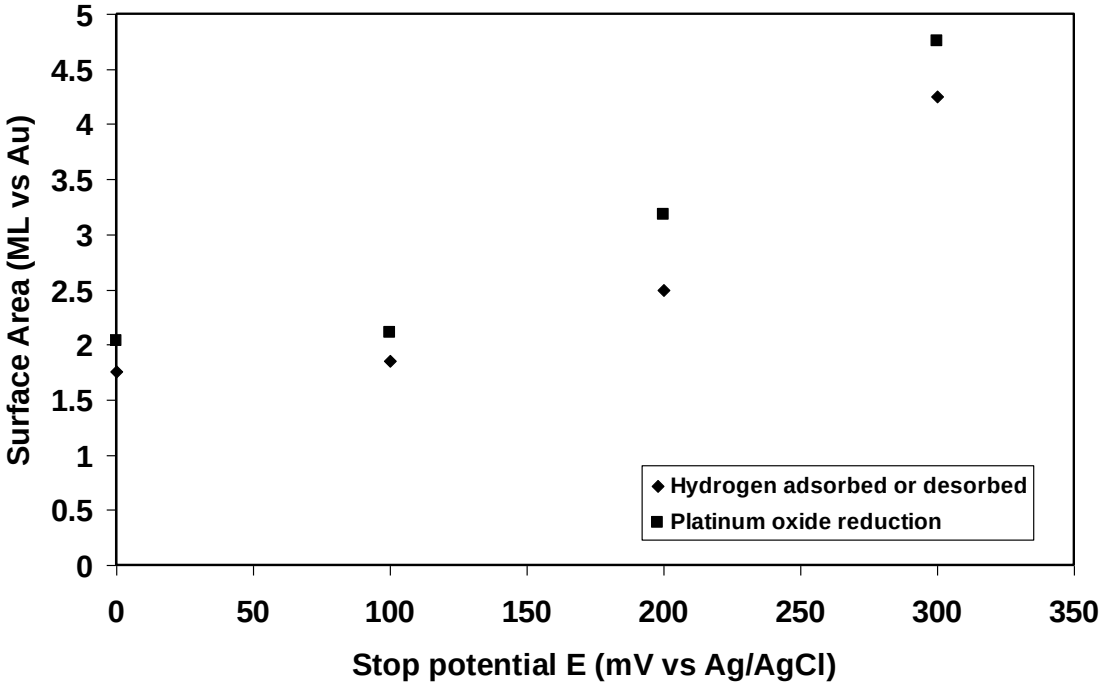

Figure 2.13. Four different 25 cycle Pt films deposited with different stop potential. Surface area (ML vs. Au) of 25 cycle Pt film calculated from Pt oxide reduction charge and Hydrogen adsorption and desorption charge in 0.5M H_2SO_4. Pt was deposited using $PtCl_4^{2-}$ ions.

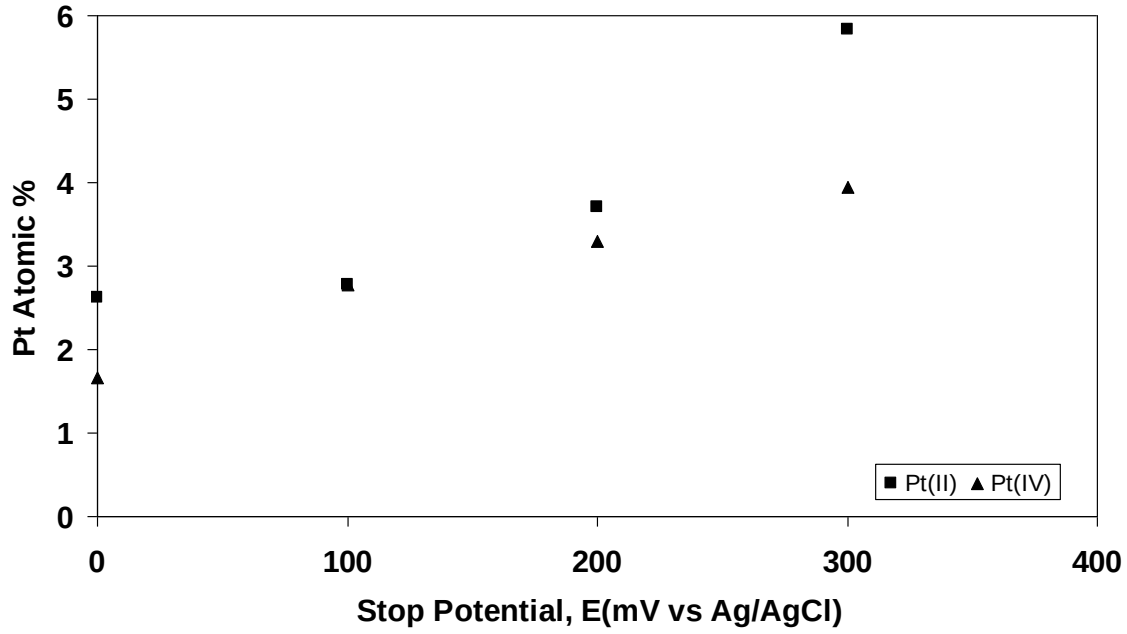

Figure 2.14. Atomic % for Pt film deposited using Pt(II) and Pt(IV) as a function of stop potentials.

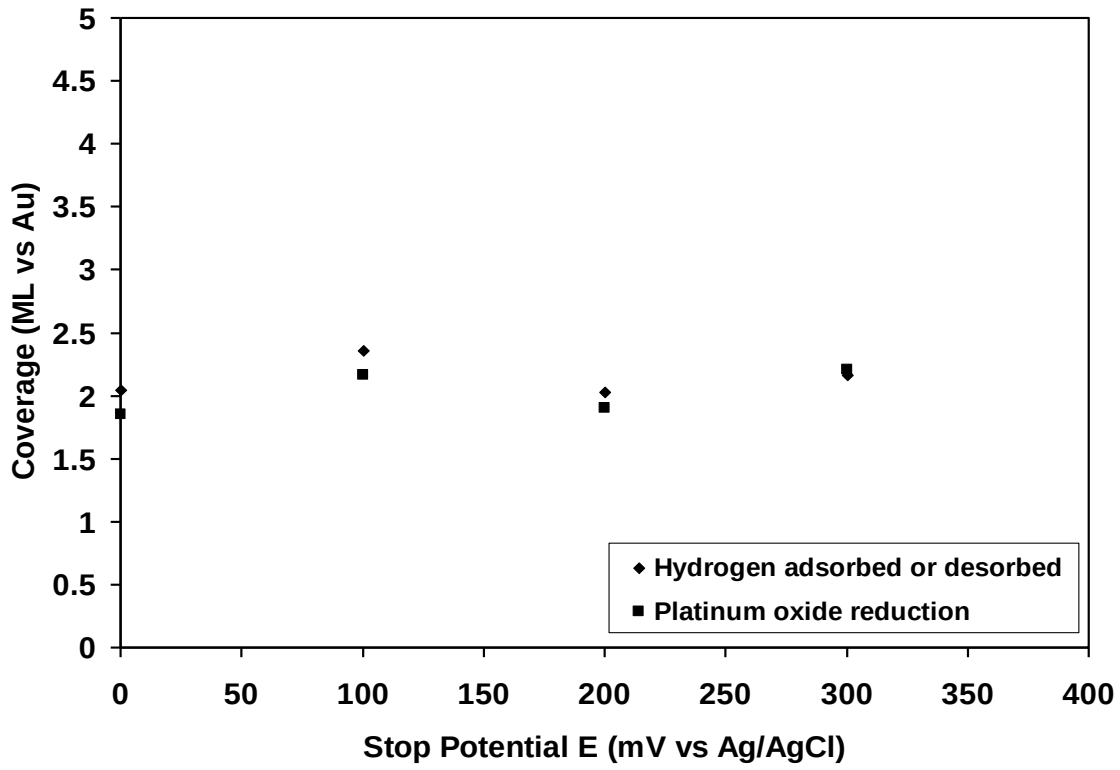

Figure 2.15. Four different 25 cycle Pt films deposited with different stop potential. Surface area (ML vs. Au) of 25 cycle Pt film calculated from Pt oxide reduction charge and Hydrogen adsorption and desorption charge in 0.5M H_2SO_4. Pt was deposited using $PtCl_6^{2-}$ ions.

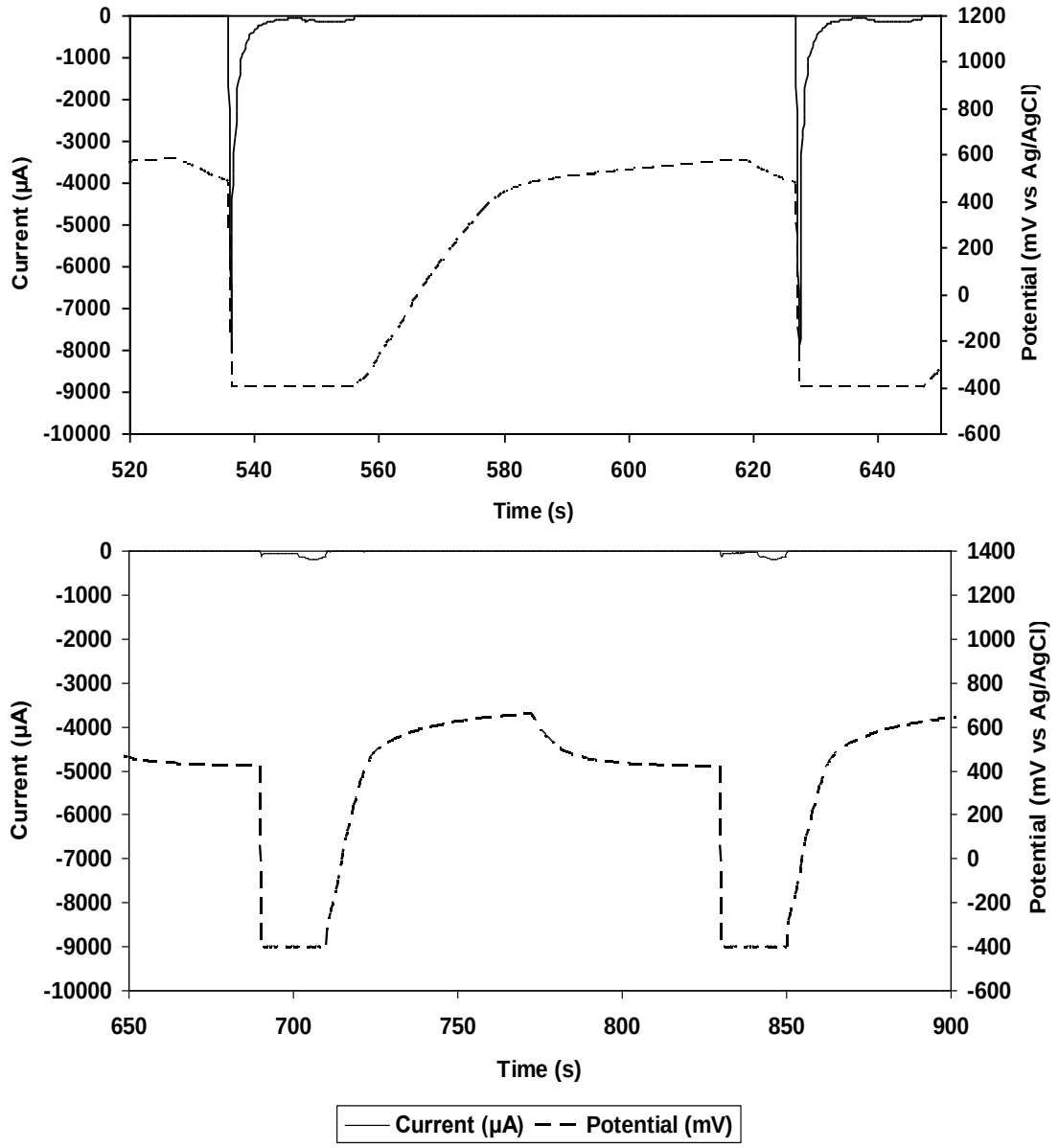

Figure 2.16. (A)Time-Current- Potential graph illustrating one Pt ALD cycle for charging current, Hydrogen evolution, reduction of adsorbed $PtCl_6^{2-}$ species and Pb UPD at -400mV. (B) Pb is deposited at -400mV and is replaced by $PtCl_4^{2-}$ ions at open circuit.

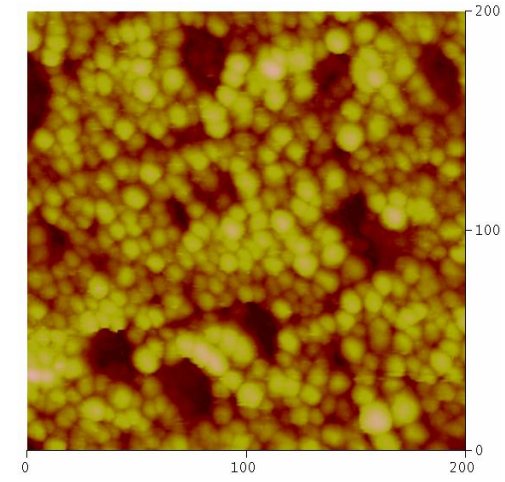

Z range	14.914 nm
Rms (Rq)	1.417 nm
Mean roughness (Ra)	1.047 nm

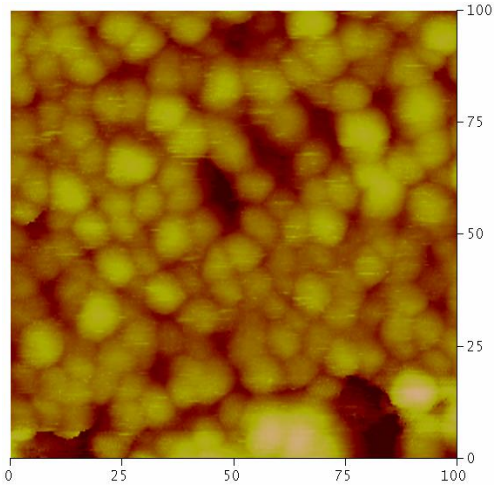

Z range	13.776 nm
Rms (Rq)	1.132 nm
Mean roughness (Ra)	0.771 nm

Figure 2.17. STM image of 25 cycle Pt film deposited on template-stripped Au using $PtCl_6^{2-}$ precursor ions,.

CHAPTER 3

PTRU NANOFILM FORMATION BY ELECTROCHEMICAL ATOMIC LAYER DEPOSITION (E-ALD)[2]

[2]Jayaraju, N., et al. To be submitted to Journal of Electrochemical Society.

Abstract

PtRu electrocatalysts are of interest as anode material in proton exchange membrane fuel cell (PEMFC), and direct methanol fuel cell (DMFC), due to their higher CO tolerance, compared with pure Platinum and other Pt based alloys. This report describes the formation of bimetallic PtRu nanofilm using the electrochemical version of atomic layer deposition (ALD). ALD is a method for the formation of materials an atomic layer at a time, using surface limited reactions. E-ALD makes use of electrochemical surface limited reactions, generally referred to as under potential deposition (UPD). UPD is the formation of an atomic layer of one element on another at a potential prior to (under) that needed to deposit the first element on itself. The formation of metal nano film using E-ALD was made possible by development of Surface Limited Redox Replacement (SLRR), where an atomic layer (UPD) of a sacrificial element is exchanged for one of a more noble element. In the present study, PtRu nanofilms were formed using SLRR of Pb UPD for Pt and Ru. The Pb UPD was replaced with ionic precursors for Pt and Ru at open circuit potential (OCP).

The ALD cycle used to form PtRu consisted of Pb UPD at -0.19V, replacement with Pt at OCP, Pb UPD again, and finally replacement with Ru OCP. PtRu nanofilms were formed by repeating the cycle a sufficient number of times to achieve the desired thickness. PtRu nanofilms with atomic proportions of 70/30, 82/18 and 50/50 Pt/Ru were formed using E-ALD. Pb UPD charges and OCP changes during replacement at OCP were monitored during the deposition process. Resulting PtRu films were characterized by CV, and CO oxidative stripping voltammetry, as a measure of catalytic activity. PtRu nanofilms showed the expectedly lower overpotentials expected, vs pure Pt or Ru.

Keywords: PtRu, E-ALD, ALD, UPD, SLRR, Fuel cell, Carbon monoxide, EPMA, electrodeposition.

Introduction

Fuel cells are considered to be possible important power sources in an overall green economy. Proton exchange membrane fuel cells (PEMFC) are composed of porous carbon electrodes, anodes and cathodes, impregnated with Pt or Pt based alloy nano-particles to catalyze both oxidations and reductions. Hydrogen works well in PEMFC, unless contaminated with CO, which is a Pt poison. Larger molecules, containing carbon, can have CO as an intermediate or byproduct, so that the Pt can become contaminated rapidly (Léger 2001; Kamarudin, Achmad et al. 2009). It has been shown that some Pt alloys better facilitate oxidation of absorbed CO, decreasing the overpotentials required to run a PEMFC. Binary, ternary and quaternary alloys, including: PtRu, PtCo, PtSn, PtMo, PtRuCo and PtRuNiZr (Igarashi, Fujino et al. 2001; Samjeské, Wang et al. 2002; Hayden, Rendall et al. 2003; Strasser, Fan et al. 2003; Whitacre, Valdez et al. 2005; Petrii 2008; Hsieh, Wu et al. 2009) have been investigated as anode materials for fuel cells. Among those alloys, PtRu has shown some of the highest catalytic activity and cell performance. It is frequently used as an anode material in proton exchange membrane fuel cells (PEMFC) and direct methanol fuel cells (DMFC) due to its increased CO tolerance (Zhang 2008) (Cha, Chen et al. 2009) (Gasteiger, Markovic et al. 1993; Gasteiger, Markovic et al. 1994; Ianniello, Schmidt et al. 1994; Gasteiger, Markovic et al. 1995; Kabbabi, Faure et al. 1998; Hoster, Iwasita et al. 2001; Liu, Song et al. 2006).

Petrii(Petrii 1965) pioneered the study of PtRu for methanol oxidation and reported higher activity for PtRu compared to Pt electrodes. Watanabe and Motoo(Watanabe and Motoo 1975; Watanabe and Motoo 1975) showed that the presence of a second alloying element, in addition to platinum, facilitated the removal of adsorbed intermediates from the catalyst surface. The superior catalytic activity of PtRu alloys can be explained as a ligand effect (electronic

effect) or by a bifunctional mechanism. In the ligand effect (Krausa and Vielstich 1994; Tong, Kim et al. 2001; Sasaki and Adzic 2008), the addition of Ru to Pt modifies the electronic properties of Pt, thereby weakening the adsorption of CO on Pt. In the bifunctional mechanism (Watanabe and Motoo 1975) (Gasteiger, Markovic et al. 1993; Gasteiger, Markovic et al. 1994; Ianniello, Schmidt et al. 1994), it is proposed that Ru adsorbs water at comparably negative potentials and provides an oxygen species to convert CO to CO_2. Although CO stripping can be used as a probe to determine the catalytic activity and the electrochemical surface area, Cu UPD is a preferred method to determine the surface areas of PtRu electrodes, because of the similarity in atomic radii of the metals.(Green and Kucernak 2002; Green and Kucernak 2002). Numerous studies (Petrii 1965; Watanabe and Motoo 1975; Watanabe and Motoo 1975; Gasteiger, Markovic et al. 1994; Gasteiger, Markovic et al. 1994; Lin, Zei et al. 1999; Markovic and Ross 2002; Maillard, Lu et al. 2005; Gavrilov, Petrii et al. 2007; Gavrilov, Savinova et al. 2007) have been performed to develop PtRu electrocatalysts with a high tolerance for CO, as their performance is directly related to fuel cell efficiency.

The majority of methods for the preparation of PtRu alloys for electrocatalysts involve thermal decomposition of precursors (Sivakumar, Ishak et al. 2005; Sivakumar and Tricoli 2006), spray pyrolysis(Chakraborty, Bischoff et al. 2005; Xue, Liu et al. 2006), sol-gel technology(Kim, Yang et al. 2003), ionic liquids(He, Liu et al. 2005; Xue, Lu et al. 2005), chemical deposition(Colmenares, Wang et al. 2006; Yan, Sun et al. 2006) and electrodeposition(Cattaneo, Sanchez de Pinto et al. 1999; Coutanceau, Rakotondrainibé et al. 2004; Rodríguez-Nieto, Morante-Catacora et al. 2004; Gavrilov, Petrii et al. 2007). Electrodeposition provides simple, cost effective, low temperature processes for growing thin films. PtRu electrodeposition on carbon supports, and their catalytic activity towards methanol

oxidation, has been well studied (Löffler, Natter et al. 2003; Natter and Hempelmann 2003; Coutanceau, Rakotondrainibé et al. 2004; Rodríguez-Nieto, Morante-Catacora et al. 2004; Gavrilov, Savinova et al. 2007). Recently, Gavrilov et al. (Gavrilov, Petrii et al. 2007) electrodeposited submicron PtRu from chloride electrolytes, at different deposition potentials, and studied their stability and electrocatalytic activity for methanol oxidation. However, the electrodeposition of Pt and Ru has proven difficult, generally resulting in surface roughening and 3-D growth.

Atomic layer deposition (ALD) is a methodology based on surface limited reactions for the formation of conformal nanofilms, one layer at a time. The electrochemical form of ALD (E-ALD) was invented in this group and initially referred to as electrochemical atomic layer epitaxy (EC-ALE). Most electrochemical surface limited reactions are referred to as underpotential deposition (UPD){Kolb, 1978 #17764;Adzic, 1984 #643;Gewirth, 1997 #655;Herrero, 2001 #2412;Magnussen, 2002 #2894}, and involves the formation of an atomic layer of one element on a second at a potential prior to, under, that needed to deposit the first element on itself. UPD is the result of the free energy of formation of a surface compound or alloy.

An atomic layer is a deposit which is one atom thick, but of an otherwise undisclosed coverage. Coverages are described in terms of monolayers (ML), where a ML is one adsorbate for every substrate surface atom. In the present report, the substrate atomic density is are approximated as equal to a Au(111) single crystal surface, where a ML corresponds to $1.35X10^{15}$ atoms/cm^2, or 217 μC/cm^2 for a one electron/surface atom.

E-ALD of metal, or elemental, nanofilms was not feasible until the invention of monolayer restricted galvanic displacement (MRGD) by Brankovic, Wang and Adzic (Brankovic, Wang et al. 2001; Brankovic, Wang et al. 2001), a process also referred to as surface

limited redox replacement (SLRR). It involves the electrodeposition of an atomic layer of a sacrificial (reactive) metal by UPD, and its exchange for an atomic layer of a less reactive, more noble element. The process involves redox exchange from a precursor solution of the desired (more noble) element, exposed to the sacrificial atomic layer, at open circuit potential (OCP). The replacement reaction is limited by the limited amount of the sacrificial atomic layer. Pt and Pd were some of the first metals formed using SLRR (Brankovic, Wang et al. 2001; Brankovic, Wang et al. 2001). Atomic level control over Pt atomic layer formation was revealed using scanning tunneling microscopy (STM). Cu UPD was used as the sacrificial layer, subsequently exchanged for Pt in a solution containing $PtCl_6^{2-}$ ions. Studies of noble metal deposition via SLRR have been extended by Vasilic and Dimitrov (Vasilic and Dimitrov 2005; Vasilic, Viyannalage et al. 2006; Viyannalage, Vasilic et al. 2007), Mroek and Weaver (Mrozek, Xie et al. 2001) and Kim and Stickney (Kim, Kim et al. 2006; Kim, Kim et al. 2007; Kim, Kim et al. 2008). The author's group have studied the use of SLRR cycles for E-ALD formation of Cu (Thambidurai, Kim et al. 2009) (Thambidurai, Gebregziabiher et al. 2010), Ru (Thambidurai, Kim et al. 2008) and Pt (Kim, Kim et al. 2006) (Jayaraju, Vairavapandian et al. 2010), on gold substrates.

Though multiple cycle metallic nanofilms of Cu, Pt, Pd and Ru have been formed formed using SLRR cycles, multi cycle bimetallic nanofilms have not Adzic et al. (Sasaki and Adzic 2008) (Ando, Sasaki et al. 2009) studied monolayer electrodeposition of Pt-Ru on a carbon support using SLRR, to activate methanol oxidation. Recently, Tumaini et al. (Mkwizu, Mathe et al. 2009) studied the deposition of bimetallic PtRu nanoclusters by SLRR of Cu on glassy carbon substrates.

In the present study, E-ALD based on SLRR cycles was used to form PtRu nanofilms on Au substrates. Pb UPD was used for the sacrificial atomic layers. $PtCl_6^{2-}$ ions were used as Pt precursors while Ru^{3+} ions were used as precursors for Ru deposition. Overpotential shifts for CO oxidation were studied on a range of PtRu deposit compositions, and treatments. For instance, CO adsorption and electrooxidation in sulfuric acid was used to incrementally remove Ru from the surface, which was then compared to CO oxidation from elemental Pt and Ru electrodes. CO oxidation studies were performed in the same flow cell system in which the deposits were formed, without their being removed. All deposits reported here were formed initially on Au on glass substrates.

Experimental

PtRu nanofilm deposition was performed using an automated electrochemical flow cell system (Electrochemcal ALD L.C.) consisting of: peristaltic pumps, Teflon solenoid valves, an electrochemical flow cell, and a potentiostat (Stickney 2002) (Wade, Ward et al. 1999) (Mathe, Cox et al. 2005). The system was controlled using custom software based on a LABVIEW (National Instruments) program. The Auxilury electrode was a gold wire embedded in the face of the Plexiglas flow cell, 1 mm from and opposite to the deposit. The Reference electrode was an Ag/AgCl (3M NaCl) (Bioanalytical systems, Inc., West Lafayette, IN) electrode, however, all potentials were reported with respect to a reversible hydrogen electrode (RHE) here. The flow cell ($4x1x0.1cm^3$) consisted of a planar Au on glass substrate, held away from the counter electrode by a 1 mm thick silicone rubber gasket. The deposition area was measured to be 3.77 cm^2. The solution flow rate was 9ml/min while pumping.

Reactant solutions were 1 mM $Pb(ClO_4)_2$, 0.1 mM $RuCl_3$, and 0.1 mM H_2PtCl_6. The Pb solution contained 0.5 M $NaClO_4$ (pH 4.5) supporting electrolyte, the Ru was 50 mM HCl (pH

1.5), and the Pt was 50 mM $HClO_4$ (pH 1.3). The blank solution was 0.5 M $NaClO_4$ (pH 4.5). CVs were performed in 0.5 M H_2SO_4. CO adsorption was carried out from 0.5 M H_2SO_4 saturated with CO. All solutions were prepared using water from a nanopure water filtration system (Barnstead, Dubuque, IA) (18MΩ) attached to the house DI water system. Chemicals were obtained from Sigma-Aldrich or Alfa Aesar. Solutions bottles were contained inside a Plexiglas box, and sparged with liquid nitrogen blow off.

The substrates were 300 nm of Au vapor deposited on glass, with a 5 nm Ti adhesion layer. The substrates were held at 280^o C during deposition, and then annealed at 400^o C for 12 hours, to produce a prominent (111) growth habit. The substrates were cleaned in nitric acid for 2 minutes and then by electrochemical cycling between 1.600 V and 0.010 V in 0.5M sulfuric acid, at 10 mV/s, prior to deposition.

The basic ALD cycle used to deposit the PtRu alloy films consisted of four major steps: a) Pb UPD at -0.19 V, b) OCP exchange of the Pb for Pt, using $PtCl_6^{2-}$ ions as precursors, c) Pb UPD at -0.19 V, d) OCP exchange of the Pb for Ru using Ru^{+3} ions as precursors. The over all E-ALD cycle was thus formation of an atomic layer of Pt, followed by one of Ru. The resulting PtRu nanofilms were characterized using cyclic voltammetry in 0.5M H_2SO_4, at 10mV/s.

Catalytic activities of the PtRu electrodes were investigated by CO stripping voltammetry, in 0.5 M H_2SO_4. Co was adsorbed by exposure to a 0.5 M H_2SO_4 solution saturated with CO, at 0.300 V for three minutes. Excess CO was rinsed away with 0.5 M H_2SO_4. The resulting adsorbed CO layer was first scanned negative to confirm the layer was complete: the absence of hydrogen adsorption or desorption (hydrogen waves). The electrode was then scanned from +0.05 V to +0.86 V, oxidizing the adsorbed CO. Those studies were performed on the as deposited PtRu films, without their being removed from the electrochemical cell.

Exposure of such to ambient would have resulted in contamination, and loss of potential control. Only the CO electrooxidation regions (0.05-0.85 V) are shown in the figures for simplicity.

Initial inspection of the deposits was performed using a Jenavert metallo-graphic microscope, 1000X. Electron probe microanalysis (EPMA) was run on a Joel 8600 wavelength dispersive scanning electron microprobe for elemental analysis.

Results and Discussions

PtRu E-ALD cycle

This article reports the E-ALD formation of PtRu nanofilms, based on SLRR cycles. The initial deposits involved the sequential deposition of one Pt atomic layer, followed by one of Ru, which is referred to here as one PtRu cycle (Figure 1). Previous studies by this group (Thambidurai, Kim et al. 2008) indicated that Ru was not easily deposited using Cu UPD for the sacrificial atomic layer. The issue involved limited difference in formal potentials for Ru and Cu, which resulted in incomplete Cu removal, and its build up each cycle. Pb UPD sacrificial atomic layers were thus chosen, as the difference in Ru and Pb formal potentials was sufficient to achieve complete removal each cycle, and previous studies had shown Pb to work for the deposition of both Pt and Ru.

Figure 2 displays three CVs, a window opening to successively lower potentials, to determine a Pb UPD potential. All three CVs started negative from 0.5 V, and displayed nearly constant current from 0.3 to 0.0 V. At 0.0 V, reduction peak A is evident (Figure 2), and consistent with Pb UPD on a Au(111) electrode (Green, Hanson et al. 1989). Bulk Pb deposition, peak B, begins near −0.21 V, and displays a small hysteresis loop, indicating a nucleation issue. Bulk Pb stripped in a sharp oxidation peak, B1, at -0.2 V, in the subsequent positive going scan. There was also a large oxidation peak, B2, at -0.1 V, corresponding to dealloying of Pb from the

Au (Green, Hanson et al. 1989). The Pb UPD stripping peak A2 shows indications of a doublet at 0.3 V. Based on the CVs in Figure 2, a Pb UPD potential of -0.19 V was selected for the formation of sacrificial atomic layers.

The E-ALD cycle program used in these studies consisted of the following steps: flow of Pb^{2+} ion solution through the cell for 10 s, at 9 mL/min and -0.19 V, to form Pb UPD. The auxiliary electrode was then disconnected, so the potential was open circuit (OCP) and the $PtCl_6^{2-}$ ion solution was flowed through the cell to facilitate exchange of Pb UPD for a Pt atomic layer. The OCP was monitored during the exchange process. Once the OCP reached 0.21 V, a "stop potential" step was applied. That is, the cell was rinsed with blank solution for 6s at OCP and then a potential of 0.31 V was applied for 5 sec, with continued rinsing. The second half of the E-ALD cycle began the same way, Pb^{2+} ion solution flowed for 10 s at -0.19 V, to form Pb UPD. The Ru^{3+} ion solution was next flowed through the cell at OCP, allowing exchange of Pb UPD for a Ru atomic layer. Once the OCP reached 0.21 V (the stop potential), the cell was rinsed with blank solution for 6 s at OCP and then at 0.31 V for 5 sec. This E-ALD cycle was designed for the sequential deposition of atomic layers of Pt and Ru, and formation of PtRu deposits. The deposits formed for this study were generally begun by running the cycle 25 times. Figure 3 displays the current-time (solid line) and potential-time (dashed line) graphs for an E-ALD cycle.

A majority of previous SLRR studies were performed using a constant exchange time. For instance, 60 s was used by Adzic to form Pt atomic layers using Cu as the sacrificial metal (Brankovic, Wang et al. 2001; Brankovic, Wang et al. 2001). However, the time needed for exchange can vary depending on the metal being deposited (Pt, Cu, Ru...etc), the pH, and the concentrations. For the present study, cycles were programmed with a "stop potential step",

which depended on the OCP during the exchange, which provided feed back on the progress of the exchange. From previous E-ALD studies using Pb UPD, it was known that all Pb should have been oxidized above 0.21 V. The control program was thus set up to monitor the OCP during exchange and once it reached 0.21 V (the stop potential) the cell was rinsed with blank for 11 s. The first 6 s were at OCP, to remove all Pt or Ru precursor ions from the cell, while the next 5 s were at 0.31 V, the OCP from drifting higher. The stop potential had to be high enough to assure all Pb was gone, yet low enough to prevent deposit oxidation. The potential-time trace in Figure 3 (dashed curve) shows the application 0.31 V for 5 s, six seconds after the OCP exceeded 0.21 V. Note the OCP gradient was steeper for Pt then Ru, suggesting that Pt exchange for Pb was more facile, possibly related to the larger difference in formal potentials. As a result, after hitting the stop potential, and flushing for 6 s, the OCP was already higher then 0.31 V, and was dropped to 0.31 V. Not so with Ru, where the potential was increased to 0.21 V (Figure 3).

The charge for Pb UPD in terms of monolayers (Pb atoms per surface Au atom), two electrons per Pb^{2+}, is displayed vs. cycle # in Figure 4A (squares for Pt and triangles for Ru). The Pb coverage used for Pt deposition increased from 0.65 ML to 0.92 ML over 25 cycles, while that for Ru increased from 0.52 ML to 0.71 ML. The resulting amounts of Pt or Ru deposited by exchange for the Pb UPD should have been controlled by Pb coverages. In principle (for SLRR) the used for deposition of Pt and Ru are provided by oxidation of the sacrificial Pb UPD layer. Since a Pt(IV) precursor is used, only half as much Pt as Pb should result, while it takes three Pb atoms to get electrons for two Ru(III) precursor ions. Based on those reaction stoichiometries, the maximum coverages of Pt and Ru expected are plotted in Figure 4B, suggesting the deposits should be 50% Pt and 50% Ru. Figure 4B also indicates a gradual increase in surface area, suggesting that some roughing is occurring over the 25 cycles.

Relative elemental coverages from EPMA indicate that the deposits were 70% Pt and 30% Ru, rather then 50/50.

The 70/30 stoichiometry probably resulted from less then 100% efficiency for the Ru exchange. Side reactions, such as oxygen reduction and hydrogen evolution, may have consumed some of the electrons from the Pb atomic layer, before the Ru layer was complete. The fact that it takes longer for the OCP to rise during the exchange of Ru for Pb then Pt for Pb (Figure 3), indicates that there would also be more time for the side reactions. Previous studies of E-ALD of Ru indicated an initial "induction period", where the Ru growth rate was low. Such induction periods have been observed in gas phase ALD studies as well, and are generally attributed to nucleation issues. Slow nucleation initially would have resulted in less Ru then expected, despite the Pb UPD coverages, with the side reactions using up the sacrificial Pb atomic layer instead of Ru.

PtRu deposits

To investigate the effect of the PtRu nanofilm bulk atomic composition of the on the electrocatalytic activity for adsorbed CO oxidation, the ALD cycle was modified to deposit PtRu alloy with different ratios. Films were made using cycles consisting of PtPtRu and PtRuRu, or two Pt steps followed by one of Ru, or one of Pt followed by two of Ru. Seventeen cycle deposits of PtPtRu and PtRuRu were grown so that the total number of atomic layer deposition steps would be equal to the 25 cycles of 70/30 PtRu deposits, discussed above. From EPMA, the PtPtRu deposits were 82% Pt and 18% Ru, and the PtRuRu deposits were 50% Pt and 50% Ru.

Steady state CVs for PtRu (70/30), PtPtRu(82/18) and PtRuRu (50/50) nanofilms, in 0.5 M H_2SO_4, are shown in Figure 5. All three displayed a single broad reduction feature, between 0.3 and 0.06 V, for oxide reduction, and some indication of hydrogen waves at lower potentials.

This voltammetric behavior has been observed for samples with well intermixed Pt and Ru components, where as Ru decorated Pt surfaces or annealed PtRu alloys tend to show double peak voltammograms (Gasteiger, Markovic et al. 1994; Davies, Hayden et al. 2002; Maillard, Lu et al. 2005). The current in the double-layer region appears to be larger than for a pure Pt electrode, which is also typical for a PtRu alloy electrode (Gavrilov, Petrii et al. 2007). The positive limit for the voltammograms was 1.1 V vs. RHE, to avoid loss of Ru and to limit place exchange, which may occur during oxidation at higher potentials. Loss of Ru at higher potentials results in development of more prominent and defined hydrogen waves typical of Pt electrode at lower potentials (Stickney, Soriaga et al. 1981).

A scheme proposed to represent a sputtered 70/30 PtRu alloy, as well schemes proposed for the 70/30, 82/18 and 50/50 PtRu deposits prepared using E-ALD, are shown in Figure 6. The sputtered PtRu alloy deposit (Figure 6A) should be a random distribution of a 70/30 mix of the two elements, both in the bulk and at the surface. According to literature, annealing a sputtered PtRu electrode generally results in surface segregation: enrichment of one component over other. Gasteiger et al. found that, for a PtRu alloy (70% Pt); annealing resulted in a surface composition of 92.1% Pt (Gasteiger, Ross Jr et al. 1993). In addition, PtRu electrodes subjected to multiple cycles in a fuel cell resulted in oxidative dissolution of Ru, further increasing the surface Pt% (Chen, Sun et al. 2006; Wang, Wang et al. 2008; Cha, Chen et al. 2009).

It is proposed here that the PtRu electrodes prepared by E-ALD should have a structure similar to that depicted in Figures 6B, 6C and 6D, before annealing or electrochemical treatments. From Figure 4B, it is expected that each atom layer deposition step should result in a ½ ML of Pt or Ru. There is no reason to think that deposits would consist of a superlattice;

alternating full atomic layers of Pt and Ru. scheme 6B suggests that small islands form for each element, each cycle, resulting in what might be called a nano-structured alloy.

The thesis behind these studies is that this approach to the formation of PtRu nanofilms is an alternative way to form catalytic surfaces, and that the surface composition may be stable longer during use because of the presence of the alloy supporting the catalytic surface, and the unique nanostructureing of the alloy (Figure 6). To investigate the activity of these films, the following CO adsorption oxidation studies were performed.

CO adsorption

Overpotentials for electrooxidation of CO on the as deposited nanofilms were investigated by CO adsorption and stripping voltammetry, without their removal from the flow cell or loss of potential control. The procedure was performed as follows: after deposit formation, CO saturated 0.5 M H_2SO_4 was flowed through the cell for 3 minutes at 0.31 V. The cell was then rinsed with CO free 0.5 M H_2SO_4 for 3 minutes at the same potential to remove any CO in solution. The adsorbed CO was then oxidatively stripped by scanning in the CO free 0.5 M H_2SO_4. Figure 7 show sets of CVs for three sequential experiments investigating CO absorption and oxidative stripping on the PtRu nanofilms (70/30). In each set, the CVs were initiated in the negative direction (solid line), which shows the absence hydrogen waves. Upon the positive going scan, the CO oxidation peak is clearly evident, where the initial onset gives an indication of the deposit activity to CO oxidation. The second CV (dashed line) shows the presence of hydrogen waves, and loss of the CO oxidation peak.

The CO adsorption process was performed prior to the CVs in Figures 7B and 7C, sequentially, on the same PtRu sample. Again, in the initial negative going scans, no hydrogen adsorption was evident, it being blocked by the adsorbed CO. The subsequent positive going scans resulted

in complete oxidation of the adsorbed CO, while the second scans verified the absence of CO, and the presence of hydrogen waves.

In each of the CVs in Figure 7, CO oxidizes in a peak starting around 0.45 V, with a peak potential of about 0.53 V. It is clear that the CO oxidation peaks get sharper with each iteration, indicating an increasingly homogenous surface, and or coverage. Hayden et al. have suggested the first scan results in cleaning some contamination on the surface which was disrupting the arrays of adsorbed CO. The second cycle results in a sharper CO oxidation peak, as the CO is more ordered (Davies, Hayden et al. 1998). It is known that nearly all organic functional groups will adsorb on Pt (Stickney, Soriaga et al. 1981), and that it is notoriously difficult to keep clean, suggesting that some cleaning of the electrode was probably required. However, it is interesting that the scan in Figure 7A looks very similar to a pure Ru electrode, nearly the same overpotential and peak shape. It is suggested here that any contamination was more likely to occur on the Pt islands (Figure 6B), while the CO adsorbed on those of Ru. In addition, some of the surface bound Ru could have been removed during the CVs, resulting in an increased Pt/Ru surface ratio, and subsequent peak shapes (Figure 7B and Figure 7C) which were more characteristic of a PtRu alloy. Similar studies for CO adsorption and oxidation were carried out using 82/18 and 50/50 Pt/Ru electrodes. Figure 8 shows the third oxidative stripping of CO from each of the three alloys: 70/30, 82/18 and 50/50 Pt/Ru. Clearly, the deposit with the higher Ru content, the 50/50 Pt/Ru showed the higher activity, the lower overpotential.

Decorated Deposits

For comparison with the PtRu E-ALD nanofilms, described above, the following set of deposits were prepared, again using E-ALD: A) Pt, B) Ru, C) a Pt decorated Ru and D) a Ru decorated Pt deposit (Figure 9). CO oxidation procedures were performed, equivalent to those

performed on the alloy deposits above. Pt nanofilm formation using E-ALD and SLRR cycles on Au substrates have been reported by this group {Kim, 2006 #87; Nagarajan, 2010 #400}, as were Ru nanofilms (Thambidurai, Kim et al. 2008). Ru modified Pt electrodes have been studied with regards to ruthenium's roll as promoter in enhancing electrocatalytic activity towards CO oxidation (Lin, Zei et al. 1999; Davies, Hayden et al. 2002; Lu, Waszczuk et al. 2002; Maillard, Lu et al. 2005). In the present studies, the Ru decorated Pt nanofilm was were prepared by first depositing 25 cycles of Pt, followed by two of Ru. Modified electrodes have been used as model electrodes for study of the activity of ad-atoms on electrode surfaces (Zei, Lei et al. 2003; Kuk and Wieckowski 2005). The Pt modified Ru electrode was prepared by depositing 25 cycles of Ru, followed by 2 cycles Pt.

Figure 10 displays electrooxidation of CO adsorbed on the catalyst deposit schemes (Figure 9), as well as on the 50/50 PtRu alloy, all formed using E-ALD. CO electrooxidation on pure Pt and pure Ru starts at 0.720V and 0.433V respectively. There is a dramatically lower overpotential for CO oxidation from Ru, compared with Pt, as is well known. The 50/50 PtRu alloy (red line) shows as well as the lowest overpotential observed in this study, as can be seen from the shift to lower potentials for initiation of the oxidation of adsorbed CO. The overpotential is 0.3 V lower then for the Pt. The Ru decorated Pt surface (pink line) shows a substantial shift of about 0.25V, compared to Pt. The Pt decorated Ru surface resulted in an increase in the CO oxidation charge but only a little over 0.1 V of decrease in overpotential compared with Pt. Onset and peak potentials for CO electrooxidation for the various deposits prepared by E-ALD are given in Table 1.

PtRu nanofilms are of importance for achieving catalysts with the, lowest loading and with long term stability during operation. An initial stability test was performed on the 50/50

PtRu alloy by subjecting the as-prepared nanofilms to 20 continuous cycles of CO adsorption and oxidation (Figure 12). The peak current for CO oxidation remained nearly constant for the first two or three CO adsorption and oxidation cycles, but then slowly decreases from cycle to cycle. Since CO adsorbs only on the surface, the top layer of metal atoms, it is important study the activity for CO oxidation of those atoms. The 50/50 PtRu alloy, prepared using 17 PtRuRu ALD cycle, was chosen for study as it showed the highest activity for CO oxidation and has higher tolerance for CO. A series of decorated 50/50 alloy deposits were formed, using 17 PtRuRu cycles: a plain 50/50 alloy, one decorated with a Pt ALD cycle, one with a PtRu ALD cycle, one with a RuRu ALD cycle, and one with a PtPt ALD cycle. The 17 PtRuRu cycle 50/50 PtRu deposit is referred to as the "base alloy". The base alloy ends with two Ru deposition steps. Figure 12 displays CO electrooxidation from the set of deposits. Although the onset potential remained about the same, respective of the decoration, there was significant variations in the peak potentials and charges. The base alloy decorated with PtRu showed the highest activity for CO electrooxidation.

Conclusions

Initial studies of electrochemical ALD cycles for the formation of bimetallic PtRu nanofilm were reported. E-ALD prepared PtRu nanofilm of 70/30, 82/18 and 50/50 Pt/ Ru composition exhibit a single broad peak in the hydrogen region, typical of PtRu alloy. PtRu alloy electrodes showed higher catalytic activity compared to pure Pt, with a negative potential shift of about 300mV. 50/50 Pt/Ru electrode showed the highest activity for CO electrooxidation compared to Pt, Ru, Ru-modified Pt, Pt-modified Ru and other Pt/Ru alloy electrodes. The deposition E-ALD program can be used to achieve the right composition in the bulk as well as at the surface. The 50/50 PtRu alloy ending with PtRu exhibited higher activity among other

surface ending layers. The EPMA data showed no evidence for the presence of Pb in the deposits.

Acknowledgements

Support from the National Science Foundation, as well as the Department of Energy, Biofuels program is acknowledged, and greatly appreciated.

References

1. Léger, J.M., *Mechanistic aspects of methanol oxidation on platinum-based electrocatalysts.* Journal of Applied Electrochemistry, 2001. **31**(7): p. 767-771.
2. Kamarudin, S.K., F. Achmad, and W.R.W. Daud, *Overview on the application of direct methanol fuel cell (DMFC) for portable electronic devices.* International Journal of Hydrogen Energy, 2009. **34**(16): p. 6902-6916.
3. Igarashi, H., et al., *CO Tolerance of Pt alloy electrocatalysts for polymer electrolyte fuel cells and the detoxification mechanism.* Physical Chemistry Chemical Physics, 2001. **3**(3): p. 306-314.
4. Petrii, O.A., *Pt-Ru electrocatalysts for fuel cells: a representative review.* Journal of Solid State Electrochemistry, 2008. **12**(5): p. 609-642.
5. Hayden, B.E., M.E. Rendall, and O. South, *Electro-oxidation of Carbon Monoxide on Well-Ordered Pt(111)/Sn Surface Alloys.* Journal of the American Chemical Society, 2003. **125**(25): p. 7738-7742.
6. Samjeské, G., et al., *CO and methanol oxidation at Pt-electrodes modified by Mo.* Electrochimica Acta, 2002. **47**(22-23): p. 3681-3692.
7. Hsieh, Y.-C., et al., *Displacement Reaction in Pulse Current Deposition of PtRu for Methanol Electro-Oxidation.* Journal of the Electrochemical Society, 2009. **156**(6): p. B735-B742.
8. Strasser, P., et al., *High Throughput Experimental and Theoretical Predictive Screening of Materials − A Comparative Study of Search Strategies for New Fuel Cell Anode Catalysts.* The Journal of Physical Chemistry B, 2003. **107**(40): p. 11013-11021.

9. Whitacre, J.F., T. Valdez, and S.R. Narayanan, *Investigation of Direct Methanol Fuel Cell Electrocatalysts Using a Robust Combinatorial Technique.* Journal of the Electrochemical Society, 2005. **152**(9): p. A1780-A1789.

10. Zhang, J., *PEM Fuel Cell Electrocatalysts and Catalyst Layers*. 2008: Springer London.

11. Cha, H.-C., C.-Y. Chen, and J.-Y. Shiu, *Investigation on the durability of direct methanol fuel cells.* Journal of Power Sources, 2009. **192**(2): p. 451-456.

12. Liu, H., et al., *A review of anode catalysis in the direct methanol fuel cell.* Journal of Power Sources, 2006. **155**(2): p. 95-110.

13. Kabbabi, A., et al., *In situ FTIRS study of the electrocatalytic oxidation of carbon monoxide and methanol at platinum-ruthenium bulk alloy electrodes.* Journal of Electroanalytical Chemistry, 1998. **444**(1): p. 41-53.

14. Gasteiger, H.A., et al., *Methanol electrooxidation on well-characterized platinum-ruthenium bulk alloys.* The Journal of Physical Chemistry, 1993. **97**(46): p. 12020-12029.

15. Gasteiger, H.A., N.M. Markovic, and P.N. Ross, *H2 and CO electrooxidation on well-characterized Pt, Ru, and Pt-Ru.2. Rotating disk electrode studies of CO/H2 mixtures at 62[thinsp][compfn]C.* J. Phys. Chem., 1995. **99**: p. 16757-16767.

16. Gasteiger, H.A., et al., *Electro-oxidation of small organic molecules on well-characterized Pt---Ru alloys.* Electrochimica Acta, 1994. **39**(11-12): p. 1825-1832.

17. Hoster, H., et al., *Pt-Ru model catalysts for anodic methanol oxidation: Influence of structure and composition on the reactivity.* Physical Chemistry Chemical Physics, 2001. **3**(3): p. 337-346.

18. Ianniello, R., et al., *CO adsorption and oxidation on Pt and Pt---Ru alloys: dependence on substrate composition.* Electrochimica Acta, 1994. **39**(11-12): p. 1863-1869.

19. Petrii, O.A., *Activity of electrolytically deposited platinum and ruthenium by the electrooxidation of methanol.* Doklady Akademii Nauk SSSR, 1965. **160**(4): p. 871-874.

20. Watanabe, M. and S. Motoo, *Electrocatalysis by ad-atoms: Part II. Enhancement of the oxidation of methanol on platinum by ruthenium ad-atoms.* Journal of Electroanalytical Chemistry, 1975. **60**(3): p. 267-273.

21. Watanabe, M. and S. Motoo, *Electrocatalysis by ad-atoms: Part III. Enhancement of the oxidation of carbon monoxide on platinum by ruthenium ad-atoms.* Journal of Electroanalytical Chemistry, 1975. **60**(3): p. 275-283.

22. Krausa, M. and W. Vielstich, *Study of the electrocatalytic influence of Pt/Ru and Ru on the oxidation of residues of small organic molecules.* Journal of Electroanalytical Chemistry, 1994. **379**(1-2): p. 307-314.

23. Tong, et al., *An NMR Investigation of CO Tolerance in a Pt/Ru Fuel Cell Catalyst.* Journal of the American Chemical Society, 2001. **124**(3): p. 468-473.

24. Sasaki, K. and R.R. Adzic, *Monolayer-Level Ru- and NbO[sub 2]-Supported Platinum Electrocatalysts for Methanol Oxidation.* Journal of the Electrochemical Society, 2008. **155**(2): p. B180-B186.

25. Gasteiger, H.A., et al., *Carbon monoxide electrooxidation on well-characterized platinum-ruthenium alloys.* The Journal of Physical Chemistry, 1994. **98**(2): p. 617-625.

26. Green, C.L. and A. Kucernak, *Determination of the platinum and ruthenium surface areas in platinum-ruthenium alloy electrocatalysts by underpotential deposition of copper. I. Unsupported catalysts.* Journal of Physical Chemistry B, 2002. **106**(5): p. 1036-1047.

27. Green, C.L. and A. Kucernak, *Determination of the Platinum and Ruthenium Surface Areas in Platinum−Ruthenium Electrocatalysts by Underpotential Deposition of Copper. 2. Effect of Surface Composition on Activity.* The Journal of Physical Chemistry B, 2002. **106**(44): p. 11446-11456.

28. Gasteiger, H.A., et al., *Temperature-Dependent Methanol Electro-Oxidation on Well-Characterized Pt-Ru Alloys.* Journal of the Electrochemical Society, 1994. **141**(7): p. 1795-1803.

29. Lin, W.F., et al., *Electrocatalytic Activity of Ru-Modified Pt(111) Electrodes toward CO Oxidation.* The Journal of Physical Chemistry B, 1999. **103**(33): p. 6968-6977.

30. Gavrilov, A.N., et al., *On the influence of the metal loading on the structure of carbon-supported PtRu catalysts and their electrocatalytic activities in CO and methanol electrooxidation.* Physical Chemistry Chemical Physics, 2007. **9**(40): p. 5476-5489.

31. Markovic, N.M. and P.N. Ross, *Surface science studies of model fuel cell electrocatalysts.* Surface Science Reports, 2002. **45**(4-6): p. 117-229.

32. Gavrilov, A.N., et al., *Pt-Ru electrodeposited on gold from chloride electrolytes.* Electrochimica Acta, 2007. **52**(8): p. 2775-2784.

33. Maillard, F., et al., *Ru-decorated Pt surfaces as model fuel cell electrocatalysts for CO electrooxidation.* Journal of Physical Chemistry B, 2005. **109**(34): p. 16230-16243.

34. Sivakumar, P., R. Ishak, and V. Tricoli, *Novel Pt-Ru nanoparticles formed by vapour deposition as efficient electrocatalyst for methanol oxidation: Part I. Preparation and physical characterization.* Electrochimica Acta, 2005. **50**(16-17): p. 3312-3319.

35. Sivakumar, P. and V. Tricoli, *Novel Pt-Ru nanoparticles formed by vapour deposition as efficient electrocatalyst for methanol oxidation: Part II. Electrocatalytic activity.* Electrochimica Acta, 2006. **51**(7): p. 1235-1243.

36. Xue, X., et al., *Physical and Electrochemical Characterizations of PtRu/C Catalysts by Spray Pyrolysis for Electrocatalytic Oxidation of Methanol.* Journal of the Electrochemical Society, 2006. **153**(5): p. E79-E84.

37. Chakraborty, D., et al., *Mixed Phase Pt-Ru Catalyst for Direct Methanol Fuel Cell Anode by Flame Aerosol Synthesis.* Journal of the Electrochemical Society, 2005. **152**(12): p. A2357-A2363.

38. Kim, J.Y., et al., *A Sol-Gel-Based Approach to Synthesize High-Surface-Area Pt-Ru Catalysts as Anodes for DMFCs.* Journal of the Electrochemical Society, 2003. **150**(11): p. A1421-A1431.

39. Xue, X., et al., *Novel preparation method of Pt-Ru/C catalyst using imidazolium ionic liquid as solvent.* Electrochimica Acta, 2005. **50**(16-17): p. 3470-3478.

40. He, P., et al., *Electrodeposition of Platinum in Room-Temperature Ionic Liquids and Electrocatalytic Effect on Electro-oxidation of Methanol.* Journal of the Electrochemical Society, 2005. **152**(4): p. E146-E153.

41. Yan, S., et al., *Polyol synthesis of highly active PtRu/C catalyst with high metal loading.* Electrochimica Acta, 2006. **52**(4): p. 1692-1696.

42. Colmenares, L., et al., *Ethanol oxidation on novel, carbon supported Pt alloy catalysts--Model studies under defined diffusion conditions.* Electrochimica Acta, 2006. **52**(1): p. 221-233.

43. Rodríguez-Nieto, F.J., T.Y. Morante-Catacora, and C.R. Cabrera, *Sequential and simultaneous electrodeposition of Pt-Ru electrocatalysts on a HOPG substrate and the electro-oxidation of methanol in aqueous sulfuric acid.* Journal of Electroanalytical Chemistry, 2004. **571**(1): p. 15-26.

44. Coutanceau, C., et al., *Preparation of Pt–Ru bimetallic anodes by galvanostatic pulse electrodeposition: characterization and application to the direct methanol fuel cell.* Journal of Applied Electrochemistry, 2004. **34**(1): p. 61-66.

45. Cattaneo, C., et al., *Characterization of platinum-ruthenium electrodeposits using XRD, AES and XPS analysis.* Journal of Electroanalytical Chemistry, 1999. **461**(1-2): p. 32-39.

46. Löffler, M.S., et al., *Preparation and characterisation of Pt-Ru model electrodes for the direct methanol fuel cell.* Electrochimica Acta, 2003. **48**(20-22): p. 3047-3051.

47. Natter, H. and R. Hempelmann, *Tailor-made nanomaterials designed by electrochemical methods.* Electrochimica Acta, 2003. **49**(1): p. 51-61.

48. Brankovic, S.R., J.X. Wang, and R.R. Adzic, *Metal monolayer deposition by replacement of metal adlayers on electrode surfaces.* Surface Science, 2001. **474**(1-3): p. L173-L179.

49. Brankovic, S.R., J.X. Wang, and R.R. Adzic, *New methods of controlled monolayer-to-multilayer deposition of Pt for designing electrocatalysts at an atomic level.* Journal of the Serbian Chemical Society, 2001. **66**(11-12): p. 887-898.

50. Vasilic, R. and N. Dimitrov, *Epitaxial growth by monolayer-restricted galvanic displacement.* Electrochemical and Solid State Letters, 2005. **8**(11): p. C173-C176.

51. Vasilic, R., L.T. Viyannalage, and N. Dimitrov, *Epitaxial growth of Ag on Au(111) by galvanic displacement of Pb and Tl monolayers.* Journal of the Electrochemical Society, 2006. **153**(9): p. C648-C655.

52. Viyannalage, L.T., R. Vasilic, and N. Dimitrov, *Epitaxial growth of Cu on Au(111) and Ag(111) by surface limited redox replacement - An electrochemical and STM study.* Journal of Physical Chemistry C, 2007. **111**(10): p. 4036-4041.

53. Mrozek, M.F., Y. Xie, and M.J. Weaver, *Surface-Enhanced Raman Scattering on Uniform Platinum-Group Overlayers: Preparation by Redox Replacement of Underpotential-Deposited Metals on Gold.* Analytical Chemistry, 2001. **73**(24): p. 5953-5960.

54. Kim, Y.-G., et al., *Platinum Nanofilm Formation by EC-ALE via Redox Replacement of UPD Copper: Studies Using in-Situ Scanning Tunneling Microscopy.* The Journal of Physical Chemistry B, 2006. **110**(36): p. 17998-18006.

55. Kim, J.Y., Y.G. Kim, and J.L. Stickney, *Copper nanofilm formation by electrochemical atomic layer deposition - Ultrahigh-vacuum electrochemical and in situ STM studies.* Journal of the Electrochemical Society, 2007. **154**(4): p. D260-D266.

56. Kim, J.Y., Y.G. Kim, and J.L. Stickney, *Cu nanofilm formation by electrochemical atomic layer deposition (ALD) in the presence of chloride ions.* Journal of Electroanalytical Chemistry, 2008. **621**(2): p. 205-213.

57. Thambidurai, C., et al., *Copper Nanofilm Formation by Electrochemical ALD.* Journal of the Electrochemical Society, 2009. **156**(8): p. D261-D268.

58. Thambidurai, C., et al., *E-ALD of Cu Nanofilms on Ru/Ta Wafers Using Surface Limited Redox Replacement.* Journal of the Electrochemical Society, 2010. **157**(8): p. D466-D471.

59. Thambidurai, C., Y.-G. Kim, and J.L. Stickney, *Electrodeposition of Ru by atomic layer deposition (ALD).* Electrochimica Acta, 2008. **53**(21): p. 6157-6164.

60. Jayaraju, N., D. Vairavapandian, and J.L. Stickney, *Electrochemical Atomic Layer Deposition (ALD) of Pt Nanofilms.* In Prep, 2010.

61. Ando, Y., K. Sasaki, and R. Adzic, *Electrocatalysts for methanol oxidation with ultra low content of Pt and Ru.* Electrochemistry Communications, 2009. **11**(6): p. 1135-1138.

62. Mkwizu, T.S., M.K. Mathe, and I. Cukrowski, *Electrodeposition of Multilayered Bimetallic Nanoclusters of Ruthenium and Platinum via Surface-Limited Redox−Replacement Reactions for Electrocatalytic Applications.* Langmuir, 2009. **26**(1): p. 570-580.

63. Stickney, J.L., *Electrochemical Atomic Layer Epitaxy (EC-ALE): Nanoscale Control in the Electrodeposition of Compound Semiconductors,* in *Advances in Electrochemical Science and Engineering,* R.C. Alkire and D.M. Kolb, Editors. 2002, Wiley-VCH: Weinheim. p. 1-105.

64. Wade, T.L., et al., *Electrodeposition of InAs.* Electrochemical and Solid-State Letters, 1999. **2**(12): p. 616-618.

65. Mathe, M.K., et al., *Formation of HgSe Thin Films Using Electrochemical Atomic Layer Epitaxy.* Journal of the Electrochemical Society, 2005. **152**(11): p. C751-C755.

66. Green, M.P., et al., *Insitu Scanning Tunneling Microscopy Studies of the Underpotential Deposition of Lead on Au(111).* Journal of Physical Chemistry, 1989. **93**(6): p. 2181-2184.

67. Davies, J.C., et al., *The electro-oxidation of carbon monoxide on ruthenium modified Pt(111).* Surface Science, 2002. **496**(1-2): p. 110-120.

68. Gasteiger, H.A., P.N. Ross Jr, and E.J. Cairns, *LEIS and AES on sputtered and annealed polycrystalline Pt-Ru bulk alloys.* Surface Science, 1993. **293**(1-2): p. 67-80.

69. Wang, Z.-B., et al., *Investigation of the performance decay of anodic PtRu catalyst with working time of direct methanol fuel cells.* Journal of Power Sources, 2008. **181**(1): p. 93-100.

70. Chen, W., et al., *The stability of a PtRu/C electrocatalyst at anode potentials in a direct methanol fuel cell.* Journal of Power Sources, 2006. **160**(2): p. 933-939.

71. Richarz, F., et al., *Surface and electrochemical characterization of electrodeposited PtRu alloys.* Surface Science, 1995. **335**: p. 361-371.

72. Davies, J.C., B.E. Hayden, and D.J. Pegg, *The electrooxidation of carbon monoxide on ruthenium modified Pt(110).* Electrochimica Acta, 1998. **44**(6-7): p. 1181-1190.

73. Stickney, J.L., et al., *A survey of factors influencing the stability of organic functional groups attached to platinum electrodes.* JEC, 1981. **125**: p. 73.

74. Lu, G.Q., P. Waszczuk, and A. Wieckowski, *Oxidation of CO adsorbed from CO saturated solutions on the Pt(111)/Ru electrode.* Journal of Electroanalytical Chemistry, 2002. **532**(1-2): p. 49-55.

75. Zei, M.S., T. Lei, and G. Ertl, *Spontaneous and electrodeposition of Pt on Ru(0001).* Zeitschrift Fur Physikalische Chemie-International Journal of Research in Physical Chemistry & Chemical Physics, 2003. **217**(5): p. 447-458.

76. Kuk, S.T. and A. Wieckowski, *Methanol electrooxidation on platinum spontaneously deposited on unsupported and carbon-supported ruthenium nanoparticles.* Journal of Power Sources, 2005. **141**(1): p. 1-7.

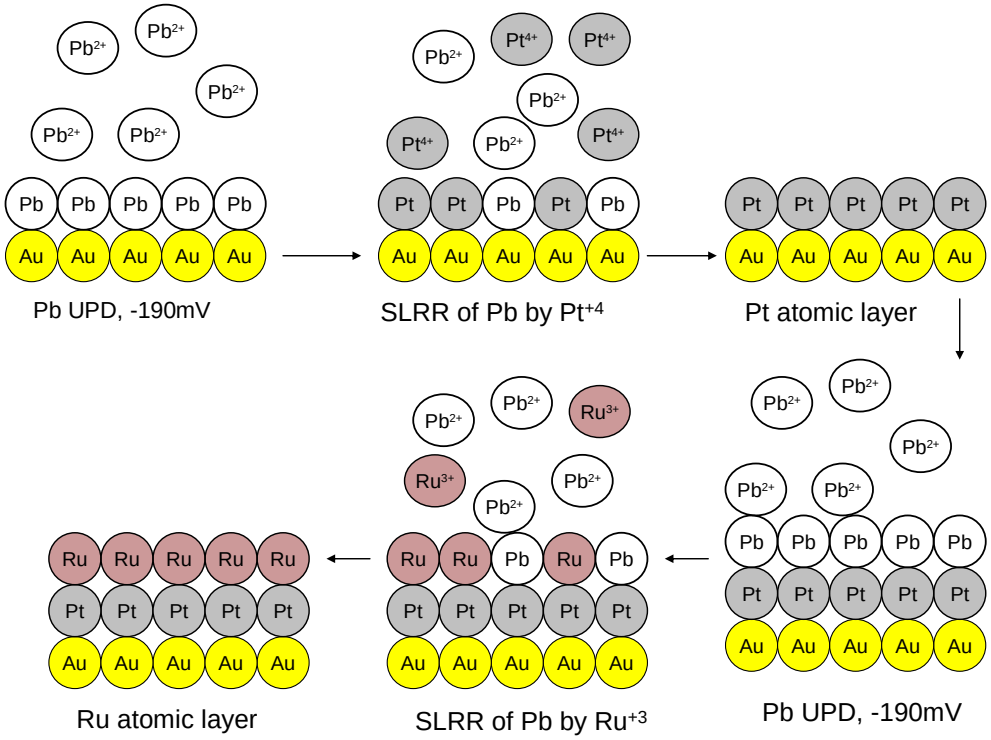

Figure 3.1. Cartoon representation for the formation of PtRu nanofilm by E-ALD and SLRR.

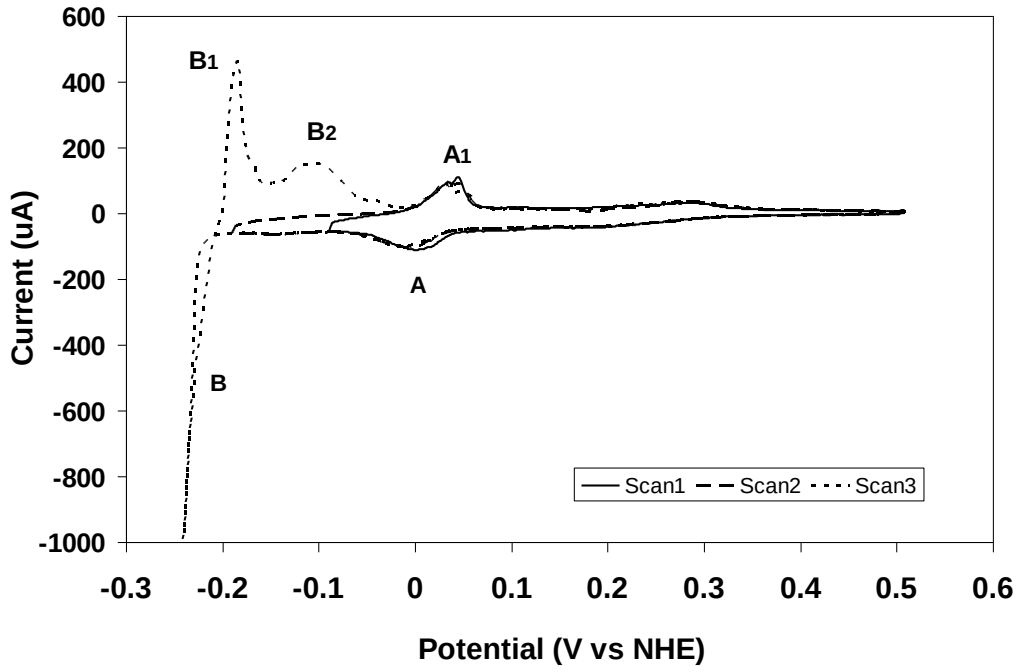

Figure 3.2. Cyclic voltammogram of Au electrode in 1mM $Pb(ClO_4)_2$ in 0.5M $NaClO_4$; pH~ 4.5; Scan rate: $10mVs^{-1}$.

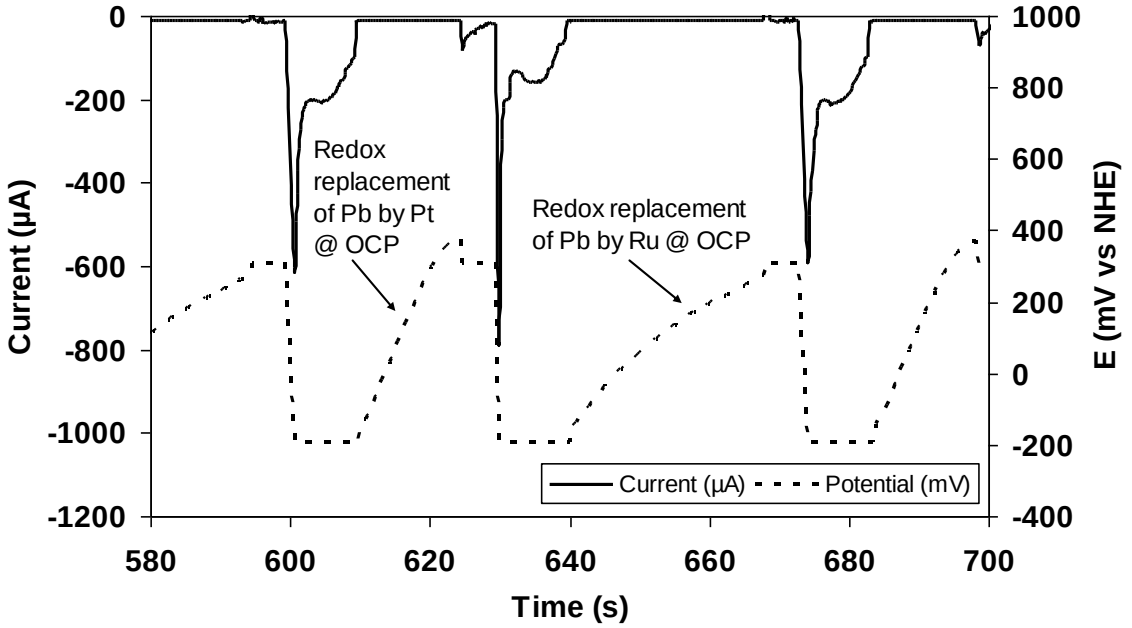

Figure 3.3. Graph of Current-Time-Potential plot for one PtRu E-ALD cycle.

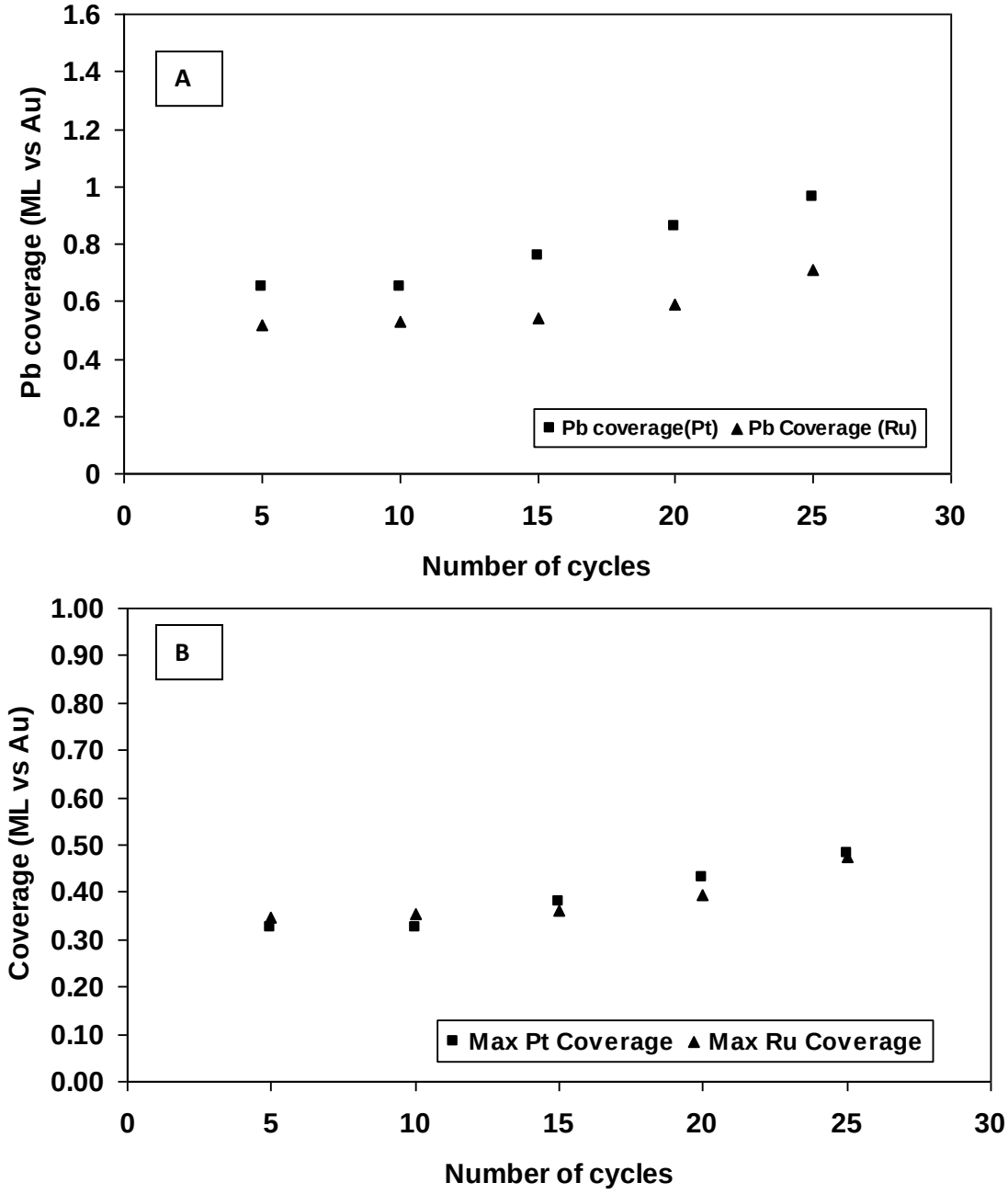

Figure 3.4. (A) Coverage for Pb UPD during Pt and Ru deposition and (B) Maximum coverage for Pt and Ru calculated from reaction stoichiometry.

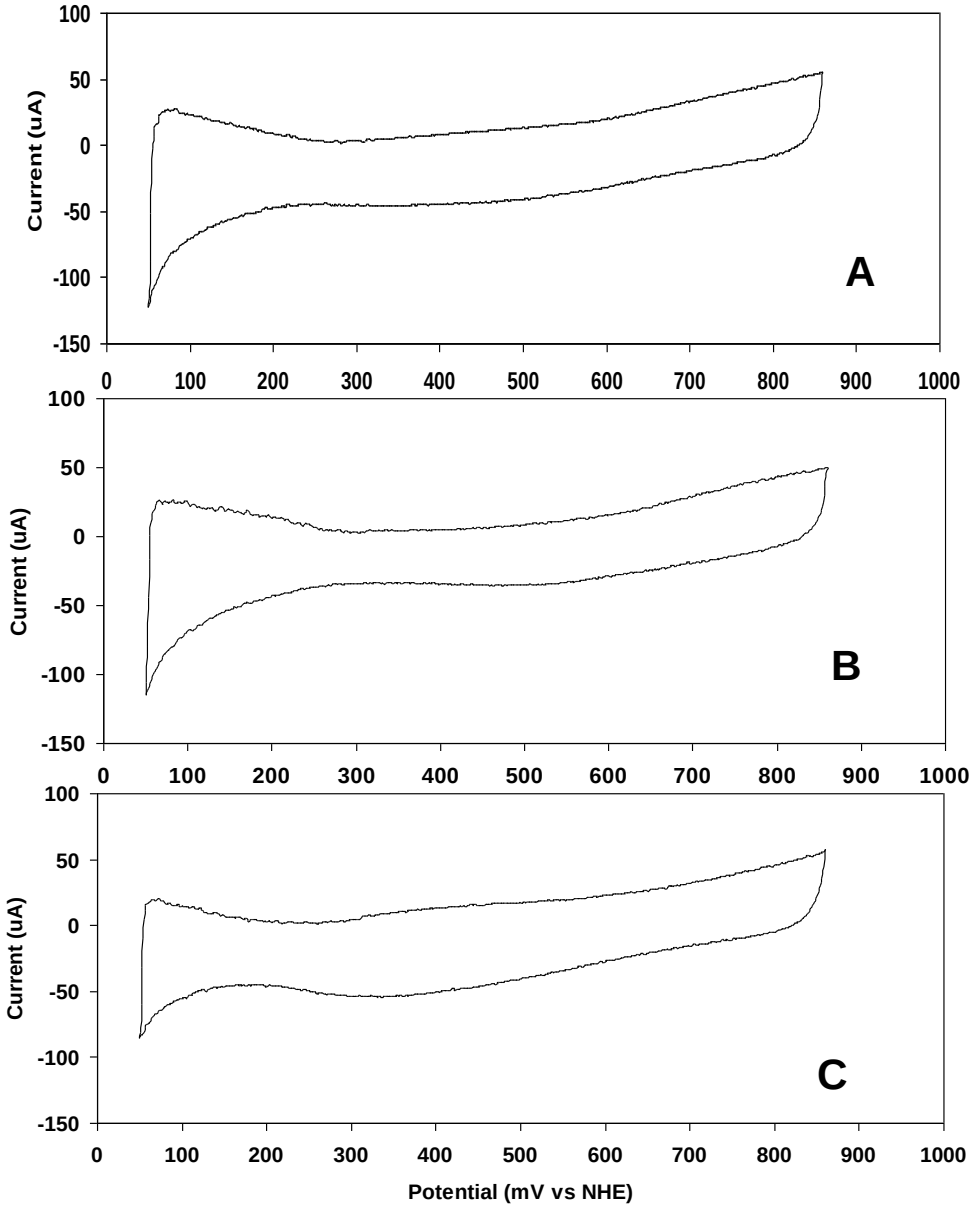

Figure 3.5. Cyclic voltammogram of PtRu electrode (A) 70/30 Pt/Ru (B) 82/18 Pt/Ru and (C) 50/50 Pt/Ru in 0.5M H_2SO_4; Scan rate: $10mVs^{-1}$.

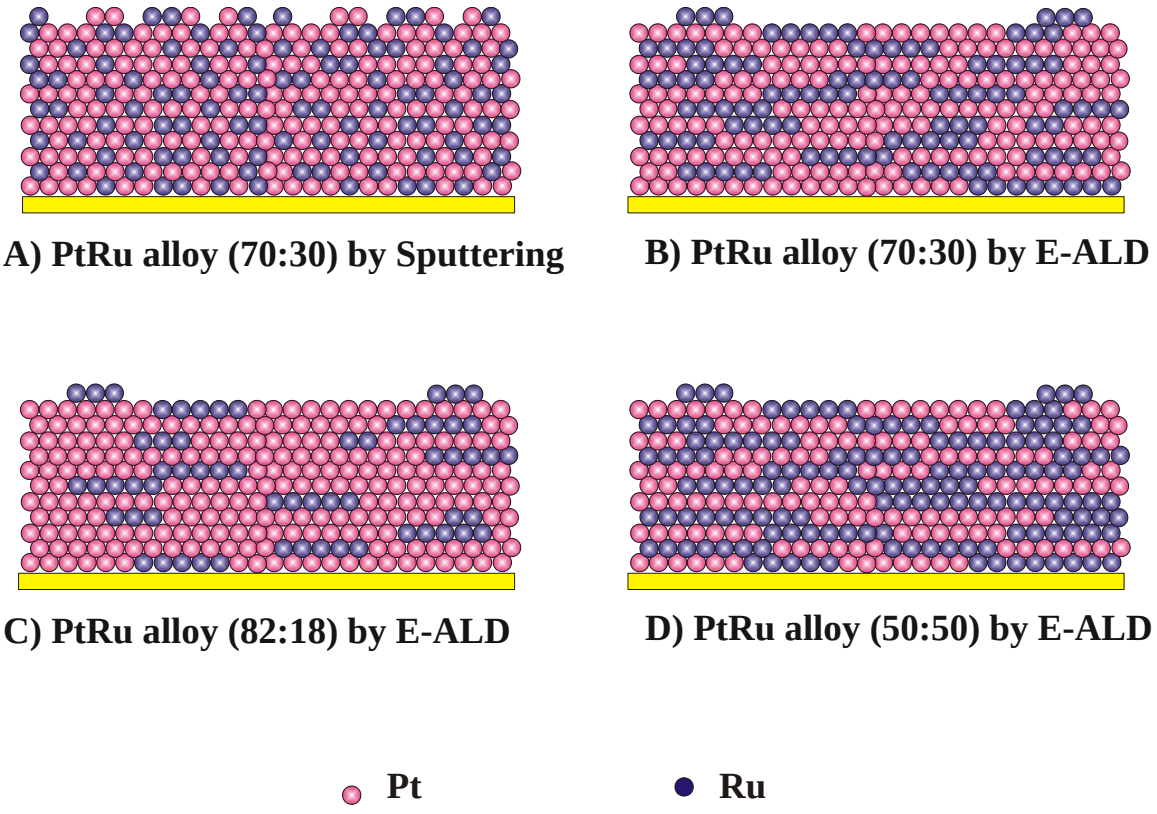

Figure 3.6. Cartoon scheme of sputtered (70/30 Pt/Ru) and E-ALD prepared PtRu (70/30Pt/Ru, 82/18 Pt/Ru and 50/50 Pt/Ru) nanofilm electrodes.

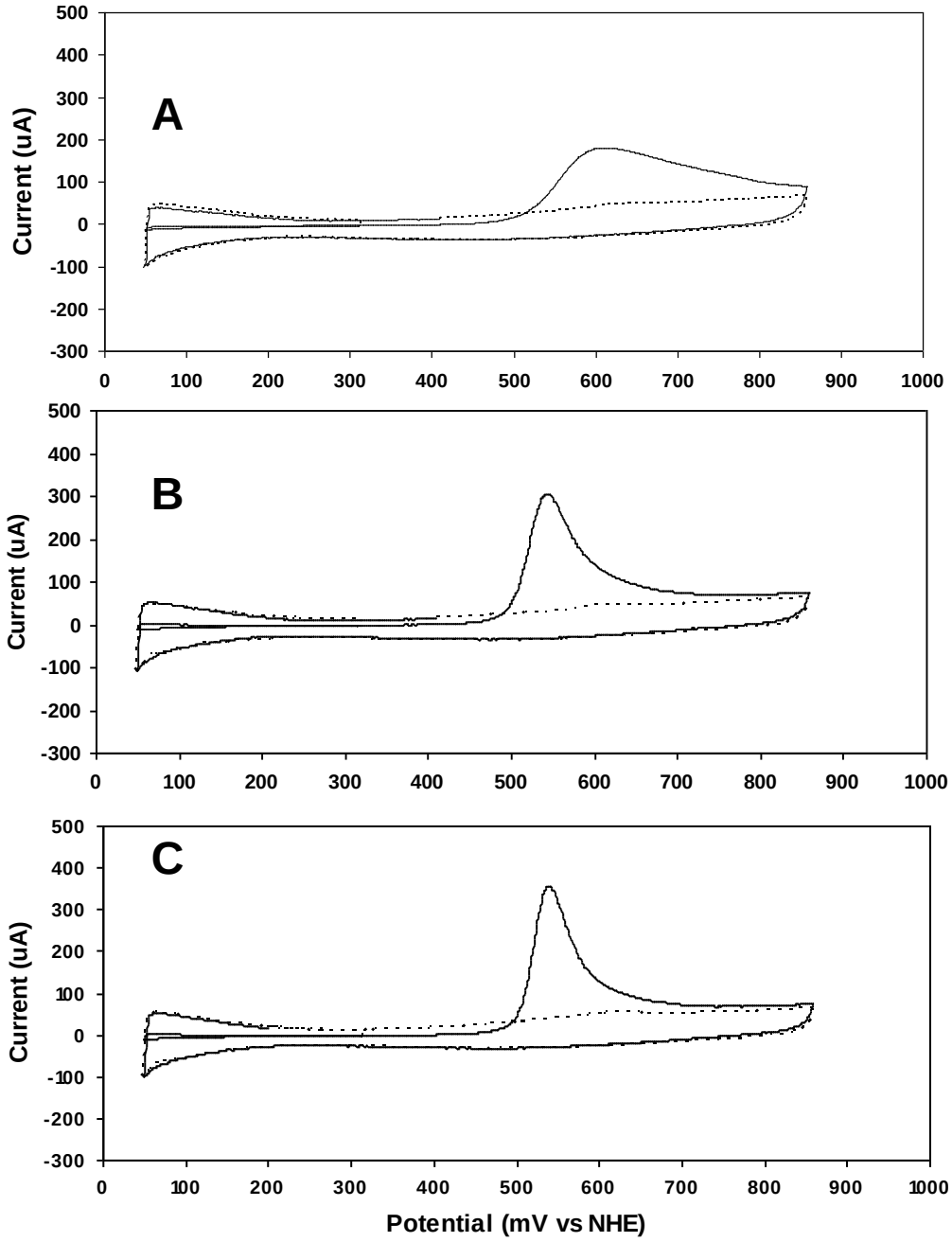

Figure 3.7. CO stripping voltammetry on PtRu electrode (70/30 Pt/Ru) in 0.5M H_2SO_4 with first (A), second (B) and third (C) continuous CO adsorption and oxidation cycles. Scan rate: $10mVs^{-1}$. (—) stripping of CO in the first positive going sweep; (----) second positive going sweep during each cycle.

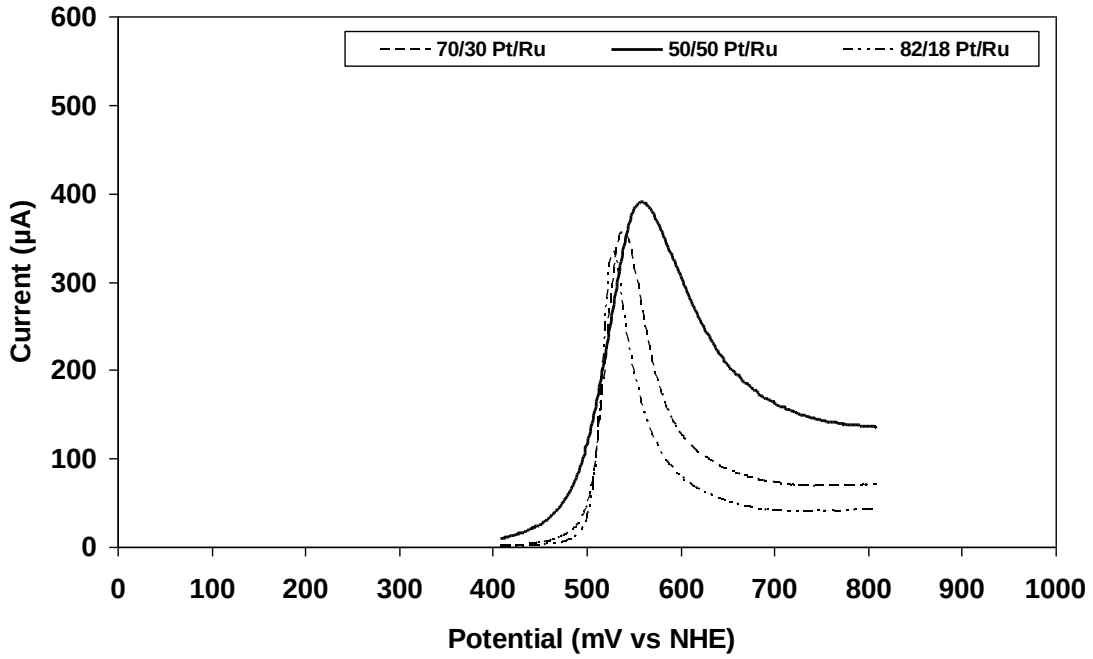

Figure 3.8. CO stripping voltammetry on various PtRu alloy electrodes in 0.5M H_2SO_4. Scan rate: $10mVs^{-1}$.

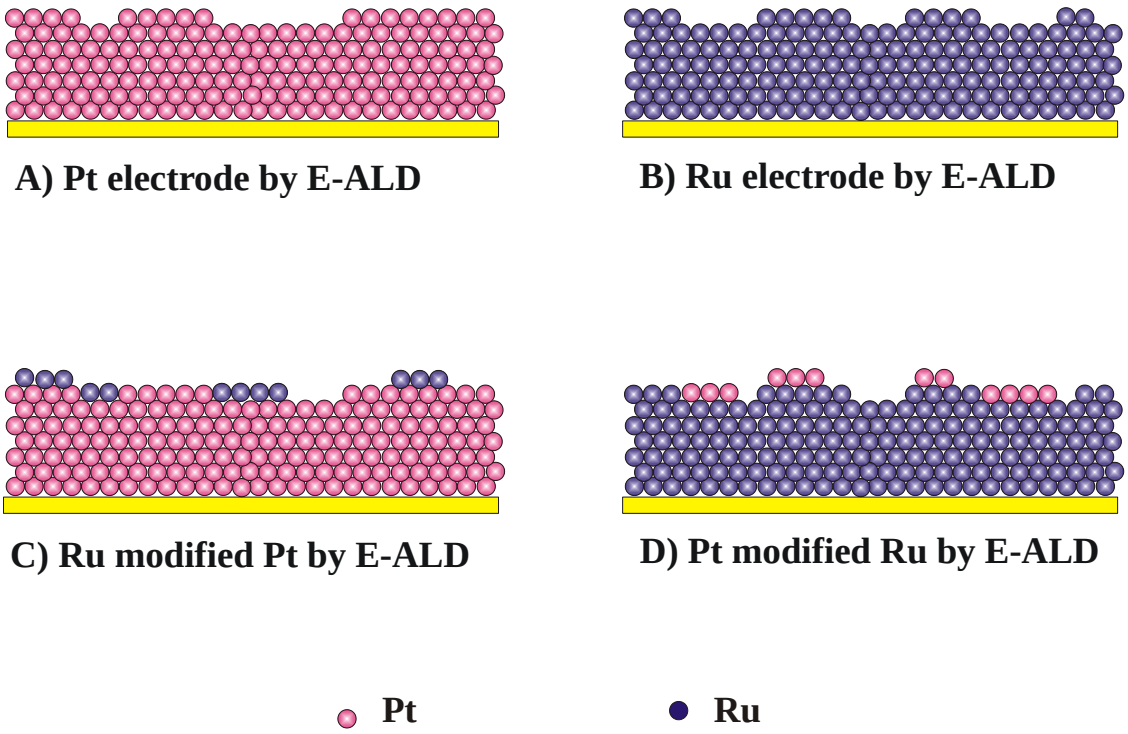

Figure 3.9. Cartoon scheme of various electrodes prepared by E-ALD.

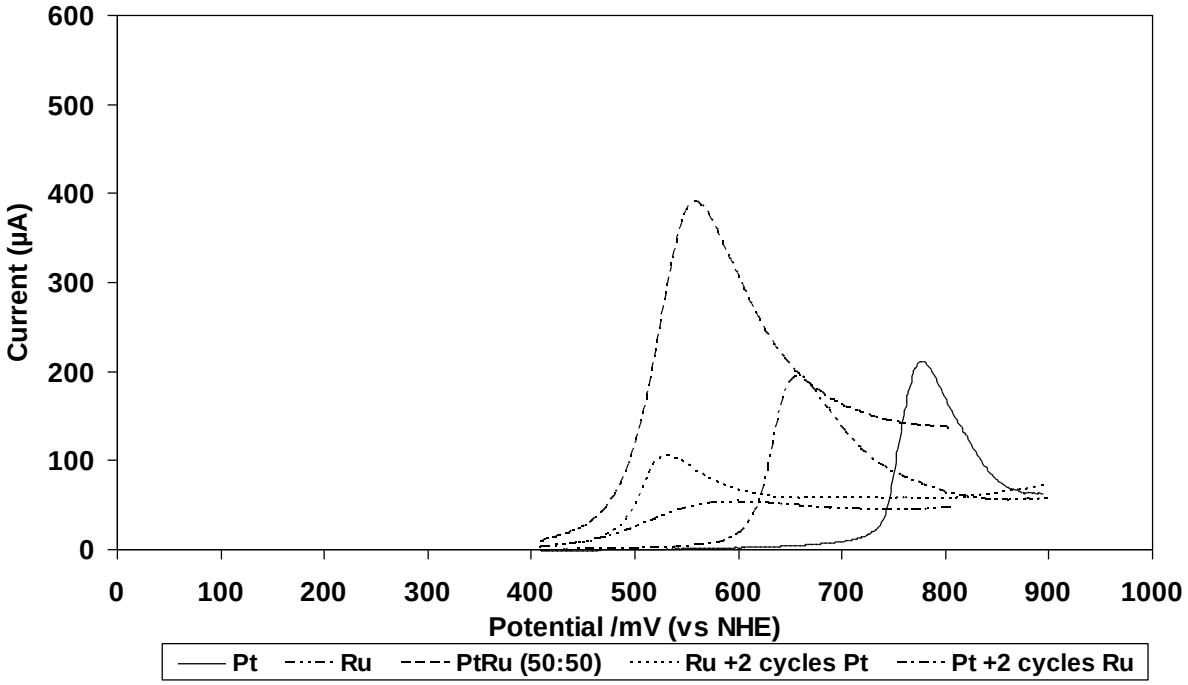

Figure 3.10. CO stripping voltammetry on Pure Pt, Pure Ru, 50/50 Pt/Ru alloy, Ru-modified Pt and Pt-modified Ru electrodes in 0.5M H_2SO_4 .Scan rate: 10mVs^{-1}.

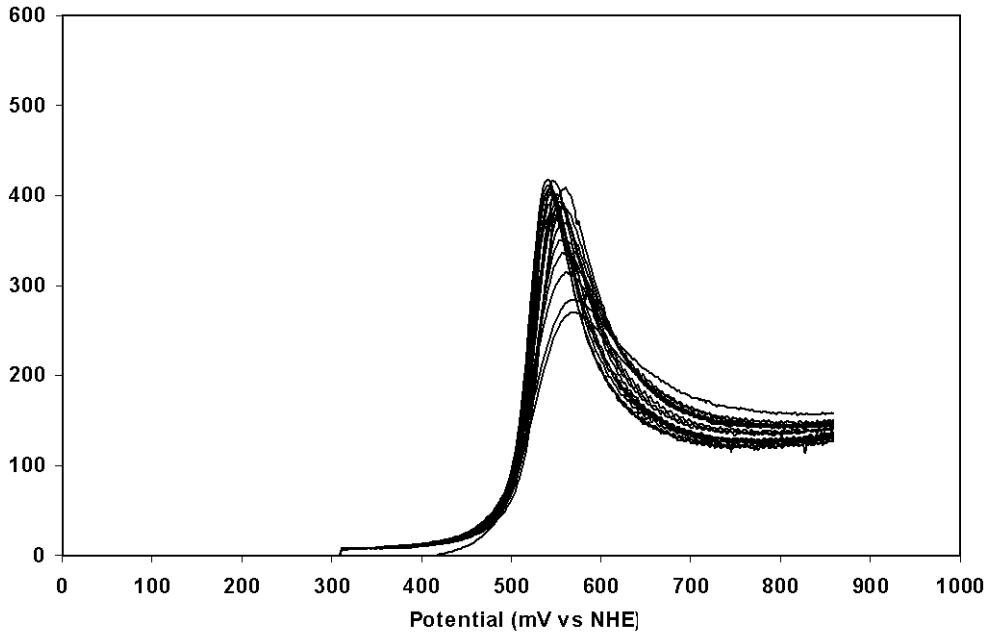

Figure 3.11. Stability test performed on 50/50 Pt/Ru alloy by subjecting to 20 continuous CO adsorption and stripping voltammetry in 0.5M H_2SO_4 .Scan rate: $10mVs^{-1}$.

Electrode type	CO oxidation onset potential (mV vs NHE)	CO oxidation peak potential (mV vs NHE)
Pure Pt	665	778
Pure Ru	433	599
Ru modified Pt	567	658
Pt modified Ru	435	531
Pt/Ru 70/30 alloy	470	545
Pt/Ru 82/18 alloy	486	530
Pt/Ru 50/50 alloy	410	561

Table 1. Summary of the onset potentials and peak potentials of CO electrooxidation for electrodes prepared by E-ALD.

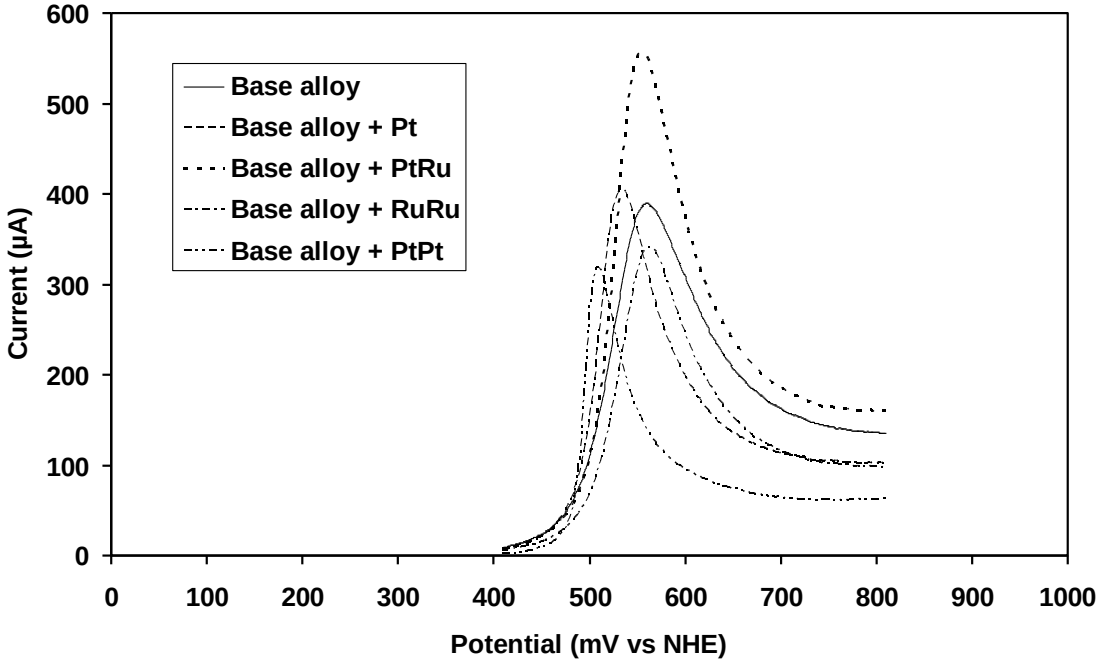

Figure 3.12. CO stripping voltammetry on 50/50 Pt/Ru (Base alloy) electrode with various surface ending layers in 0.5M H_2SO_4. Scan rate: $10mVs^{-1}$.

CHAPTER 4

RU MODIFIED PT NANOFILM FORMATION BY ELECTROCHEMICAL ATOMIC LAYER DEPOSITION (E-ALD)[3] AND THEIR CATALYTIC ACTIVITY TOWARDS CO ELECTROOXIDATION

[3]Jayaraju, N., et al. To be submitted to Journal of Electrochemical Society.

Abstract

This article concerns the Electrochemical Atomic Layer Deposition (E-ALD) of Ru modified Pt nanofilm electrode as an electrocatalyst for fuel cell applications. PtRu are a better electrocatalyst than Pt for the electrooxidation of CO and are widely used as an anode material in fuel cells. Electrochemical ALD is based on underpotential deposition (UPD) and surface limited redox replacement (SLRR). SLRR also referred to as galvanic displacement, where an atomic layer of a sacrificial element is first deposited by UPD, and is then exchanged for the element of interest. Pb is used as the sacrificial metal. Electrodeposition was carried out in an automated flow cell system. Ru modified Pt electrodes were prepared by depositing 25 cycle Pt film followed by 1 cycle Ru. Deposition of Pt and Ru were done by replacing Pb atomic layer with Pt^{4+} and Ru^{3+} ions respectively at open circuit potential. Pb UPD at -190mV was used to deposit Pt whereas the amount of Ru deposited is varied by choosing different Pb deposition potentials in the UPD range between 10mV to -240mV. The amount of Pb deposited at different UPD potentials ensures different Ru coverages. The charge for Pb deposition and OCP changes during replacement are monitored as a function of time. The catalytic activities were studied by CO stripping voltammetry in 0.5M sulphuric acid. Ru/Pt electrode exhibits higher CO tolerance with negative potential shift of about 150mV compared to pure pt electrode.

Keywords: Fuel Cell, Pt, Ru, E-ALD, UPD, ALD, SLRR, CO.

Introduction

Pt and Pt based alloy electrodes are used as electrocatalysts in proton exchange membrane fuel cells (PEMFCs) and direct methanol fuel cells (DMFCs). Carbon monoxide (CO), one of the intermediates formed during methanol oxidation in DMFCs or the trace amounts present in the Hydrogen fuel in PEMFCs, adsorbs strongly on to Pt sites. CO acts as a poisoning agent and reduces the performance of fuel cells. The adsorbed CO has to be removed at a much negative potential to activate the catalytic sites. Pt based alloy electrode [1-5] are investigated as anode materials in the fuel cells as they higher tolerance towards CO.

Watanabe and Motoo[6-7] studied the electrooxidation of CO and showed that the addition of Ru to platinum increases the CO tolerance. In the ligand effect [8-9], the addition of Ru modifies the electronic interactions of Pt, thereby weakening the adsorption of CO on Pt. In the bifunctional mechanism [7, 10], Ru adsorbs water at comparably lower potentials and provides the oxygen species for the oxidation of CO to CO_2. Since then numerous studies have been carried out on surfaces of different morphologies such as bulk PtRu alloys [11-13], Ru modified Pt single crystal [14-16], Pt modified Ru [17-18] and PtRu nanoparticles[19-20]. Several groups have studied Pt electrodes modified by ruthenium as model electrocatalysts for fuel cells.

Although most of the work is focused on the study of bimetallic PtRu (50:50) alloy as they showed highest catalytic activity for CO oxidation[11-12, 21-22], it is essential to have a better understanding of the role of Ru towards CO electrooxidation. Numerous research groups have studied the modified electrodes as model electrocatalysts for fuell cells. Ru modified Pt electrode refers to the deposition of 2D nanosized Ru islands dispersed on Pt substrates as observed in STM [23-24]. As the top layer is the most active layer for the oxidation of fuel in a

fuel cell, the study on Pt electrodes modified or decorated with Ru will provide a relationship between ad-atom coverage and reactivity. Ru modified Pt electrodes are prepared by one of the following methods: electrodeposition of Ru on Pt [14] [23] [24] [25] [19], spontaneous deposition of Ru on Pt [26] [25, 27-41] [19], Redox replacement reaction of less noble metal [42-44] and metal vapor deposition [16] [45] [30].

Several research groups have studied the Ru/Pt bimetallic system as electrocatalysts for methanol and CO oxidation [14, 16, 19-20, 24, 29-30, 34, 46-47]. Most of the studies are focused on Ru/Pt nanoparticles and Ru modified Pt (111) surface. Maillard et al. [19-20, 47] showed higher activity for methanol electrooxidation on Ru deposited Pt nanoparticle on carbon than PtRu alloy. Waszczuk et al.[46] showed similar results on Pt/Ru nanoparticle on gold support. CO oxidation on Pt single crystal electrodes modified with Ru[14, 16, 24-25, 29-30, 34, 45] has been well studied and they reported an enhancement in the oxidation of CO compared to pure Pt electrodes. A split peak was observed for CO oxidation on Ru modified Pt single crystals and Pt nanoparticles due to the presence of two CO populations on the electrode surface. Spectroscopy method such as Fourier transformed infrared (FTIR) [14, 19, 23, 25] have identified the CO adsorbed on Pt and CO adsorbed on Ru sites. The mechanism for CO oxidation is still not clear but it shows that the surface structure of Ru on Pt directly impacts the activity for CO oxidation.

Electrochemical deposition of monoatomic 2D noble metals by Monolayer Restricted Galvanic Displacement (MRGD) were shown by Brankovic and Adzic [48], where they deposited a less noble metal at UPD and replaced with a more noble metal at open circuit. They showed that two-dimensional growth of monoatomic Pt or Pd monolayers on Au by exchange of Pt^{+4} or Pd^{+2} ions for Cu at open circuit. MRGD are referred to as surface limited redox replacement (SLRR) reactions. Electrodeposition of noble metals by galvanic displacement have

been studied by Vasilic and Dimitrov [49-50], Mroek and Weaver [51] and Kim and Stickney [52-56]}.

Electrochemical surface limited reactions also referred to as underpotential deposition (UPD) [57]. UPD involves the formation of an atomic layer of one element on a second at a potential prior to that needed to deposit the element on itself. UPD is a thermodynamic process, where an atomic layer is formed as the result of the free energy of formation of a surface compound or alloy. Electrochemical atomic layer deposition (E-ALD) had been successfully used to grow wide variety of compound semiconductors [39, 58-64]. More recently the author's group has studied the use of UPD and SLRR cycles for the formation of E-ALD of metal nanofilms Cu [65] [55], Ru [66] and Pt [56].

Metal surfaces modified with various metal monolayers exhibit properties very different from the individual bulk metals [67]. The change in electronic properties is shown to improve the catalytic activities of the modified electrodes [68]. The catalytic activities of the modified electrodes are determined not only by the type of metal monolayer used but also depend on their distribution on the surface. Adzic et al. studied Pt monolayer deposition on metals and alloy carbon supported nanoparticles [69] as well as bimetallic systems consisting of transition metal monolayer (Ir, Ru, Rh, Re, Pt and Os) over Au, Pd or Pt layers, for oxygen reduction in fuel cells [42].

In the following studies, deposition of Ru modified Pt electrodes were prepared using E-ALD in an automated flow cell system using. Pb was used as the sacrificial metal for the SLRR. The Pt ALD cycle and Ru ALD cycle were used to prepare the modified electrodes. The maximum Ru coverage was calculated based on reaction stoichiometry. The catalytic activity of

Ru modified Pt electrodes towards CO electrooxidation are investigated by cyclic voltammetry in 0.5M sulfuric acid without taking the deposits from the cell.

Experimental

The solutions used were 1mM $Pb(ClO_4)_2$, 0.1mM $RuCl_3$ and 0.1mM $H_2PtCl_6.6H_2O$. The Pb solution was made with 0.5M $NaClO_4$ (pH 4.5). The Ru solution was made with 50 mM HCl (pH 1.5). The Pt solution was made with 50 mM $HClO_4$ (pH 1.3). The blank solution was 0.5M $NaClO_4$ (pH 4.5). Cyclic voltammograms were performed using 0.5M H_2SO_4. CO adsorption were carried out in CO saturated 0.5M H_2SO_4. Solutions were prepared using water from a Nanopure water filtration system (Barnstead, Dubuque, IA) (18MΩ) attached to the house DI water system. Chemicals were reagent grade or better. All the solution bottles were purged with nitrogen before the deposition process.

Electrochemical atomic layer depositions were conducted in an automated electrochemical flow cell system consisting of pump, valves, Plexiglas flow cell and a potentiostat [60, 70]. Computer using LABVIEW program controlled the components of the automated system. Most of the hardware used was previously described. A gold wire embedded in the Plexiglas flow cell was used as the auxiliary electrode. An Ag/AgCl (3M NaCl) (Bioanalytical systems, Inc.) electrode was used as reference electrode and all potentials, E, are quoted with respect to reversible hydrogen electrode (RHE). Glass slides with 3nm Ti adhesion layer and 300nm thick gold were used as substrates. Au was vapor deposited onto substrates held 280^o C, and then the deposits were annealed at 400^o C for 12 hours, resulting in a prominent (111) growth habit. These gold electrodes were cleaned in concentrated nitric acid by immersion for 2 minutes and then by electrochemical cycling upon insertion into the flow cell (0.5M H_2SO_4; Scan rate $10mVs^{-1}$).

Ru modified Pt electrodes are prepared using Pt ALD cycle and Ru ALD cycle. Pb was used as the sacrificial element for the redox replacement reaction. Pt ALD cycle contains steps where Pb atomic layer are replaced by Pt. Ru ALD cycle contains steps where Ru replaces Pb atomic layer. A program was used to deposit the modified electrodes. The solution flow rate of 9 mL/min was used during the deposition process. The geometric electrode area of deposition is $3.77cm^2$.

The electrodes prepared were characterized by cyclic voltammetry in 0.5M H_2SO_4 and the catalytic activity are studied by CO adsorption and electroxidation. Studies were performed in-situ on the as deposited film without taking them out of the cell. Cyclic voltammograms were recorded at a scan rate of $10mVs^{-1}$. The electrolytes are pumped in to the flow cell at a flow rate of 4mL/min from two different bottles, one containing 0.5M H_2SO_4 and the other containing CO saturated H_2SO_4. CO was adsorbed on to the electrode by flushing in CO saturated H_2SO_4 at 0.300V for 3 minutes and then rinsed out with 0.5M H_2SO_4 for 3 minutes, while the electrode was held at 0.300V. In the voltammetric experiments, the initial sweep was in the negative direction till 0.050V and the positive scan limit is set at 0.860V.

Results and Discussions

Deposition of ruthenium modified Pt electrodes by electrochemical ALD (E-ALD) using UPD and SLRR are reported in this paper. UPD and SLRR are incorporated in an ALD cycle for the deposition of Pt or Ru. They are referred to as Pt ALD and Ru ALD cycle. The cartoon representation of the Pt and Ru ALD cycle is shown in (Figure 1A and 1B). Pb was chosen as the sacrificial metal and is deposited at UPD to form an atomic layer. The sacrificial layer was then exposed to a solution containing ions of the desired element (noble metal) at open circuit for the redox replacement reaction to take place. $PtCl_6^{2-}$ ions are used in Pt ALD cycle while Ru^{3+} ions

are used in Ru ALD cycle. This process will result in an atomic layer of the noble metal (Pt or Ru).

Pb was used as the sacrificial metal for the deposition of Pt and Ru as previous studies in this group by Chandru et al.[66] showed that Ru cannot be deposited using Cu as the sacrificial metal. The driving force for the SLRR reaction ΔE between the sacrificial element and the depositing element should be large enough for the reaction to occur. Under potential deposition (UDP) of Pb on Au had been well studied by the author's group and others [71]. The UPD potential is determined from the cyclic voltammogram of Pb on Au.

The cyclic voltammogram of Pb is shown in Figure 3. Two continuous scan is shown here each to a more negative potentials. The CV displays a wide window for Pb UPD from 0.0V to -0.210V. Bulk Pb deposition begins near -0.220V, and displays a hysteresis loop, indicating a nucleation growth. Bulk Pb is stripped at -0.2V in the subsequent positive scan. Dealloying of Pb from Au is also evident at -0.1V, consistent with the literature [71]. Based on the CVs in Figure 3, a potential of -0.19V was selected for the deposition of Pb sacrifial layers in Pt ALD cycle to grow Pt nanofilm. Pb deposition potential in a Ru ALD cycle was varied between 10mV and -240mV vs. NHE to vary the Ru coverage on the surface.

Pt nanofilm deposition and Ru nanofilm deposition by E-ALD are described in detail by the author's group. The specific program for Pt depositions consists of: Pumping of the Pb^{2+} ions solution through the cell for 10 s, at -0.19 V, to form Pb UPD. The potential was then let go open circuit (OCP) and the $PtCl_6^{2-}$ ion solution was then pumped through the cell to facilitate the exchange of Pb UPD for a Pt atomic layer. The oxidation of Pb provides electrons for Pt deposition. The open circuit potential was monitored during the displacement process. Once the

OCP reached 0.21 V (the "stop potential"), the cell was rinsed with the blank solution for 6s at OCP and then 0.31 V for 5sec.

The Ru ALD cycle began the same way, Pb^{2+} ion solution pumped for 10 s at -0.010 V, for Pb UPD. Next, the Ru^{3+} ion solution was pumped through the cell at OCP, allowing exchange of Pb UPD for a Ru atomic layer. Once the OCP reached 0.21 V (the stop potential), the cell was rinsed with the blank solution, for 6s at OCP and then at 0.31 V for 5sec. The current-time (solid line) and potential-time (dashed line) plots for one E-ALD cycle of Pt and Ru are shown in Figure 3A and Figure3B respectively. The dotted line represents the OCP change-time during the replacement reaction.

Detailed studies of the Pt nanofilm formation and the significance of "Stop Potential" are previously reported by the author's group and will not be discussed here [56]. The Ru ALD cycles that were used for modifying the Pt surface will be discussed in detail. The amounts of Ru deposited were controlled by the amount of Pb deposited as the electrons are provided by Pb oxidation. The deposition of Ru from Ru^{+3} is a 3-electron process and should result in 2/3 coverage of the Pb atomic layer. Coverages are calculated and reported in (ML vs. Au (111)). The maximum Ru deposited were calculated from the Pb deposition charge and the reaction stoichiometry between Pb and Ru. The amount of Ru is then varied by simply varying the Pb deposition potential in the UPD region.

Previous studies on Ru modified Pt (111) electrodes have shown monoatomic Ru island by STM [23] with 10% of Ru deposited exhibiting a bilayer configuration. This bilayer behavior is seen for Ru coverages larger than 0.40ML [26, 72]. The bilayer growth is exhibited on Ru deposited on Pt by ebeam evaporation at room temperature as Ru-Ru exhibits strong interaction compared to Pt-Ru [73-74].

In the initial studies the Ru modified Pt electrodes are prepared by depositing a Pt nanofilm followed by Ru atomic layer. In all the studies, a 25 cycles Pt nanofilm deposited on gold, Pb UPD of -190mV, serves as the substrate. The software was programmed to continuously deposit 25 cycles Pt and one cycle Ru. The amount of Ru in each of the deposits was varied by choosing different Pb UPD potentials in the range of $-240mV \geq E \leq 10mV$. For the first electrode, a Pb UPD potential of 10mV was chosen to deposit Ru (Figure 3B). The charge for Pb deposition is 0.24ML, which correlates to a maximum coverage of 0.16ML Ru. Immediately after deposition the electrode is held at 0.31V in the cell and is at potential control all the time. The catalytic activities are studied by CO adsorption and oxidation. The adsorption were carried out for 3 minutes in CO saturated 0.5M H_2SO_4 and then rinsed out with CO free 0.5M H_2SO_4 for 3 minutes, while the electrode was held at 0.31V. Figure 4 shows CO stripping voltammetry in 0.5M H_2SO_4 with Ru coverage of 0.16ML. The initial negative going scan shows no hydrogen adsorption, as the surface has been blocked by adsorbed CO. After each CO adsorption, two continuous scan were done between 60mV and 860mV. The first positive scan is to completely oxidize the CO and the second positive scan is to verify that all CO is completely oxidized. The CO oxidation starts around 600mV and a single peak for CO electrooxidation takes place with the peak potential is at 706mV. The entire sequences starting from preparing the electrodes to CO oxidation were repeated with different Ru coverage. Figure 5 lists the Pb deposition potentials, Pb coverage as well as the maximum Ru coverage that could be achieved.

The CO oxidation of the modified electrodes with Ru coverage of 0.16, 0.20, 0.35, 0.39 and 0.83 ML under the voltammetric conditions is shown in Figure 6. CO stripping voltammetry performed on a 25 cycles Pt deposit and a 25 cycles Ru deposit were used for comparison (Figure 6) with the modified electrodes. The CO oxidation on Ru electrode starts at 430mV with

a peak potential of 580mV. The onset and peak potential for the Pt electrode are 730mV and 790mV respectively. The Ru modified electrodes shows a substantial enhancement in the electrocatalytic oxidation of adsorbed CO. Increasing the amounts of Ru shifts both the CO electrooxidation peak potential and the onset potential to more negative values compared to CO oxidation on pure Pt electrode. For the electrode modified with 0.83 ML Ru, a negative potential shift of about 130mV (onset potential) compared to pure Pt can be seen. A single broad peak (A shoulder appears to the right) is observed compared the split peak observed on Ru modified Pt single crystal as reported in the literature [25, 30, 34, 75] and Ru modified Pt nanoparticles [19]. The addition of Ru on Pt increased the CO tolerance of the electrodes compared to pure Pt electrodes. The single broad peak may also be a result of contaminted Pt substrate as Pt electrode gets contaminated quickly with the solutions being flowed continuously [56, 76]. A sharp peak appears on a cleaner surface. To investigate the effect of surface cleaning, 25 cycles Pt nanofilm was prepared and the electrode was cycled in 0.5M H_2SO_4 between 50mV and 1410mV. The steady state voltammogram of a clean Pt electrode is shown in Figure 7. Ru coverage of 0.35ML was deposited on to the electrode. The differences in the CO oxidation on the modified electrodes without (dotted line) and with cleaning (solid line) the Pt electrodes are shown in Figure 8. A sharp peak was observed on the clean Pt electrode with Ru compared to the broad peak observed on contaminated Pt. For all further studies, the Pt electrode was cleaned before Ru deposition.

In the second set of experiment the Ru modified Pt electrodes were prepared by adding Ru in small incremental on to the same Pt electrode. A 25 cycle Pt nanofilm was prepared and cleaned in 0.5M H_2SO_4 by potential cycling. Ru was then deposited on to Pt at a Pb UPD potential of 10mV, resulting in coverage of 0.31ML Ru. Immediately after Ru deposition, CO

adsorption and electrooxidation were carried out on the electrode. Figure 10 shows CO stripping voltammograms recorded in 0.5M H_2SO_4 at a scan rate of $10mVs^{-1}$ for the oxidation of adsorbed CO. After each CO adsorption, two continuous scan were done between 60mV and 860mV. The first positive scan (solid line) completely oxidizes the adsorbed CO, which is confirmed by the second scan (dotted line). The CO oxidation starts around 600mV and a single peak for CO electrooxidation takes place with the peak potential is at 706mV. The process of Ru deposition, CO adsorption and oxidation were carried out for 5 consecutive cycles to study the effect of CO electrooxidation with increasing Ru content. Figure 11 shows the CO stripping voltammetry after each Ru addition. It can be seen that the onset and peak potential shifts positive after each addition contrary to that expected. The onset and peak potential for CO oxidation was expected to shift negative with each addition. This indicates that at lower Ru coverage, CO adsorption and oxidation significantly affects the Ru layer. Also Ru dissolution is possible in the acidic medium when scanned till 850mV.

Since it appears that Ru is being lost after CO adsorption and oxidation, the experiment was designed to deposit 5 consecutive cycles Ru (Pb at 10mV) followed by CO adsorption and oxidation. Figure 12 shows the CVs for three continuous CO adsorption and oxidation. The first CO oxidation peak exhibits a broad feature while the second and third CO oxidation peak appears to be relatively unchanged. The adsorption of oxygen species occurs at potentials 530mV, approximately 220mV more negative than on Pt electrode. Also it can be seen that in Figure 12 the peaks shifts negative compared to Figure 11 where the peaks shifted positive, indicating a more homogeneous distribution of bimetallic pairs and stable structure being formed on the surface.

In order to see how stable these structures were on to the Pt surface, 12 continuous cycles of CO adsorption and oxidation were performed in the flow cell under the voltammetric conditions. Pb UPD of -190mV was chosen for Ru deposition cycle. Stability study involves the following steps: Pt nanofilm deposition, cleaning of Pt electrode by potential cycling to reach the steady state voltammogram given in Figure 7, one cycle Ru and 12 continuous cycle CO adsorption and oxidation. Figure 13 is a sequence of CO adsorption followed by oxidation, from the surface of Pt nanofilm on which 0.35 ML Ru were deposited. The first CO oxidation is similar to that seen in Figure 6 and Figure 8 for 0.35 ML Ru coverage. The CO oxidation peak shifts positive from cycle to cycle and the 12^{th} cycle CO oxidation peak resembles that on the Pt electrode. The amount of Ru is systematically reduced by this process, due to a small amount of dissolution in the acidic blank when scanned till 860mV.

The stability tests were repeated with 2 cycles Ru and three cycles Ru on Pt nanofilm. Figure 14 and Figure 15 shows the CO oxidation with 0.75ML Ru and 1.34 ML Ru. Pt electrode modified with 1.34 ML Ru shows a stable CO oxidation compared to the Pt electrode modified with one cycle and two cycles Ru, indicating a more stable structure on the surface.

Conclusions

Ru modified Pt nanofilm deposition by electrochemical ALD was reported. Pb was used as the sacrificial metal for the deposition of Pt and Ru. Ru atomic layer was deposited on a 25 cycle Pt nanofilms. Ru coverages varying between 0.16 ML - 0.83 ML were deposited and their activity towards CO electrooxidation were studied. The electrocatalytic activity of the Ru modified Pt electrodes showed higher CO tolerance with a negative potential shift of about 200mV compared to Pure Pt electrodes.

Acknowledgements

Support from the National Science Foundation, as well as the Department of Energy, is acknowledged, and greatly appreciated.

References

1. Igarashi, H., et al., *CO Tolerance of Pt alloy electrocatalysts for polymer electrolyte fuel cells and the detoxification mechanism.* Physical Chemistry Chemical Physics, 2001. **3**(3): p. 306-314.
2. Petrii, O.A., *Pt-Ru electrocatalysts for fuel cells: a representative review.* Journal of Solid State Electrochemistry, 2008. **12**(5): p. 609-642.
3. Hsieh, Y.-C., et al., *Displacement Reaction in Pulse Current Deposition of PtRu for Methanol Electro-Oxidation.* Journal of the Electrochemical Society, 2009. **156**(6): p. B735-B742.
4. Strasser, P., et al., *High Throughput Experimental and Theoretical Predictive Screening of Materials − A Comparative Study of Search Strategies for New Fuel Cell Anode Catalysts.* The Journal of Physical Chemistry B, 2003. **107**(40): p. 11013-11021.
5. Whitacre, J.F., T. Valdez, and S.R. Narayanan, *Investigation of Direct Methanol Fuel Cell Electrocatalysts Using a Robust Combinatorial Technique.* Journal of the Electrochemical Society, 2005. **152**(9): p. A1780-A1789.
6. Watanabe, M. and S. Motoo, *Electrocatalysis by ad-atoms: Part II. Enhancement of the oxidation of methanol on platinum by ruthenium ad-atoms.* Journal of Electroanalytical Chemistry, 1975. **60**(3): p. 267-273.
7. Watanabe, M. and S. Motoo, *Electrocatalysis by ad-atoms: Part III. Enhancement of the oxidation of carbon monoxide on platinum by ruthenium ad-atoms.* Journal of Electroanalytical Chemistry, 1975. **60**(3): p. 275-283.

8. Krausa, M. and W. Vielstich, *Study of the electrocatalytic influence of Pt/Ru and Ru on the oxidation of residues of small organic molecules.* Journal of Electroanalytical Chemistry, 1994. **379**(1-2): p. 307-314.

9. Tong, et al., *An NMR Investigation of CO Tolerance in a Pt/Ru Fuel Cell Catalyst.* Journal of the American Chemical Society, 2001. **124**(3): p. 468-473.

10. Yajima, T., et al., *Adsorbed water for the electro-oxidation of methanol at Pt-Ru alloy.* Chemical Communications, 2003(7): p. 828-829.

11. Ianniello, R., et al., *CO adsorption and oxidation on Pt and Pt---Ru alloys: dependence on substrate composition.* Electrochimica Acta, 1994. **39**(11-12): p. 1863-1869.

12. Gasteiger, H.A., et al., *Carbon monoxide electrooxidation on well-characterized platinum-ruthenium alloys.* The Journal of Physical Chemistry, 1994. **98**(2): p. 617-625.

13. Gasteiger, H.A., et al., *Electro-oxidation of small organic molecules on well-characterized Pt---Ru alloys.* Electrochimica Acta, 1994. **39**(11-12): p. 1825-1832.

14. Friedrich, K.A., et al., *CO adsorption and oxidation on a Pt(111) electrode modified by ruthenium deposition: an IR spectroscopic study.* Journal of Electroanalytical Chemistry, 1996. **402**(1-2): p. 123-128.

15. Chrzanowski, W., H. Kim, and A. Wieckowski, *Enhancement in methanol oxidation by spontaneously deposited ruthenium on low-index platinum electrodes.* Catalysis Letters, 1998. **50**(1): p. 69-75.

16. Davies, J.C., B.E. Hayden, and D.J. Pegg, *The electrooxidation of carbon monoxide on ruthenium modified Pt(110).* Electrochimica Acta, 1998. **44**(6-7): p. 1181-1190.

17. Zei, M.S., T. Lei, and G. Ertl, *Spontaneous and electrodeposition of Pt on Ru(0001).* Zeitschrift Fur Physikalische Chemie-International Journal of Research in Physical Chemistry & Chemical Physics, 2003. **217**(5): p. 447-458.

18. Kuk, S.T. and A. Wieckowski, *Methanol electrooxidation on platinum spontaneously deposited on unsupported and carbon-supported ruthenium nanoparticles.* Journal of Power Sources, 2005. **141**(1): p. 1-7.

19. Maillard, F., et al., *Electrooxidation of Carbon Monoxide at Ruthenium-Modified Platinum Nano-particles: Evidence for CO Surface Mobility.* Fuel Cells, 2002. **2**(3-4): p. 143-152.

20. Maillard, F., F. Gloaguen, and J.M. Leger, *Preparation of methanol oxidation electrocatalysts: ruthenium deposition on carbon-supported platinum nanoparticles.* Journal of Applied Electrochemistry, 2003. **33**(1): p. 1-8.

21. Iwasita, T., et al., Electrochim. Acta, 1994. **39**: p. 1817.

22. Kabbabi, A., et al., *In situ FTIRS study of the electrocatalytic oxidation of carbon monoxide and methanol at platinum-ruthenium bulk alloy electrodes.* Journal of Electroanalytical Chemistry, 1998. **444**(1): p. 41-53.

23. Cramm, S., et al., *Surface structural and chemical characterization of Pt/Ru composite electrodes: A combined study by XPS, STM and IR spectroscopy.* Fresenius Journal of Analytical Chemistry, 1997. **358**(1-2): p. 189-192.

24. Lin, W.F., et al., *Electrocatalytic Activity of Ru-Modified Pt(111) Electrodes toward CO Oxidation.* The Journal of Physical Chemistry B, 1999. **103**(33): p. 6968-6977.

25. Friedrich, K.A., et al., *Fundamental aspects in electrocatalysis: from the reactivity of single-crystals to fuel cell electrocatalysts.* Journal of Electroanalytical Chemistry, 2002. **524-525**: p. 261-272.

26. Herrero, E., J.M. Feliu, and A. Wieckowski, *Scanning tunneling microscopy images of ruthenium submonolayers spontaneously deposited on a Pt(111) electrode.* Langmuir, 1999. **15**(15): p. 4944-4948.

27. Crown, A. and A. Wieckowski, *Scanning tunneling microscopy investigations of ruthenium- and osmium-modified Pt(100) and Pt(110) single crystal substrates.* Physical Chemistry Chemical Physics, 2001. **3**(16): p. 3290-3296.

28. Babu, P.K., et al., *Electronic Alterations Caused by Ruthenium in Pt-Ru Alloy Nanoparticles as Revealed by Electrochemical NMR.* The Journal of Physical Chemistry B, 2003. **107**(31): p. 7595-7600.

29. Brankovic, S.R., et al., *Electrosorption and catalytic properties of bare and Pt modified single crystal and nanostructured Ru surfaces.* Journal of Electroanalytical Chemistry, 2002. **524-525**: p. 231-241.

30. Davies, J.C., et al., *The electro-oxidation of carbon monoxide on ruthenium modified Pt(111).* Surface Science, 2002. **496**(1-2): p. 110-120.

31. Goswami, J., et al., *Properties of Platinum Films by Liquid-Source MOCVD in H 2 and O 2.* Integrated Ferroelectrics, 2002. **42**(1): p. 13 - 23.

32. Green, C.L. and A. Kucernak, *Determination of the Platinum and Ruthenium Surface Areas in Platinum−Ruthenium Electrocatalysts by Underpotential Deposition of Copper. 2. Effect of Surface Composition on Activity.* The Journal of Physical Chemistry B, 2002. **106**(44): p. 11446-11456.

33. Gülzow, E., et al., *Study of membrane electrode assemblies for direct methanol fuel cells.* Journal of Power Sources, 2002. **105**(2): p. 261-266.

34. Lu, G.Q., P. Waszczuk, and A. Wieckowski, *Oxidation of CO adsorbed from CO saturated solutions on the Pt(111)/Ru electrode.* Journal of Electroanalytical Chemistry, 2002. **532**(1-2): p. 49-55.

35. Markovic, N.M. and P.N. Ross, *Surface science studies of model fuel cell electrocatalysts.* Surface Science Reports, 2002. **45**(4-6): p. 117-229.

36. Samjeské, G., et al., *CO and methanol oxidation at Pt-electrodes modified by Mo.* Electrochimica Acta, 2002. **47**(22-23): p. 3681-3692.

37. Strbac, S., et al., *In situ STM imaging of spontaneously deposited ruthenium on Au(111).* Surface Science, 2002. **517**(1-3): p. 207-218.

38. Valet, O., et al., *Study of platinum thin films deposited by MOCVD as electrodes for oxide applications.* Microelectronic Engineering, 2002. **64**(1-4): p. 457-463.

39. Varazo, K., et al., *Formation of the first monolayers of CdTe on Au(111) by electrochemical atomic layer epitaxy (EC-ALE): studied by LEED, Auger, XPS, and in-situ STM.* Journal of Electroanalytical Chemistry, 2002. **522**(1): p. 104-114.

40. Waibel, H.F., et al., *Initial stages of Pt deposition on Au(111) and Au(100).* Electrochimica Acta, 2002. **47**(9): p. 1461-1467.

41. Waszczuk, P., et al., *UHV and electrochemical studies of CO and methanol adsorbed at platinum/ruthenium surfaces, and reference to fuel cell catalysis.* Electrochimica Acta, 2002. **47**(22-23): p. 3637-3652.

42. Zhou, W.P., et al., *Improving Electrocatalysts for O-2 Reduction by Fine-Tuning the Pt-Support Interaction: Pt Monolayer on the Surfaces of a Pd3Fe(111) Single-Crystal Alloy.* Journal of the American Chemical Society, 2009. **131**(35): p. 12755-12762.

43. Xing, Y., et al., *Enhancing Oxygen Reduction Reaction Activity via Pd,àíAu Alloy Sublayer Mediation of Pt Monolayer Electrocatalysts.* The Journal of Physical Chemistry Letters, 2010. **1**(21): p. 3238-3242.

44. Zhang, J.L., et al., *Mixed-metal Pt monolayer electrocatalysts for enhanced oxygen reduction kinetics.* Journal of the American Chemical Society, 2005. **127**(36): p. 12480-12481.

45. Davies, J.C., B.E. Hayden, and D.J. Pegg, *The modification of Pt(110) by ruthenium: CO adsorption and electro-oxidation.* Surface Science, 2000. **467**(1-3): p. 118-130.

46. Waszczuk, P., et al., *Methanol Electrooxidation on Platinum/Ruthenium Nanoparticle Catalysts.* Journal of Catalysis, 2001. **203**(1): p. 1-6.

47. Maillard, F., et al., *Ru-decorated Pt surfaces as model fuel cell electrocatalysts for CO electrooxidation.* Journal of Physical Chemistry B, 2005. **109**(34): p. 16230-16243.

48. Brankovic, S.R., J.X. Wang, and R.R. Adzic, *Metal monolayer deposition by replacement of metal adlayers on electrode surfaces.* Surface Science, 2001. **474**(1-3): p. L173-L179.

49. Vasilic, R. and N. Dimitrov, *Epitaxial growth by monolayer-restricted galvanic displacement.* Electrochemical and Solid State Letters, 2005. **8**(11): p. C173-C176.

50. Vasilic, R., L.T. Viyannalage, and N. Dimitrov, *Epitaxial growth of Ag on Au(111) by galvanic displacement of Pb and Tl monolayers.* Journal of the Electrochemical Society, 2006. **153**(9): p. C648-C655.

51. Mrozek, M.F., Y. Xie, and M.J. Weaver, *Surface-Enhanced Raman Scattering on Uniform Platinum-Group Overlayers: Preparation by Redox Replacement of Underpotential-Deposited Metals on Gold.* Analytical Chemistry, 2001. **73**(24): p. 5953-5960.

52. Kim, Y.-G., et al., *Platinum Nanofilm Formation by EC-ALE via Redox Replacement of UPD Copper: Studies Using in-Situ Scanning Tunneling Microscopy.* The Journal of Physical Chemistry B, 2006. **110**(36): p. 17998-18006.

53. Kim, J.Y., Y.G. Kim, and J.L. Stickney, *Copper nanofilm formation by electrochemical atomic layer deposition - Ultrahigh-vacuum electrochemical and in situ STM studies.* Journal of the Electrochemical Society, 2007. **154**(4): p. D260-D266.

54. Kim, J.Y., Y.G. Kim, and J.L. Stickney, *Cu nanofilm formation by electrochemical atomic layer deposition (ALD) in the presence of chloride ions.* Journal of Electroanalytical Chemistry, 2008. **621**(2): p. 205-213.

55. Thambidurai, C., et al., *E-ALD of Cu Nanofilms on Ru/Ta Wafers Using Surface Limited Redox Replacement.* Journal of the Electrochemical Society, 2010. **157**(8): p. D466-D471.

56. Jayaraju, N., D. Vairavapandian, and J.L. Stickney, *Electrochemical Atomic Layer Deposition (ALD) of Pt Nanofilms.* In Prep, 2010.

57. Kolb, D.M., *Physical and Electrochemcial Properties of Metal Monolayers on Metallic Substrates*, in *Advances in Electrochemistry and Electrochemical Engineering*, H. Gerischer and C.W. Tobias, Editors. 1978, John Wiley: New York. p. 125.

58. Innocenti, M., et al., *CdS and ZnS Deposition on Ag(111) by Electrochemical Atomic Layer Epitaxy.* Journal of the Electrochemical Society, 2001. **148**(5): p. C357-C362.

59. Mathe, M.K., et al., *Deposition of CdSe by EC-ALE.* Journal of Crystal Growth, 2004. **271**(1-2): p. 55-64.

60. Mathe, M.K., et al., *Formation of HgSe Thin Films Using Electrochemical Atomic Layer Epitaxy.* Journal of the Electrochemical Society, 2005. **152**(11): p. C751-C755.

61. Venkatasamy, V., et al., *Deposition of HgTe by electrochemical atomic layer epitaxy (EC-ALE).* Journal of Electroanalytical Chemistry, 2006. **589**(2): p. 195-202.

62. Wade, T.L., et al., *Electrodeposition of InAs.* Electrochemical and Solid-State Letters, 1999. **2**(12): p. 616-618.

63. Wade, T.L., et al., *Electrochemical formation of a III-V compound semiconductor superlattice: InAs/InSb.* Journal of Electroanalytical Chemistry, 2001. **500**(1-2): p. 322-332.

64. Banga, D.O., et al., *Formation of PbTe nanofilms by electrochemical atomic layer deposition (ALD).* Electrochimica Acta, 2008. **53**(23): p. 6988-6994.

65. Thambidurai, C., et al., *Copper Nanofilm Formation by Electrochemical ALD.* Journal of the Electrochemical Society, 2009. **156**(8): p. D261-D268.

66. Thambidurai, C., Y.-G. Kim, and J.L. Stickney, *Electrodeposition of Ru by atomic layer deposition (ALD).* Electrochimica Acta, 2008. **53**(21): p. 6157-6164.

67. Ruckman, M.W. and M. Strongin, *Monolayer Metal Films on Metallic Surfaces: Correlation between Electronic Structure and Molecular Chemisorption.* Accounts of Chemical Research, 1994. **27**(8): p. 250-256.

68. Zhang, J., et al., *Controlling the Catalytic Activity of Platinum-Monolayer Electrocatalysts for Oxygen Reduction with Different Substrates13.* Angewandte Chemie International Edition, 2005. **44**(14): p. 2132-2135.

69. Adzic, R.R., et al., *Platinum Monolayer Fuel Cell Electrocatalysts.* Topics in Catalysis, 2007. **46**(3/4): p. 249-262.

70. Stickney, J.L., *Electrochemical Atomic Layer Epitaxy (EC-ALE): Nanoscale Control in the Electrodeposition of Compound Semiconductors*, in *Advances in Electrochemical Science and Engineering*, R.C. Alkire and D.M. Kolb, Editors. 2002, Wiley-VCH: Weinheim. p. 1-105.

71. Green, M.P., et al., *Insitu Scanning Tunneling Microscopy Studies of the Underpotential Deposition of Lead on Au(111).* Journal of Physical Chemistry, 1989. **93**(6): p. 2181-2184.

72. Lin, W.F., T. Iwasita, and W. Vielstich, *Catalysis of CO electrooxidation at Pt, Ru, and PtRu alloy. An in situ FTIR study.* Journal of Physical Chemistry B, 1999. **103**(16): p. 3250-3257.

73. A.Berko, et al., *From bilayer to monolayer growth: Temperature effects in the growth of Ru on Pt(111).* Surface Science, 2009. **603**(16): p. 2556-2563.

74. Bergbreiter, A., et al., *On the origin of Ru bilayer island growth on Pt(111).* Vacuum, 2009. **84**(1): p. 13-18.

75. Massong, H., et al., Electrochim. Acta, 2000. **46**: p. 701.

76. López-Cudero, A., et al., *CO electrooxidation on carbon supported platinum nanoparticles: Effect of aggregation.* Journal of Electroanalytical Chemistry, 2009. **In Press, Corrected Proof**.

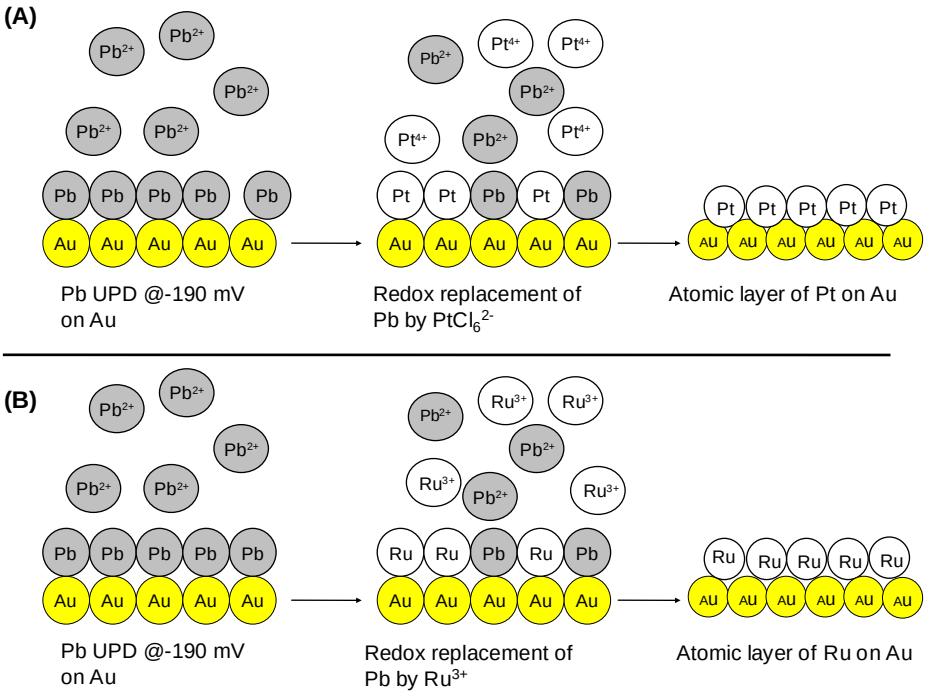

Figure 4.1. Cartoon representation of A) Pt E-ALD cycle and B) Ru E-ALD cycle.

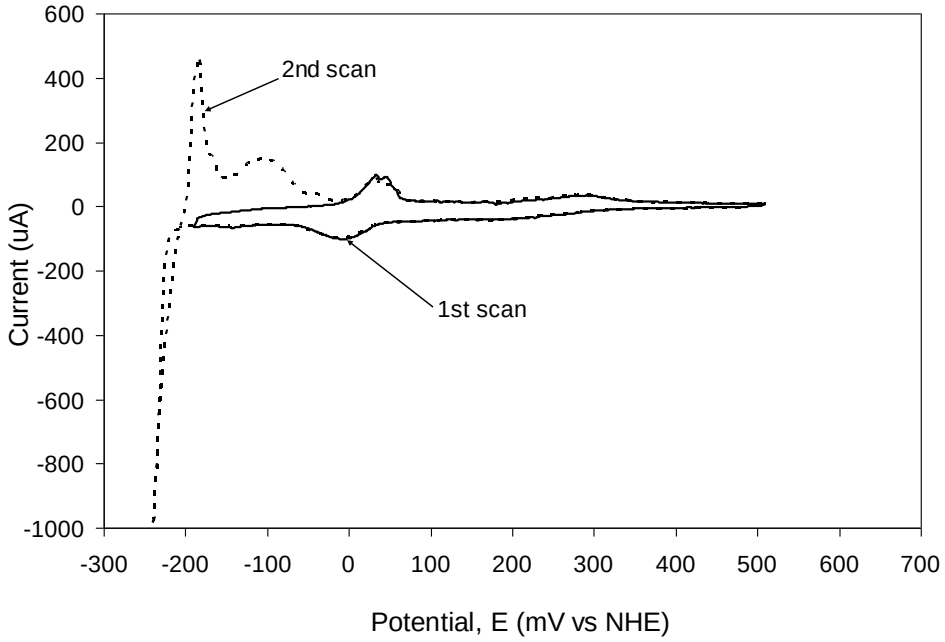

Figure 4.2. Cyclic voltammogram of Au in 1mM $Pb(ClO_4)_2$ with 0.5M $NaClO_4$; pH~ 4.5; Scan rate: $10mVs^{-1}$.

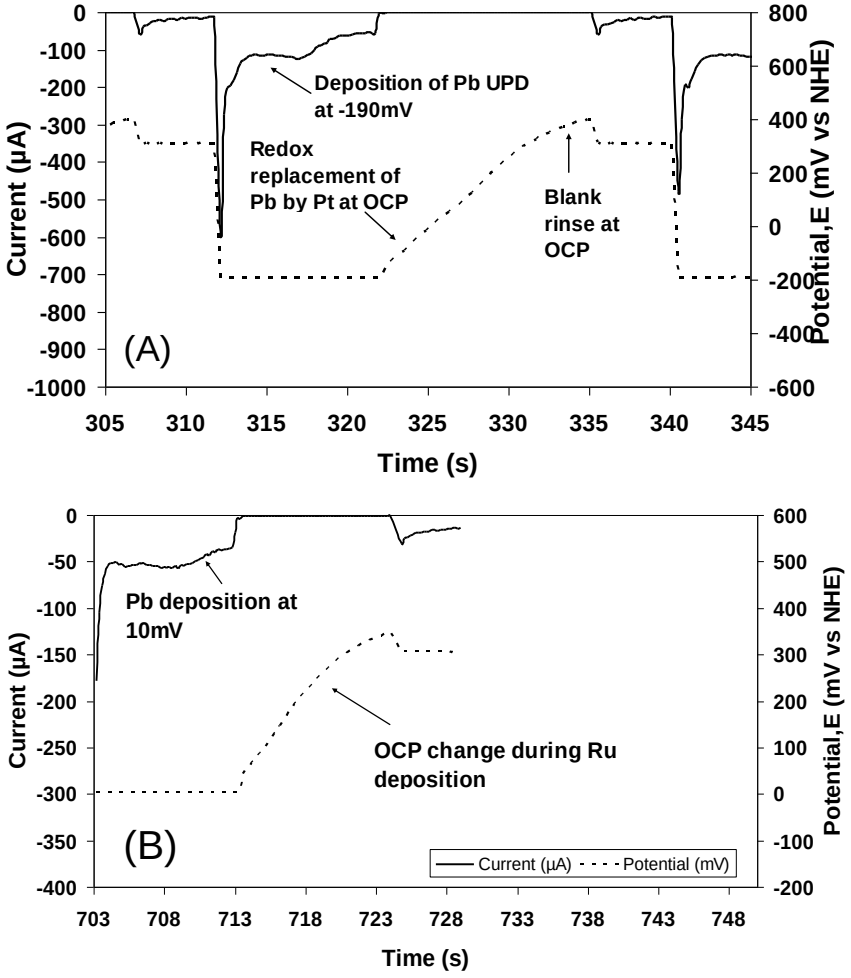

Figure 4.3. Time-Current-Potential graph for: A) one Pt E-ALD cycle and B) one Ru E-ALD cycle.

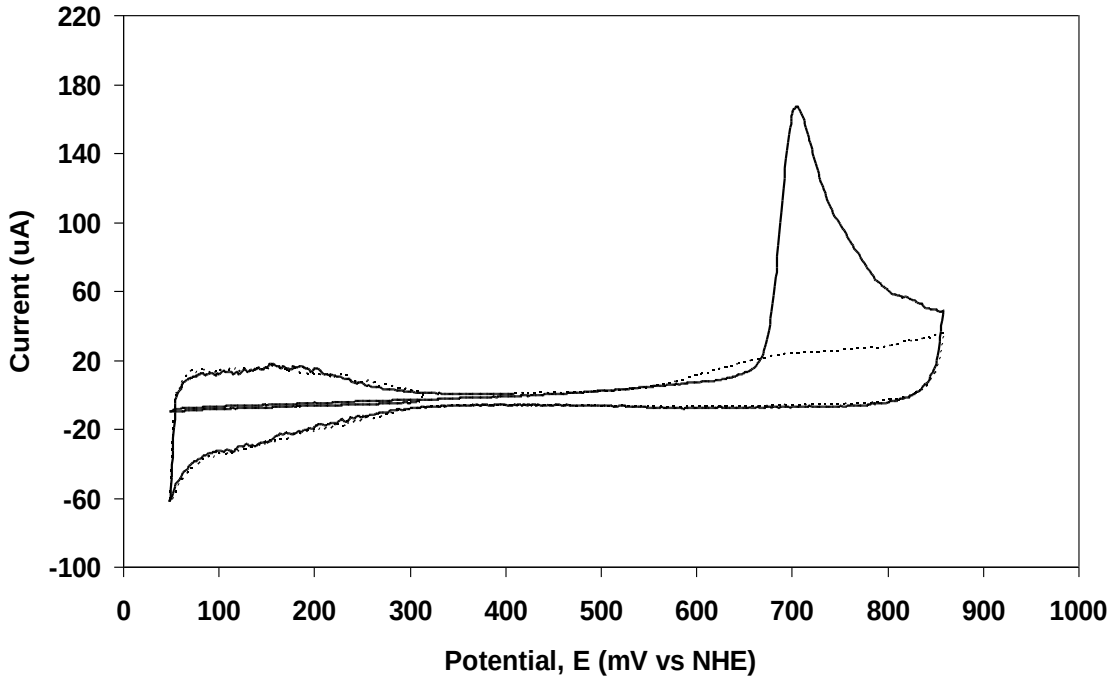

Figure 4.4. Cyclic voltammetry (0.5M H_2SO_4, 10mVs^{-1}) for CO stripping on 0.16ML Ru modified Pt electrode.

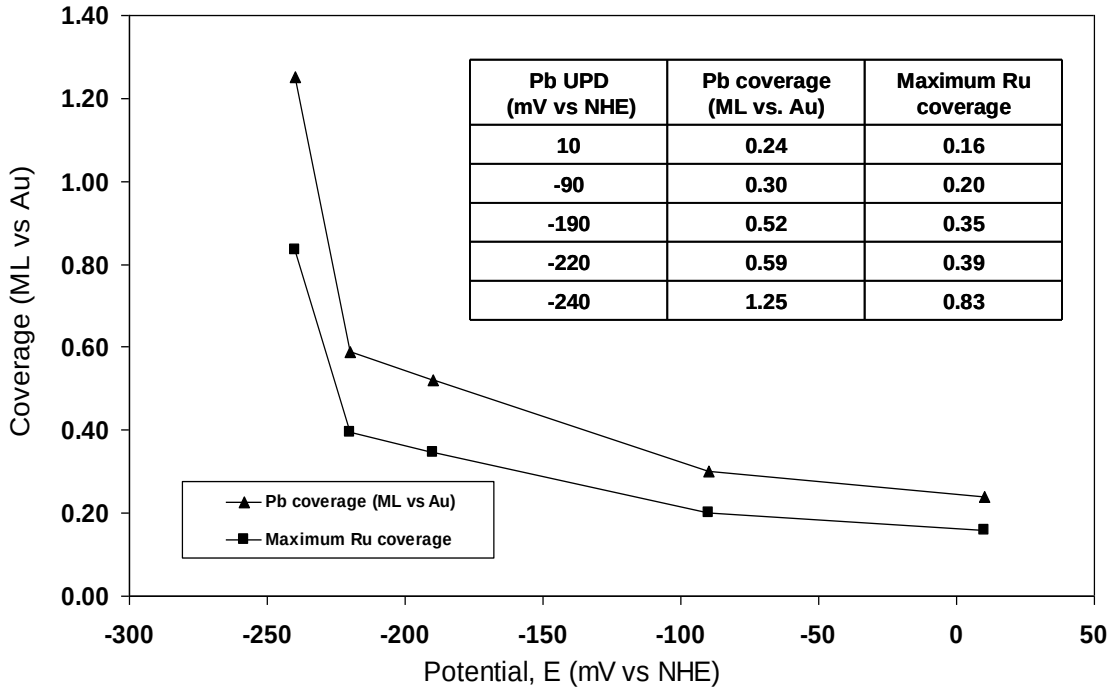

Pb UPD (mV vs NHE)	Pb coverage (ML vs. Au)	Maximum Ru coverage
10	0.24	0.16
-90	0.30	0.20
-190	0.52	0.35
-220	0.59	0.39
-240	1.25	0.83

Figure 4.5. (▲) Points represent the Pb coverage and (■) represents the maximum Ru coverage possible from reaction stoichiometry at the corresponding Pb deposition potentials used for modifying the Pt surface.

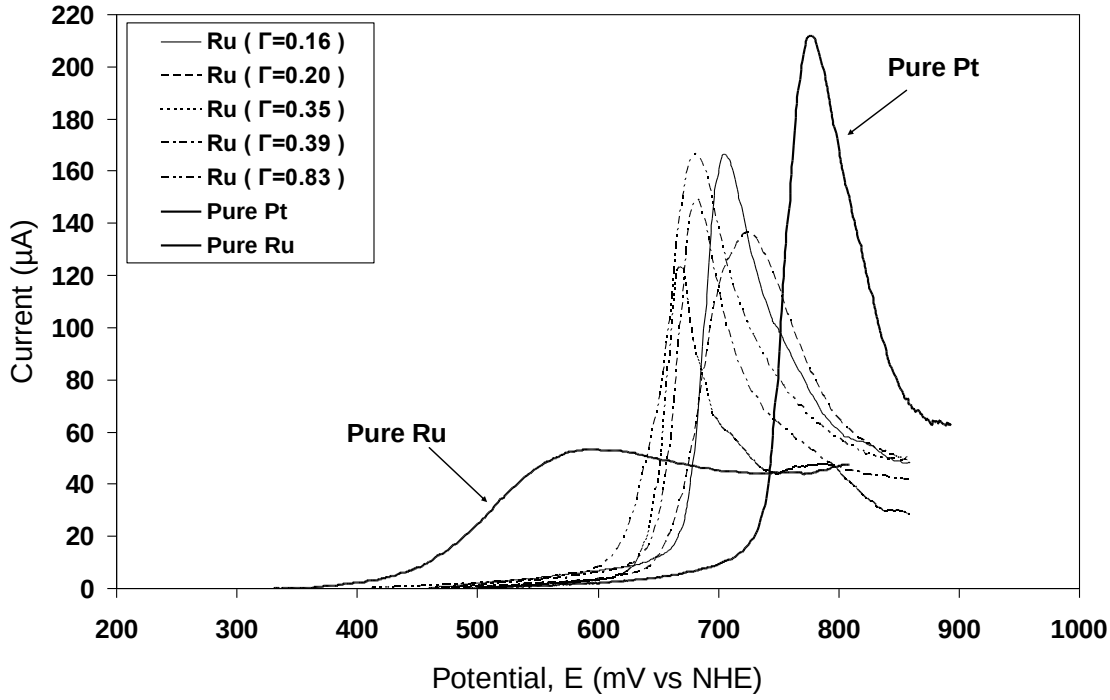

Figure 4.6. CO oxidation curves on the Pt electrode modified with 0.16ML, 0.20ML, 0.35ML, 0.39ML and 0.83 ML Ru in 0.5M H_2SO_4; Scan rate: $10mVs^{-1}$.

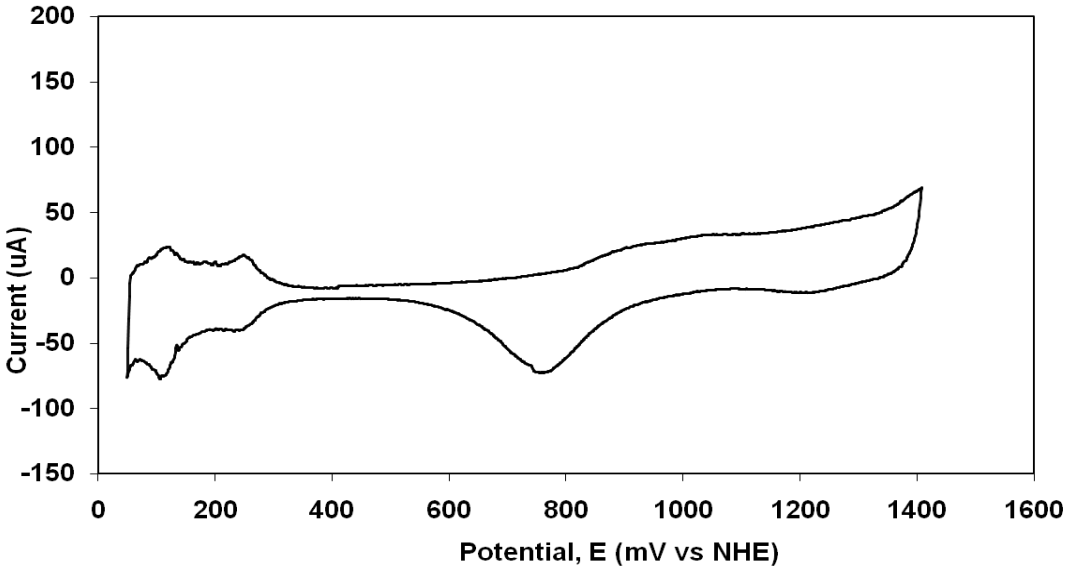

Figure 4.7. CV of a clean Pt electrode in 0.5M H_2SO_4; Scan rate: $10mVs^{-1}$.

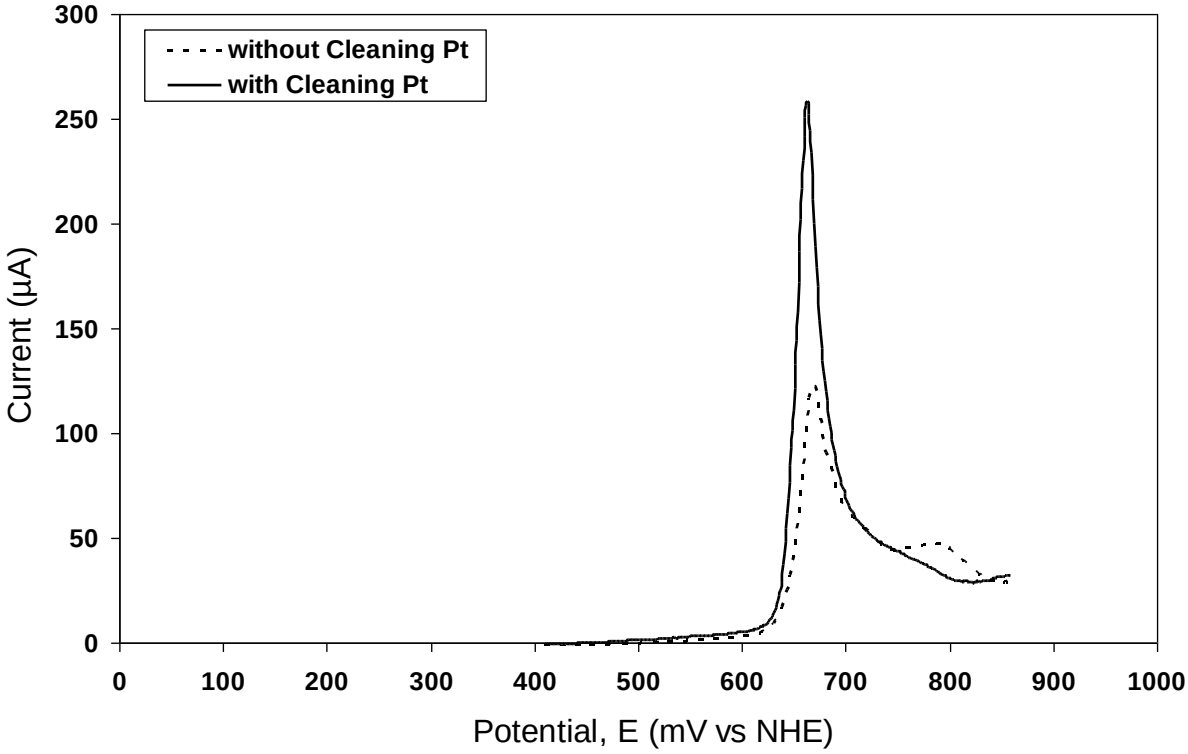

Figure 4.8. CO oxidation on the Pt electrode modified with 0.35ML Ru in 0.5M H_2SO_4; Scan rate: 10mVs^{-1}. (---) Represents Ru on contaminated Pt nanofilm and (—) represents Ru on cleaned Pt nanofilm electrode.

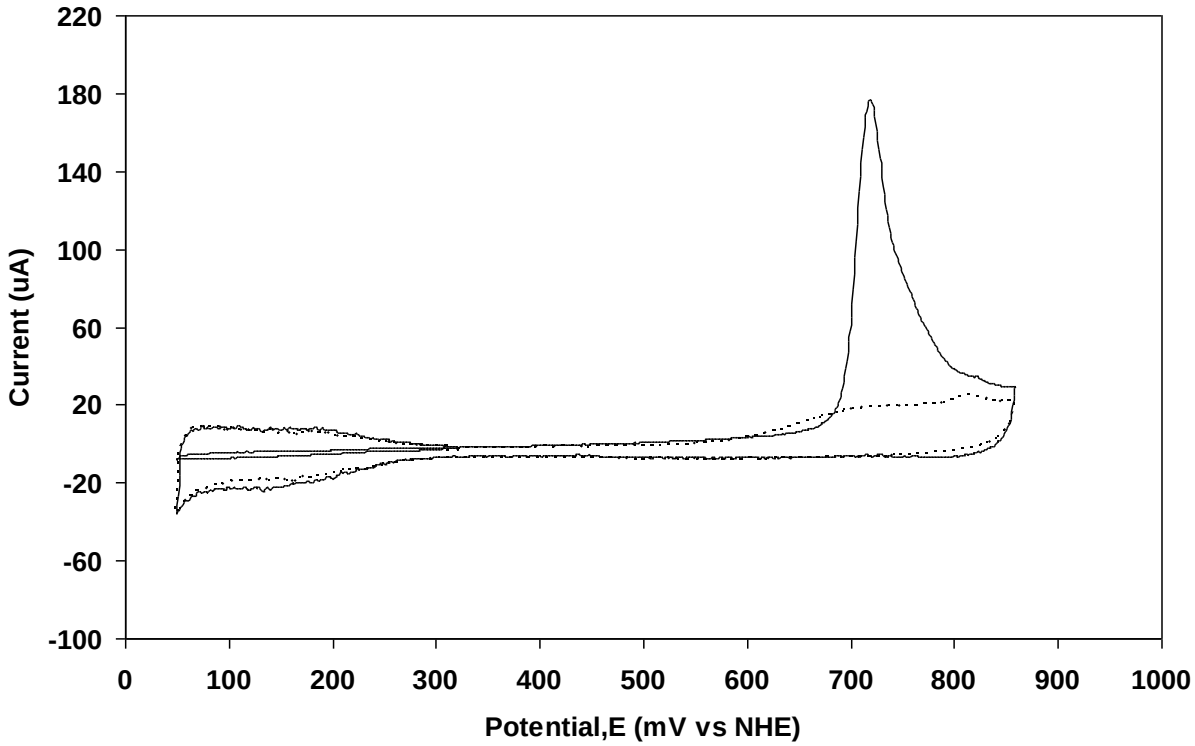

Figure 4.9. CO stripping voltammogram (0.5M H_2SO_4, 10mVs^{-1}) on the Pt surface modified with 0.31ML Ru.

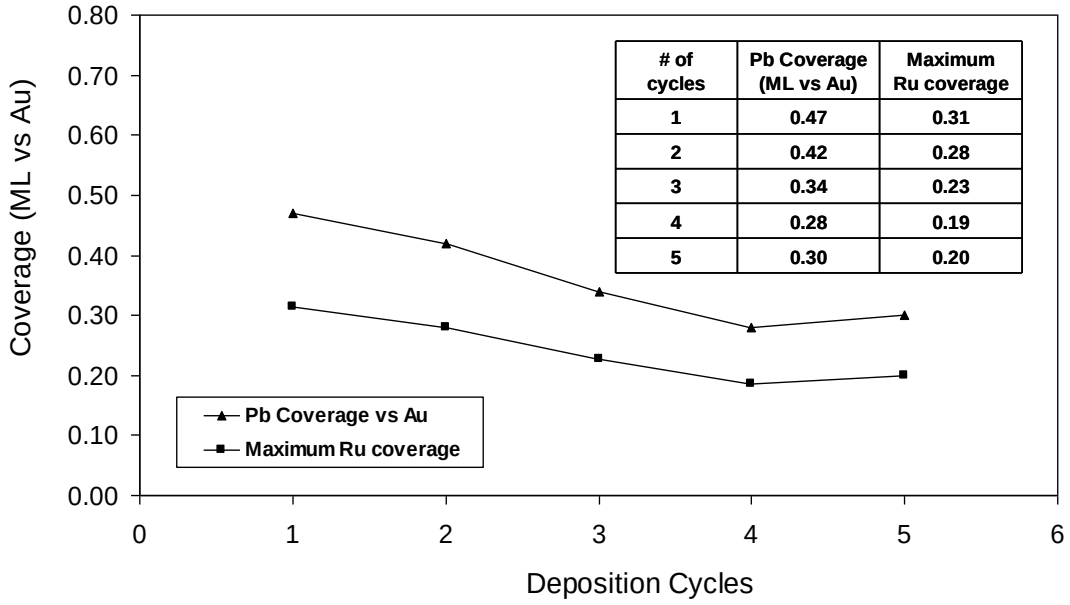

# of cycles	Pb Coverage (ML vs Au)	Maximum Ru coverage
1	0.47	0.31
2	0.42	0.28
3	0.34	0.23
4	0.28	0.19
5	0.30	0.20

Figure 4.10. (▲) Points represent Pb coverage and (■) represents the maximum Ru coverage possible from reaction stoichiometry as a function of deposition cycles.

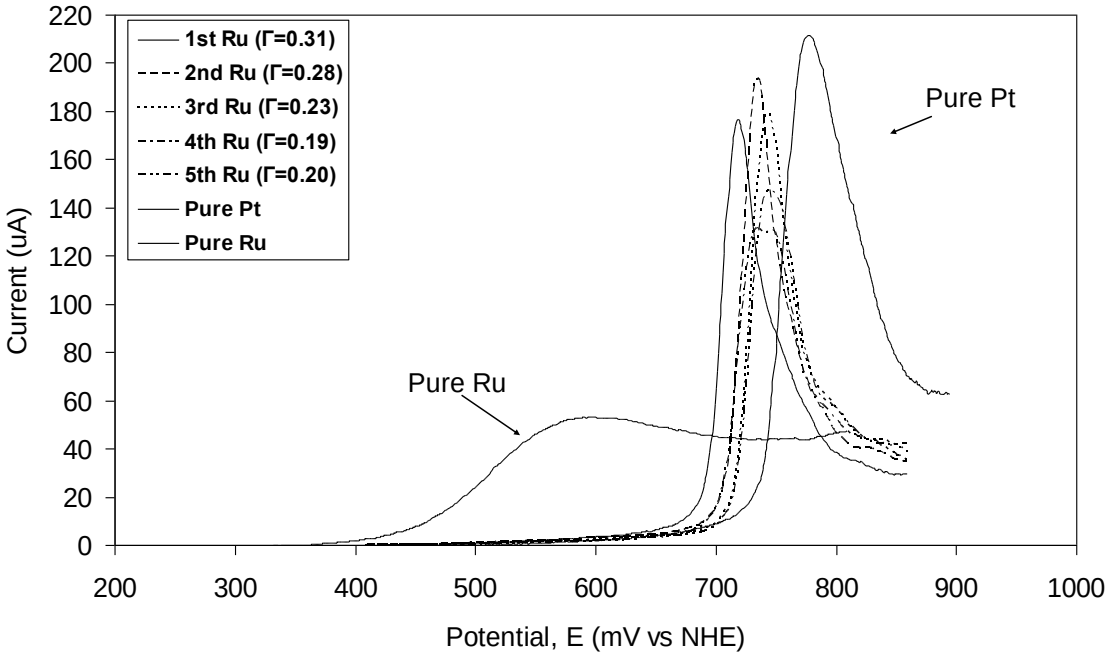

Figure 4.11. CO oxidation curves obtained after each cycle Ru deposition on the same Pt electrode (0.5M H_2SO_4, 10mVs^{-1}).

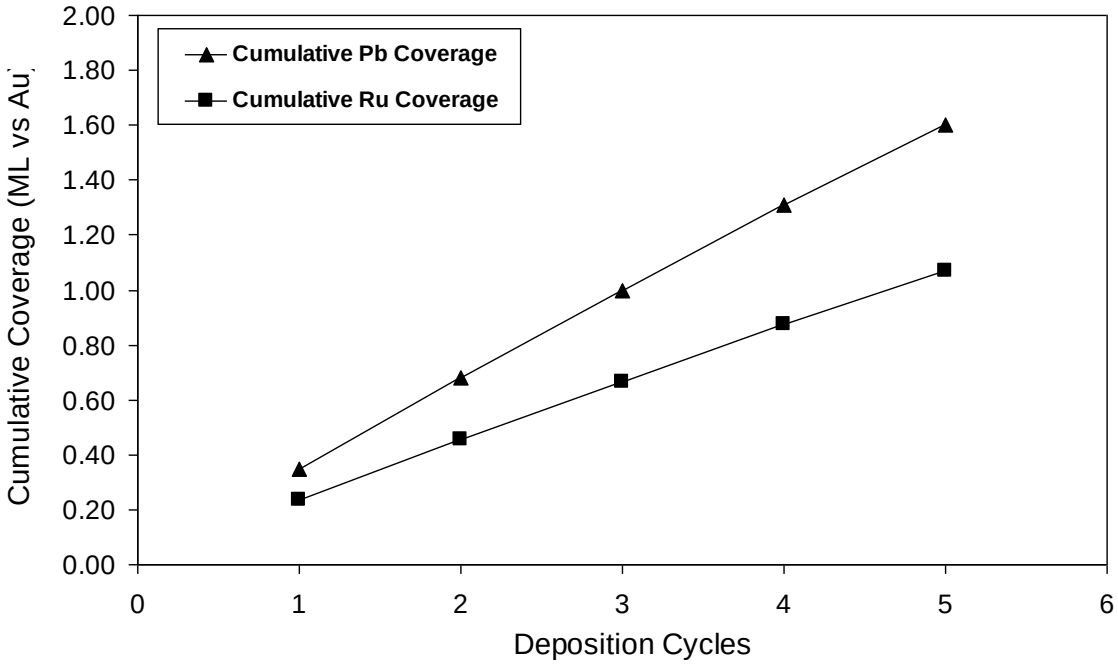

Figure 4.12. Cumulative Pb coverage (▲) and maximum Ru coverage (■) as a function of deposition cycles.

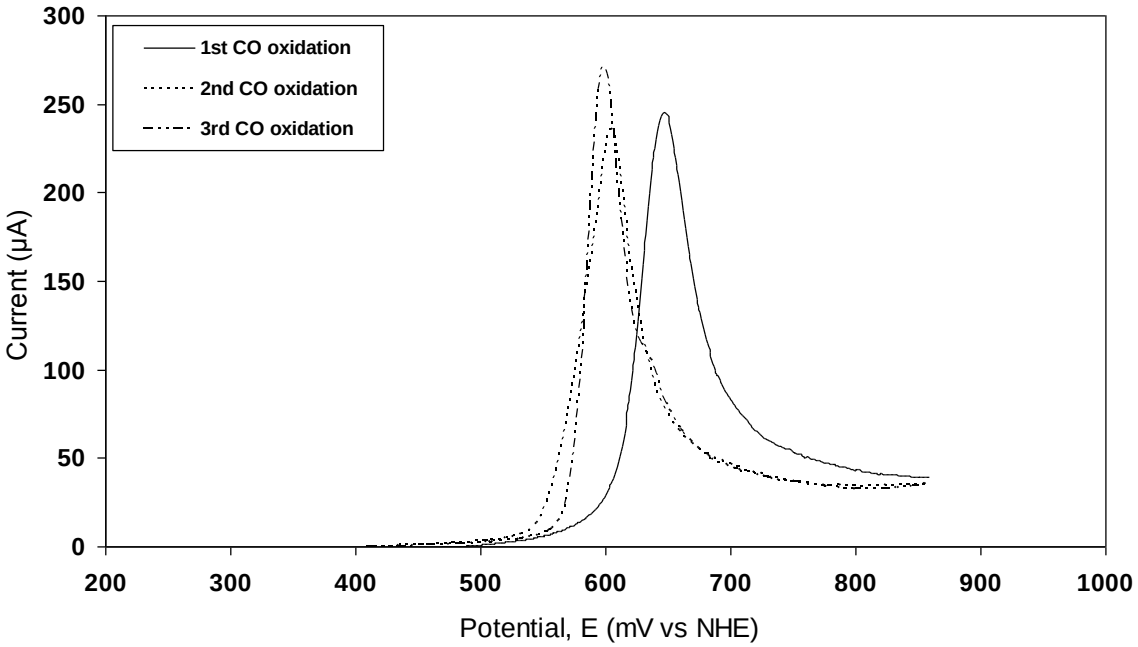

Figure 4.13. Three continuous CO stripping curves on the Pt electrode modified with 1.07 ML Ru (0.5M H_2SO_4, 10mVs^{-1}).

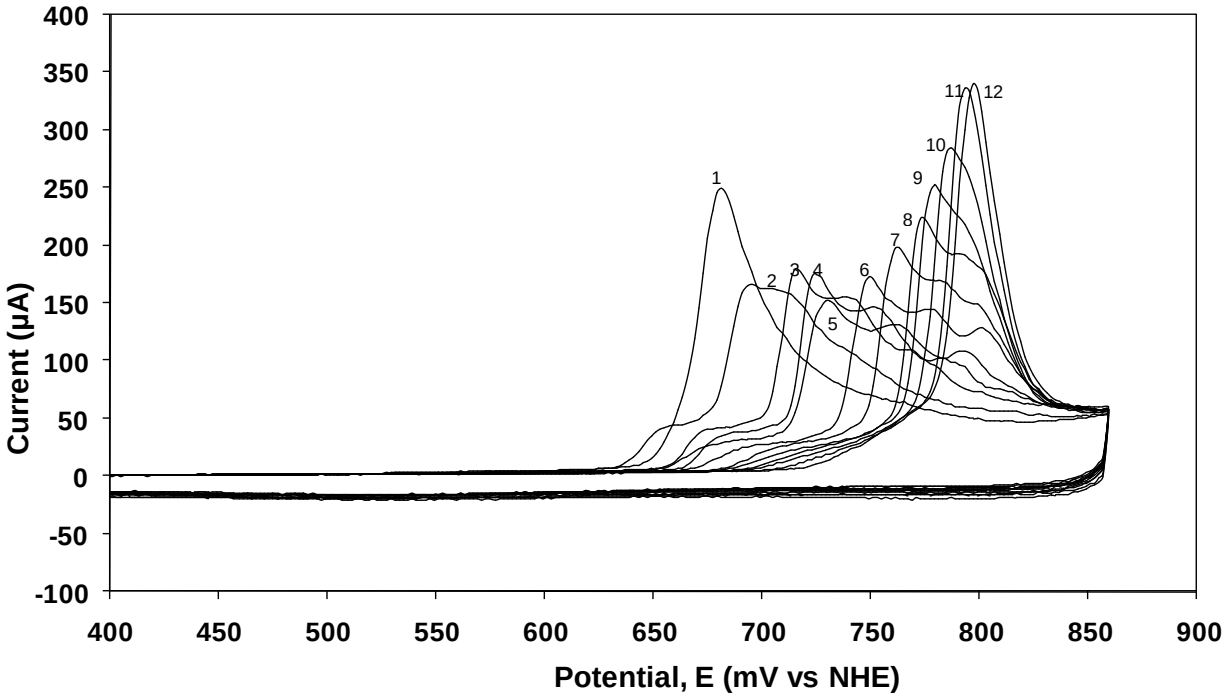

Figure 4.14. Twelve continuous CO stripping curves on the Pt electrode modified with 0.35 ML Ru (0.5M H_2SO_4, 10mVs^{-1}).

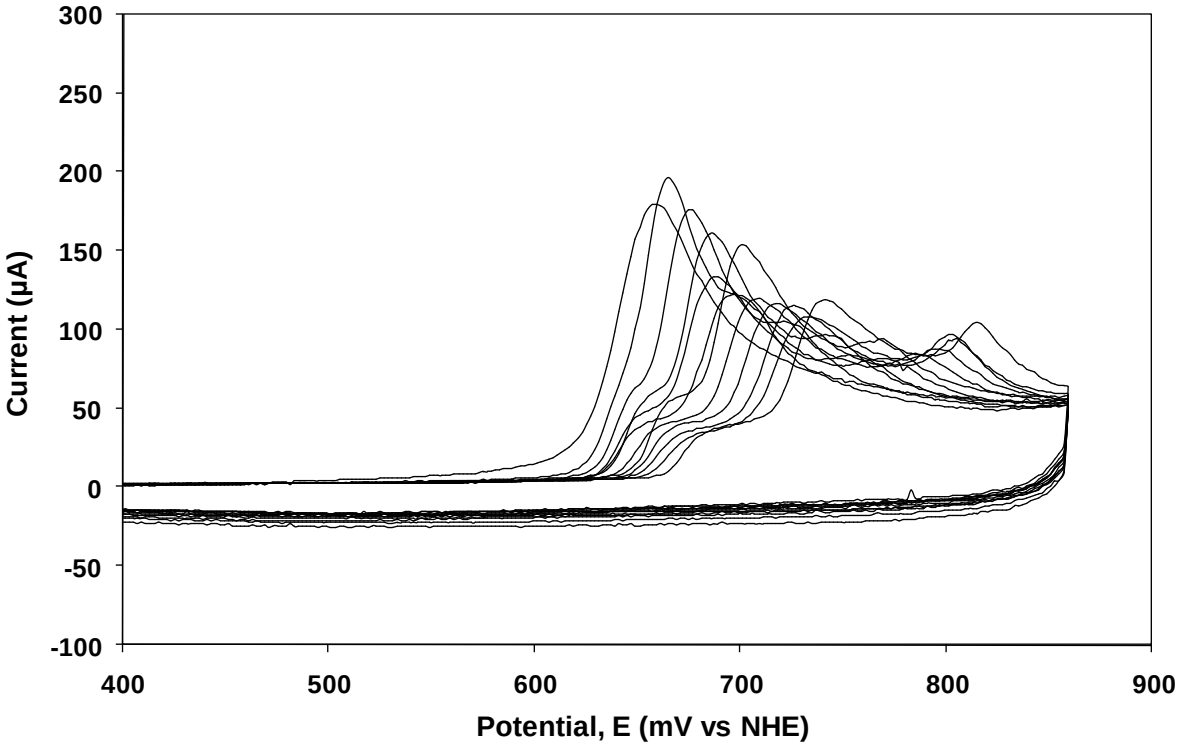

Figure 4.15. Twelve continuous CO stripping curves on the Pt electrode modified with 0.75 ML Ru (0.5M H_2SO_4, 10mVs^{-1}).

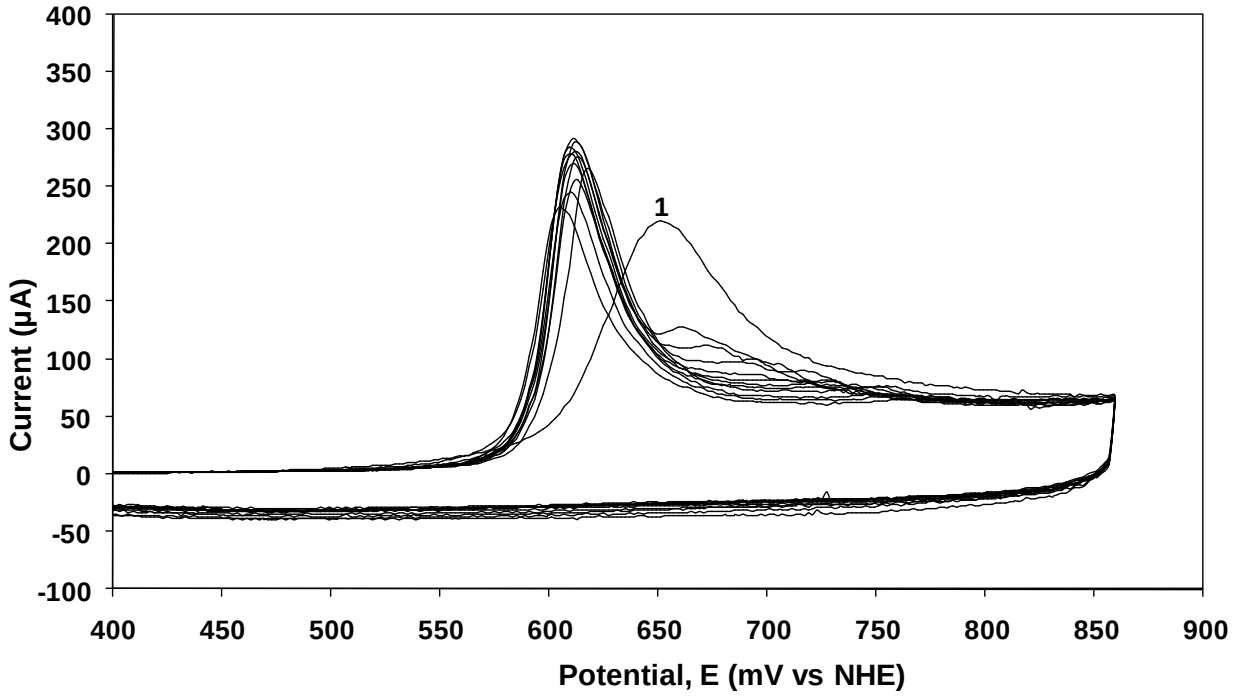

Figure 4.16. Twelve continuous CO stripping curves on the Pt electrode modified with 1.34 ML Ru (0.5M H_2SO_4, 10mVs^{-1}).

CHAPTER 5

CO OXIDATION STUDIES ON PT NANOFILM PREPARED BY ELECTROCHEMICAL ATOMIC LAYER DEPOSITION (E-ALD)

[5]Jayaraju, N., et al. To be submitted to Journal of Electrochemical Society.

Abstract

Pt is an active material in fuel cells and catalysis. This paper describes various studies performed to clean the platinum nanofilm formed via electrochemical atomic layer deposition (E-ALD). Atomic layer deposition (ALD) is the formation of materials an atomic layer at a time using surface limited reactions. E-ALD is the application of electrochemical surface limited reactions, such as under potential deposition (UPD) and surface limited redox replacement (SLRR) reactions, to the formation of nanofilms of materials using an ALD cycle. UPD is deposition of an atomic layer of one element on a second, at a potential prior to (under) that needed to deposit on itself. SLRR is where a sacrificial atomic layer of one element, formed by UPD, is spontaneously replaced with an atomic layer of a more noble element. E-ALD is the repeated application of such a process, cycle, to form a nanofilm of the desired material. Pb was used as the sacrificial metal while Pt(II) was used as the precursor ions. The Pt nanofilm formed doesn't show the prominent hydrogen adsorption and desorption peaks as a result of contaminants on the surface. Scanning in the hydrogen evolution region, Modified E-ALD cycle, and CO adsorption and oxidation studies were performed to clean the surface off the contaminants. Pt films were characterized using cyclic voltammetry (CV), electron probe micro analysis (EPMA) and CO electrooxidation.

Keywords: PtRu, E-ALD, UPD, SLRR, Fuel cell, Carbon monoxide, EPMA.

Introduction

Pt nanofilm finds enormous applications in the field of fuel cells and catalysis. Thin films of metals can be grown by a variety of techniques such as molecular beam epitaxy (MBE) [1-3], chemical vapor deposition (CVD) [4-5], physical vapor deposition (PVD) [6], metallorganic chemical vapor deposition (MOCVD) [7-9] and electrodeposition[10-14]. Pt nanofilm by electrodeposition usually results in 3-D growth and surface roughening [15] [16]. The development of better ways to deposit Pt and its alloys with 2D control will benefit the formation of catalytic materials with known structure and morphology.

Pt being an important electrocatalyst, the electrochemical formation of Pt nano particles and films, has been studied by researchers around the world. CO is one of the widely studied molecules by electrochemists. The adsorption and electrooxidation behavior on Pt single crystals and Pt nanoparticles gives information about the surface structure of the electrodes. Also CO is one of the intermediates formed during the oxidation of fuel in a fuel cell. CO adsorbs strongly on to the reaction active sites of the electrodes resulting in slower kinetics. These molecules have to be removed to open up all the active sites for fuel oxidation (methanol, formic acid...etc). The electrooxidation studies on the Pt electrodes will give an insight on the reaction mechanism and are used as model catalysts. Various Pt based alloy electrodes and Pt modified by Metal M (M = Ru, Sn....) electrodes are studied as the anode catalyst.

CO electrooxidation on the nanoparticles usually results in a split peak behavior [17] [18]. The peak splitting is attributed to the size of the nanoparticles [19] [20], predominant oxidation on terraces and edges.

Pt deposition tends to form clusters [21] and usually results in “platinum black”, a very high surface area form of metallic Pt. Detailed studies have been performed of the

electrodeposition of Pt on Au, and the formation of Pt nanoparticles [22-24]. Electrodeposition of Pt nanoparticles on highly oriented pyrolytic graphite was achieved by Lu et al. [11].

One method for promoting layer by layer growth is atomic layer deposition (ALD) {George, 2010 #17619}. ALD describes a family of deposition methodologies where materials are formed an atomic layer at a time, using surface limited reactions. The electrochemical analog of ALD, E-ALD, was invented in this group [25-26], thought it was initially referred to as electrochemical atomic layer epitaxy (EC-ALE) for historical reasons{Suntola, 1977 #17749}. Most electrochemical surface limited reactions are referred to as underpotential deposition (UPD) [27-30]. UPD is the formation of an atomic layer of one element on a second at a potential prior to (under) that needed to deposit the element on itself. An atomic layer refers to a deposit which is only one atom thick, without specific reference to the coverage. Coverage is frequently described in terms of monolayers (ML), where a ML, in this report, corresponds to one adsorbate atom for every substrate surface atom. UPD is a thermodynamic phenomenon where one element deposits on a second, driven by the free energy of formation of a surface compound or alloy. Initial E-ALD studies focused on the formation of compounds, where one element was deposited on a second at an underpotential, and then vice-versa.

E-ALD of metal (or elemental) nanofilms was felt by the PI to not be possible, until the development of monolayer restricted galvanic displacement (MRGD) by Brankovic, Wang and Adzic [31-32] and Weaver [33]. MRGD has also been referred to as surface limited redox replacement (SLRR). It involves the electrodeposition of an atomic layer of a sacrificial element by UPD. That layer is then replaced by exposure to a solution containing precursor ions of a more noble element, at open circuit potential (OCP). The replacement reaction is limited by the amount of the sacrificial element, generally less then a monolayer. Deposition of single

monolayers of Pt and Pd were some of the first examples of SLRR [31-32], where atomic level control was revealed by scanning tunneling microscopy (STM) of the resulting Pt atomic layers.

Deposition of more noble metal by surface limited redox replacement reaction had been extended by others for the formation of thin film and modification of electrodes with a foreign adatom[33-37]. The author's group has studied the use of SLRR as cycles for E-ALD formation of Cu [38],[Thambidurai, 2010 #429] Pt [39-41]and Ru [42] nanofilm on Au substrates, as well as PtRu structured alloys (in preparation).

The driving force for SLRR is the potential difference between the sacrificial and the depositing metal, which will vary as the reaction progresses, dropping the sacrificial element's coverage and increasing the depositing element's. Changes in the solution composition will be a factor as well. Noble metal atomic layers have been deposited using Cu[31] [43] [37] [44] [45], Ni, and Pb [34] [38, 42] as sacrificial atomic layers.

The present study investigates E-ALD using SLRR cycles to form Pt nanofilms on Au on glass substrates. Pb was used as the sacrificial metal and Pt^{+2} precursors was used for the exchange process. An automated electrochemical flow deposition system (Electrochemical ALD L.C.) was used to form the deposits. Pt electrodes were subjected to CO adsorption and electrooxidation by cyclic voltammetry in 0.5M sulfuric acid without taking the deposits from the cell.

Experimental

Solutions used included 1mM $PbClO_4$, 0.1mM K_2PtCl_4, 0.1mM H_2PtCl_6, 0.5M H_2SO_4 and 0.5M $NaClO_4$. The Pb solutions were made with 0.5 M $NaClO_4$ (pH 4.5). The Pt solutions were made with 50 mM $HClO_4$ (pH 1.3). The 0.5M H_2SO_4 and 0.5M $NaClO_4$ were used as blank solutions. All solutions were prepared using water from a nanopure water filtration system

(Barnstead, Dubuque, IA) (18Ω), attached to the house DI water system. Chemicals were obtained from sigma-Aldrich or Alfa Aesar. Solution bottles were contained inside a Plexiglas box and were deaerated by bubbling with dry nitrogen, prior to deposition.

Pt nanofilm deposits were formed using an automated electrochemical flow cell system (Electrochemical ALD L.C.), similar to those previously described [46-47]. The system is controlled using a Labview program (National Instruments). The components of the system consist of: Peristaltic pumps, Teflon solenoid valves, an electrochemical flow cell and a potentiostat. A gold wire, embedded in the Plexiglas flow cell face, was used as the auxiliary electrode. An Ag/AgCl (3M NaCl) (Bioanalytical Systems, Inc., West Lafayette, IN) was used as the reference electrode and all potentials, E are quoted with reference to reversible hydrogen electrode (RHE). The flow cell ($4X1X0.1cm^3$) consisted of a planar substrate held away from a counter electrode by a 1mm thick silicone rubber gasket. The deposition area was 3.77 cm^2, and a solution flow rate of 9 ml/min was used.

The Pt nanofilms were generally formed using 25 E-ALD cycles, on Au on glass substrates. The glass slides, after etching in dilute HF, were initially coated with a 5 nm adhesion layer of titanium, and then 300 nm of Au. The substrates were held at 280°C during deposition, and then annealed at 400°C for 12 hours, producing a prominent (111) growth mode. The gold substrates were cleaned in nitric acid for 2 minutes and then repeatedly cycled between 1600 mV and 10 mV in 0.5M sulfuric acid prior to deposition, at 10 mV/s. The Au substrates were characterized using cyclic voltammetry in 0.5 M H_2SO_4.

The Pt nanofilm electrodes were characterized by cyclic voltammetry in 0.5M H_2SO_4. CO adsorption and electrooxidation studies were performed in-situ on the as deposited film without taking them out of the cell. The electrolytes are pumped in to the flow cell at a flow rate

of 4mL/min from two different bottles, one containing 0.5M H_2SO_4 and the other containing CO saturated H_2SO_4. CO was adsorbed on to the electrode by flushing in CO saturated H_2SO_4 at 0.300V for 3 minutes and then rinsed out with 0.5M H_2SO_4 for 3 minutes, while the electrode was held at 0.300V. Cyclic voltammograms were recorded at a scan rate of $10mVs^{-1}$.

The deposits were initially inspected using a Jenavert metallo-graphic optical microscope, at 1000X. Electron probe microanalysis (EPMA) was run using a Joel 8600 wavelength dispersive scanning electron microprobe, for elemental analysis.

Results and Discussion

Pt nanofilm deposits were formed using Pb UPD as the sacrificial metal, and a cartoon depicting that E-ALD SLRR cycle is shown in Figure 1. Pb was deposited at its underpotential on Au resulting in an atomic layer. The Pb UPD was then exchanged for $PtCl_4^{2-}$ ions at OCP. Pb UPD potential was determined form cyclic voltammetry.

A window opening consisting of two CVs for a Au substrate in the Pb^{2+} solution, each to an increasingly negative potential, is shown in Figure 2. The scans all started at 500 mV and displayed a slowly increasing change to lower potentials, with a peak at 10 mV, consistent with Pb UPD on a Au(1 1 1) electrode [48]. Bulk Pb deposition began near −220 mV, and stripped in a sharp oxidation peak at -190 mV, in the subsequent positive going scan. There was also a broad oxidation peak around −100 mV, corresponding to dealloying of Pb from the Au substrate [48]. Pb UPD stripping consisted of a small peak at 60 mV, with a couple of smaller features on top. Based on the CVs in Figure 4, -190mV was selected for the formation of the sacrificial Pb atomic layers.

In the present study nanofilms formed using Pb sacrificial metal will be discussed. The cycle consisted of pumping in Pb^{2+}, for 10s at -190mV, to form Pb UPD. $PtCl_4^{2-}$ ions were

pumped in at open circuit potential for the redox replacement of Pb for Pt. A control program was set up to monitor the OCP during replacement and once it reached 0 mV a "stop potential step" was performed. The step involved flushing the cell for with blank for 11 s. For the first 6 s the cell remained at OCP, so that any Pt precursor ions would be flushed from the cell, and Pt ions would electrodeposit. For the next 5 seconds of blank rinsing, a controlled potential of 100 mV was used. It was believed that any last traces of Pb will strip from the surface at 100 mV.

Pb UPD at -190 mV resulted in a coverage of 0.54 ML, both on Au and Pt. It was shown that potentials above 0 mV generally result in completely oxidation of the Pb layer which led to the use of "Stop Potential". Detailed studies using Cu and Pb as the sacrificial metal for the formation on Pt nanofilms by E-ALD and the significance of using stop potential were discussed elsewhere. EPMA showed 3 atomic % Pt in the 25 cycle deposit with no evidence for Pb.

The resulting Pt nanofilms were then characterized using CVs in 0.5 M sulfuric acid at a scan rate of 10 mV/s. This will give us information about the cleanliness of the electrode and also the active surface area can be determined. Figure 4 is the first CV after deposition, and shows little of the expected hydrogen waves expected, suggesting contamination. The deposit was cleaned; by cycling between 1400 mV and -160 mV to reach a steady state as shown in Figure 5. The coverages were based on the assumption that the surface resembled a Pt(111), and one electron for hydrogen adsorption for each surface atom, and two for oxide reduction. The voltammetric profile of Pt consisting of hydrogen adsorption and desorption waves is considered as the fingerprint of a clean Pt electrode.

Pt is notoriously difficult to keep clean {Hubbard, 1978 #659}, as it strongly adsorbs organic molecules containing nearly any functional group [49]. The best Pt CVs are run under extremely stringent conditions, in ultra clean Pyrex cells {Clavilier, 1980 #15019; Clavilier,

1992 #14970; 2004 #14948; Zolfaghari, 1997 #4873}. In the present studies, the electrochemical flow cell was constructed using Plexi Glass, and solution was flowing over the surface of the deposit most of the time, so some contamination was expected. To decrease contamination, the cells could be made out of Pyrex glass and everything could be kept scrupulously clean. It is understood by practitioners of Pt single crystal electrochemistry that experimental times must be minimized to keep the Pt clean.

Initial attempts at cleaning the electrodes were made by scanning multiple times in the hydrogen evolution region (0.5 M sulfuric acid; 10mV/s). The potential window is kept below 400mV without going positive in to the platinum oxidation region. After 20 cycles scanning, Figure 5 shows the CV of the Pt nanofilm exhibiting a prominent hydrogen adsorption and desorption wave.

It gets really harder to clean the Pt nanofilm after 25 cycle deposition as the contamination builds up in each cycle. In order to clean the Pt during each cycle, the E-ALD cycle was modified. During each cycle, after Pt deposition, the potential was switched to 1200mV for 10s and then back to 400mV for 10s. The positive potential will oxidize the Pt surface and form an oxide layer. This will also help to remove any contaminants off the surface. The potential of 400mV will reduce the platinum oxide to platinum. Figure 6 shows the CV of Pt nanofilm exhibiting a prominent hydrogen adsorption and desorption wave

Alternatively, the Pt surface could be protected with a surfactant that can prevent contamination of the Pt surface while allowing the chemistry to continue. Initial attempts at using surfactants such as I atoms and CO look promising [43, 50]. The first studies of the SLRR of Pt by this group, involved the use of an atomic layer of I atoms to protect the surface [43].

After 25 cycle Pt deposition, CO adsorption and electrooxidation were performed on the as deposited Pt nanofilms to study the nature of the deposit. CO adsorption was carried out as it helps to desorb any contaminants off the surface. The first and second CO oxidation curves are shown in Figure 8A and Figure 8B. Previous studies revealed that CO stripping voltammogram is sensitive to the surface structure. The first CO oxidation shows a broad stripping feature with a peak potential of 780mV. The second CO oxidation exhibits a sharp peak with a peak potential of 800mV. The sharp oxidation peak during the second CV is a result of surface cleaning (desorption of the contaminants). The active sites on Pt can be calculated by integrating the charges under the CO stripping curve ($2e^-$ process for CO to CO_2)

After the second CO oxidation, the voltammogram in the hydrogen adsorption and desorption region results in the appearance of the hydrogen waves. can be seen after the second CO oxidation

Conclusions

Initial studies of the deposition of Pt films by electrochemical ALD were reported. EPMA results confirmed the formation of Pt films using ALD. There was no evidence for the presence of Pb in the deposits. The deposit appears to have contaminants on the surface. Electrochemical potential cycling between +1400 mV and -160 mV was done to clean the Pt film for reproducible hydrogen adsorption and desorption peaks to appear. Extensive cycling in the hydrogen evolution region, CO adsorption and electrooxidation results in the surface cleaning of the Pt electrodes with the appearance hydrogen adsorption and desorption peaks.

Acknowledgments:

Support from the National Science foundation, Division of Materials Research, and the Department of Energy, …… is gratefully acknowledged.

References

1. Nishikawa, K., M. Yamamoto, and T. Kingetsu, *Dependence of electrical resistivity on surface topography of MBE-grown Pt film.* Applied Surface Science, 1997. **113-114**: p. 412-416.
2. Kato, T., et al., *Magnetic anisotropy of MBE grown MnPt3 and CrPt3 ordered alloy films.* Journal of Magnetism and Magnetic Materials, 2004. **272-276**(Part 2): p. 778-779.
3. Makarov, D., et al., *Growth of Pt thin films on WSe2.* Surface Science, 2007. **601**(9): p. 2032-2037.
4. Garcia, J.R.V. and T. Goto, *Chemical Vapor Deposition of Iridium, Platinum, Rhodium and Palladium.* MATERIALS TRANSACTIONS, 2003. **44**(9): p. 1717-1728.
5. Huang, S.-F., et al., *Preparation of Pt-Ru Alloyed Thin Films Using a Single-Source CVD Precursor.* Chemical Vapor Deposition, 2003. **9**(3): p. 157-161.
6. Mattox, D.M., *Physical Sputtering and Sputter Deposition (Sputtering)*, in *Handbook of Physical Vapor Deposition (PVD) Processing (Second Edition)*. 2010, William Andrew Publishing: Boston. p. 237-286.
7. Kwon, J.-H. and S.-G. Yoon, *Preparation of Pt thin films deposited by metalorganic chemical vapor deposition for ferroelectric thin films.* Thin Solid Films, 1997. **303**(1-2): p. 136-142.
8. Valet, O., et al., *Study of platinum thin films deposited by MOCVD as electrodes for oxide applications.* Microelectronic Engineering, 2002. **64**(1-4): p. 457-463.
9. Goswami, J., et al., *MOCVD of Platinum Films from (CH3)3CH3CpPt and Pt(acac)2: Nanostructure, Conformality, and Electrical Resistivity.* Chemical Vapor Deposition, 2003. **9**(4): p. 213-220.

10. Duarte, M.M.E., et al., *Platinum particles electrodeposition on carbon substrates.* Electrochemistry Communications, 2006. **8**(1): p. 159-164.

11. Lu, G. and G. Zangari, *Electrodeposition of Platinum on Highly Oriented Pyrolytic Graphite. Part I: Electrochemical Characterization.* The Journal of Physical Chemistry B, 2005. **109**(16): p. 7998-8007.

12. Lu, G. and G. Zangari, *Electrodeposition of platinum nanoparticles on highly oriented pyrolitic graphite: Part II: Morphological characterization by atomic force microscopy.* Electrochimica Acta, 2006. **51**(12): p. 2531-2538.

13. Choi, K.H., H.S. Kim, and T.H. Lee, *Electrode fabrication for proton exchange membrane fuel cells by pulse electrodeposition.* Journal of Power Sources, 1998. **75**(2): p. 230-235.

14. Itaya, K., H. Takahashi, and I. Uchida, *Electrodeposition of Pt ultramicroparticles in Nafion films on glassy carbon electrodes.* Journal of Electroanalytical Chemistry, 1986. **208**(2): p. 373-382.

15. Saitou, M., *Electrochemical characterization of platinum black electrodeposited from electrolyte including lead acetate trihydrate.* Surface and Coatings Technology, 2006. **201**(6): p. 3611-3614.

16. Zhou, L., Y.F. Cheng, and M. Amrein, *Fabrication by electrolytic deposition of platinum black electrocatalyst for oxidation of ammonia in alkaline solution.* Journal of Power Sources, 2008. **177**(1): p. 50-55.

17. Arenz, M., et al., *The effect of the particle size on the kinetics of CO electrooxidation on high surface area Pt catalysts.* Journal of the American Chemical Society, 2005. **127**(18): p. 6819-6829.

18. Mayrhofer, K.J.J., et al., *CO surface electrochemistry on Pt-nanoparticles: A selective review.* Electrochimica Acta, 2005. **50**(25-26): p. 5144-5154.

19. Maillard, F., et al., *Infrared spectroscopic study of CO adsorption and electro-oxidation on carbon-supported Pt nanoparticles: Interparticle versus intraparticle heterogeneity.* Journal of Physical Chemistry B, 2004. **108**(46): p. 17893-17904.

20. Kinge, S., et al., *Dependence of CO oxidation on Pt nanoparticle shape: a shape-selective approach to the synthesis of PEMFC catalysts.* Applied Organometallic Chemistry, 2008. **22**(1): p. 49-54.

21. Bauer, E. and J.H. van der Merwe, *Structure and growth of crystalline superlattices: From monolayer to superlattice.* Physical Review B, 1986. **33**(Copyright (C) 2009 The American Physical Society): p. 3657.

22. Uosaki, K., et al., *Electrochemical Epitaxial Growth of a Pt(111) Phase on an Au(111) Electrode.* The Journal of Physical Chemistry B, 1997. **101**(38): p. 7566-7572.

23. Waibel, H.F., et al., *Initial stages of Pt deposition on Au(111) and Au(100).* Electrochimica Acta, 2002. **47**(9): p. 1461-1467.

24. Nagahara, Y., et al., *In Situ Scanning Tunneling Microscopy Examination of Molecular Adlayers of Haloplatinate Complexes and Electrochemically Produced Platinum Nanoparticles on Au(111).* The Journal of Physical Chemistry B, 2004. **108**(10): p. 3224-3230.

25. Gregory, B.W. and J.L. Stickney, *Electrochemical atomic layer epitaxy (ECALE).* Journal of Electroanalytical Chemistry, 1991. **300**(1-2): p. 543-561.

26. Gregory, B.W., D.W. Suggs, and J.L. Stickney, *Conditions for the deposition of cadmium telluride (CdTe) by electrochemical atomic layer epitaxy.* Journal of the Electrochemical Society, 1991. **138**(5): p. 1279-84.

27. Kolb, D.M., *Physical and Electrochemcial Properties of Metal Monolayers on Metallic Substrates*, in *Advances in Electrochemistry and Electrochemical Engineering*, H. Gerischer and C.W. Tobias, Editors. 1978, John Wiley: New York. p. 125.

28. Adzic, R.R., *Electrocatalytic Properties of the Surfaces Modified by Foreign Metal Ad Atoms*, in *Advances in Electrochemistry and Electrochemical Engineering*, H. Gerishcher and C.W. Tobias, Editors. 1984, Wiley-Interscience: New York. p. 159.

29. Gewirth, A.A. and B.K. Niece, *Electrochemical applications of in situ scanning probe microscopy.* Chemical Reviews, 1997. **97**(4): p. 1129-1162.

30. Herrero, E., L.J. Buller, and H.D. Abruna, *Underpotential Deposition at Single Crystal Surfaces of Au, Pt, Ag and Other Materials.* Chemical Reviews, 2001. **101**(7): p. 1897-1930.

31. Brankovic, S.R., J.X. Wang, and R.R. Adzic, *Metal monolayer deposition by replacement of metal adlayers on electrode surfaces.* Surface Science, 2001. **474**(1-3): p. L173-L179.

32. Brankovic, S.R., J.X. Wang, and R.R. Adzic, *New methods of controlled monolayer-to-multilayer deposition of Pt for designing electrocatalysts at an atomic level.* Journal of the Serbian Chemical Society, 2001. **66**(11-12): p. 887-898.

33. Mrozek, M.F., Y. Xie, and M.J. Weaver, *Surface-Enhanced Raman Scattering on Uniform Platinum-Group Overlayers: Preparation by Redox Replacement of Underpotential-Deposited Metals on Gold.* Analytical Chemistry, 2001. **73**(24): p. 5953-5960.

34. Viyannalage, L.T., R. Vasilic, and N. Dimitrov, *Epitaxial growth of Cu on Au(111) and Ag(111) by surface limited redox replacement - An electrochemical and STM study.* Journal of Physical Chemistry C, 2007. **111**(10): p. 4036-4041.

35. Vasilic, R., L.T. Viyannalage, and N. Dimitrov, *Epitaxial growth of Ag on Au(111) by galvanic displacement of Pb and Tl monolayers.* Journal of the Electrochemical Society, 2006. **153**(9): p. C648-C655.

36. Rettew, R.E., J.W. Guthrie, and F.M. Alamgir, *Layer-by-Layer Pt Growth on Polycrystalline Au: Surface-Limited Redox Replacement of Overpotentially Deposited Ni Monolayers.* Journal of the Electrochemical Society, 2009. **156**(11): p. D513-D516.

37. Adzic, R.R., et al., *Platinum Monolayer Fuel Cell Electrocatalysts.* Topics in Catalysis, 2007. **46**(3/4): p. 249-262.

38. Thambidurai, C., et al., *Copper Nanofilm Formation by Electrochemical ALD.* Journal of the Electrochemical Society, 2009. **156**(8): p. D261-D268.

39. Kim, J.Y., Y.G. Kim, and J.L. Stickney, *Copper nanofilm formation by electrochemical atomic layer deposition - Ultrahigh-vacuum electrochemical and in situ STM studies.* Journal of the Electrochemical Society, 2007. **154**(4): p. D260-D266.

40. Kim, J.Y., Y.G. Kim, and J.L. Stickney, *Cu nanofilm formation by electrochemical atomic layer deposition (ALD) in the presence of chloride ions.* Journal of Electroanalytical Chemistry, 2008. **621**(2): p. 205-213.

41. Jayaraju, N., D. Vairavapandian, and J.L. Stickney, *Electrochemical Atomic Layer Deposition (ALD) of Pt Nanofilms.* In Prep, 2010.

42. Thambidurai, C., Y.-G. Kim, and J.L. Stickney, *Electrodeposition of Ru by atomic layer deposition (ALD).* Electrochimica Acta, 2008. **53**(21): p. 6157-6164.

43. Kim, Y.-G., et al., *Platinum Nanofilm Formation by EC-ALE via Redox Replacement of UPD Copper: Studies Using in-Situ Scanning Tunneling Microscopy.* The Journal of Physical Chemistry B, 2006. **110**(36): p. 17998-18006.

44. Yu, Y.L., et al., *The study of Pt@Au electrocatalyst based on Cu underpotential deposition and Pt redox replacement.* Electrochimica Acta, 2009. **54**(11): p. 3092-3097.

45. Qu, D., C.W.J. Lee, and K. Uosaki, *Pt Nano-Layer Formation by Redox Replacement of Cu Adlayer on Au(111) Surface.* Bulletin of the Korean Chemical Society, 2009. **30**(12): p. 2875-2876.

46. Stickney, J.L., *Electrochemical Atomic Layer Epitaxy (EC-ALE): Nanoscale Control in the Electrodeposition of Compound Semiconductors,* in *Advances in Electrochemical Science and Engineering,* R.C. Alkire and D.M. Kolb, Editors. 2002, Wiley-VCH: Weinheim. p. 1-105.

47. Mathe, M.K., et al., *Formation of HgSe Thin Films Using Electrochemical Atomic Layer Epitaxy.* Journal of the Electrochemical Society, 2005. **152**(11): p. C751-C755.

48. Green, M.P., et al., *Insitu Scanning Tunneling Microscopy Studies of the Underpotential Deposition of Lead on Au(111).* Journal of Physical Chemistry, 1989. **93**(6): p. 2181-2184.

49. Stickney, J.L., et al., *A survey of factors influencing the stability of organic functional groups attached to platinum electrodes.* JEC, 1981. **125**: p. 73.

50. Strbac, S., et al., *In situ STM imaging of spontaneously deposited ruthenium on Au(111).* Surface Science, 2002. **517**(1-3): p. 207-218.

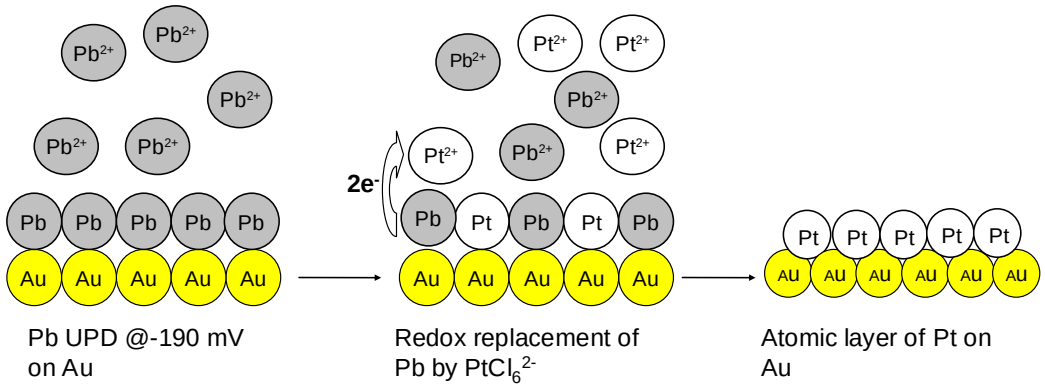

Figure 5.1. Cartoon representation for the formation of Pt nanofilm by E-ALD and SLRR

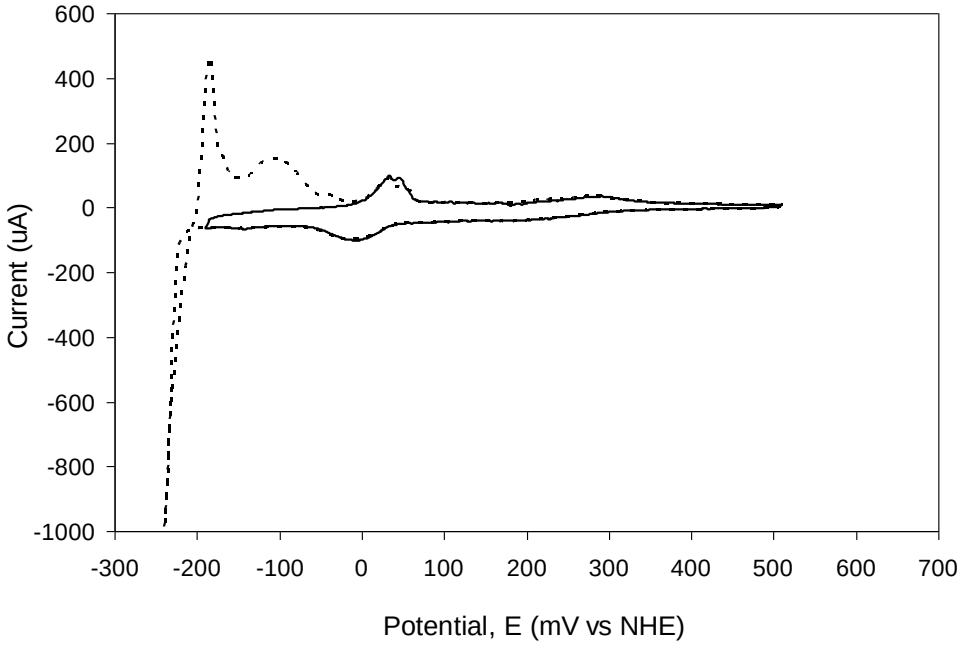

Figure 5.2. Cyclic voltammogram of Au in 1mM $Pb(ClO_4)_2$ in 0.5M $NaClO_4$; pH~ 4.5; Scan rate: $10mVs^{-1}$.

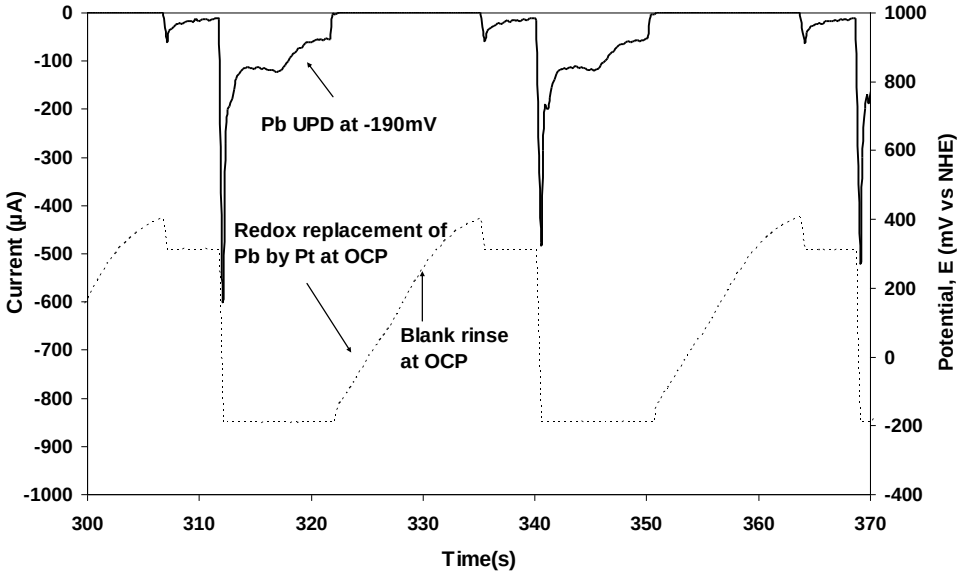

Figure 5.3. Graph of Current – Time – Potential plot for one Pt E-ALD cycle.

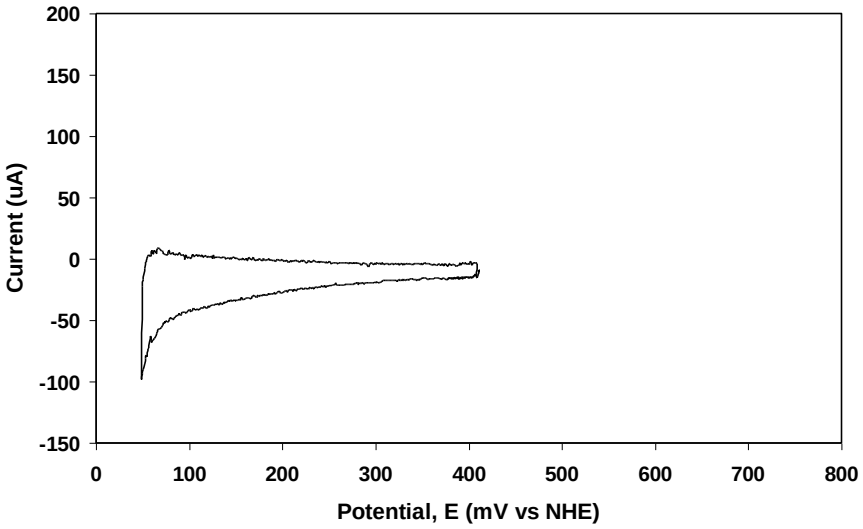

Figure 5.4. Cyclic voltammogram of Pt in 0.5M H_2SO_4 between 400mV and 50mV; Scan rate: $10mVs^{-1}$.

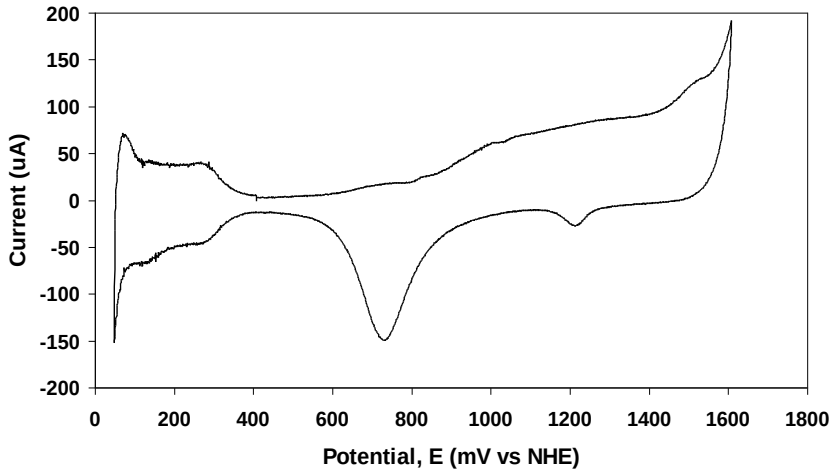

Figure 5.5. Cyclic voltammogram of Pt in 0.5M H_2SO_4 between 1600mV and 50mV; Scan rate: $10mVs^{-1}$.

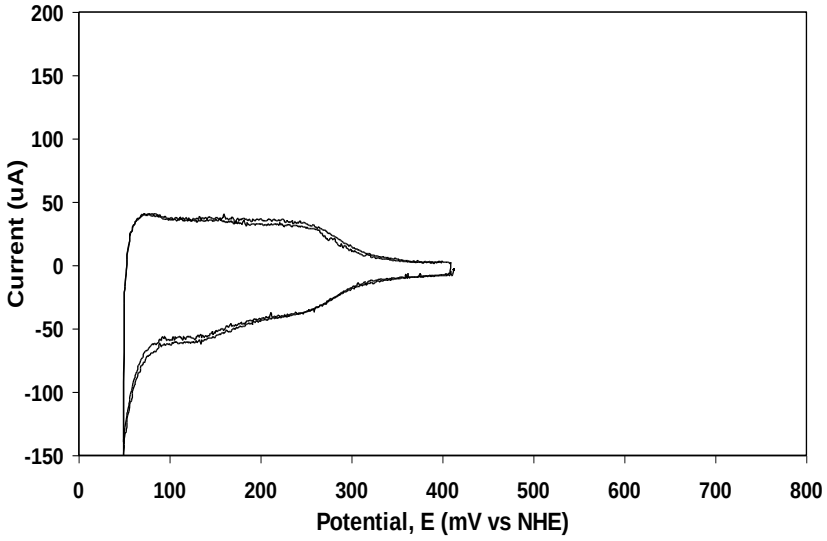

Figure 5.6. Cyclic voltammogram of Pt in 0.5M H_2SO_4 between 410mV and 50mV; Scan rate: $10mVs^{-1}$.

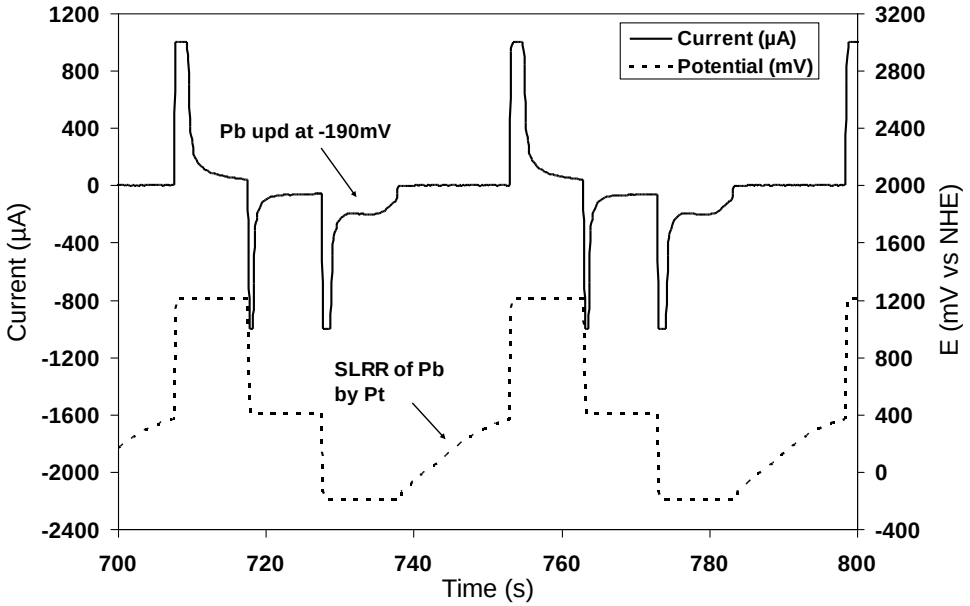

Figure 5.7. Graph of Current – Time – Potential plot for one Pt E-ALD cycle. After Pt deposition the potential was switched between 1200mV and 400mV in blank to clean the surface off the contaminants.

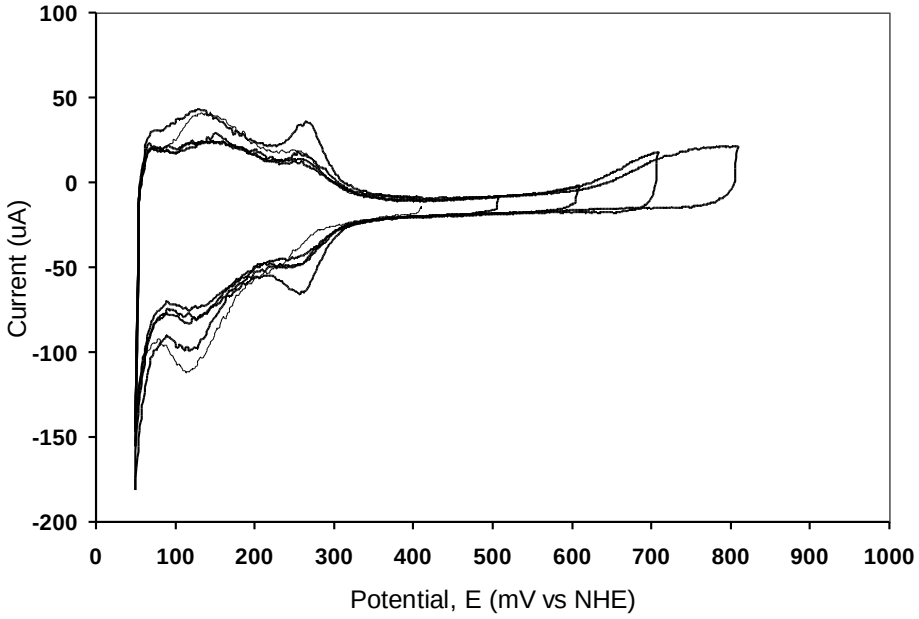

Figure 5.8. Cyclic voltammogram of Pt in 0.5M H_2SO_4; Scan rate: $10mVs^{-1}$.

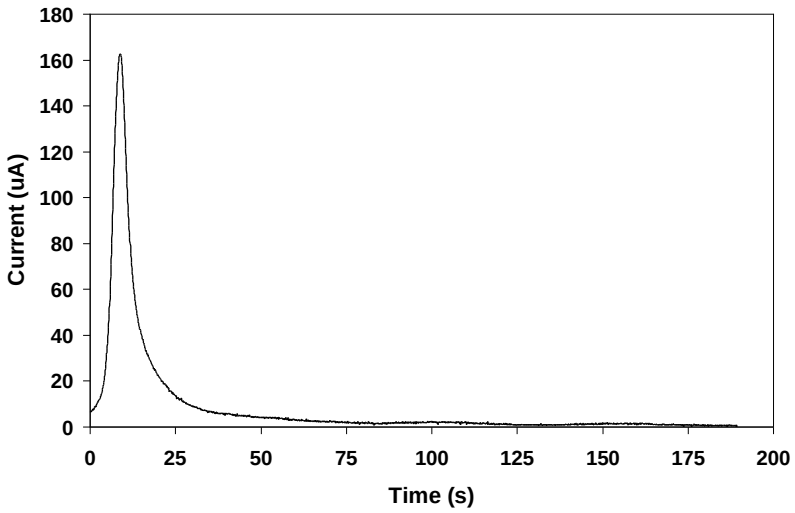

Figure 5.9. Chronoamperometric oxidation of adsorbed CO on the Pt nanofilm at 750mV.

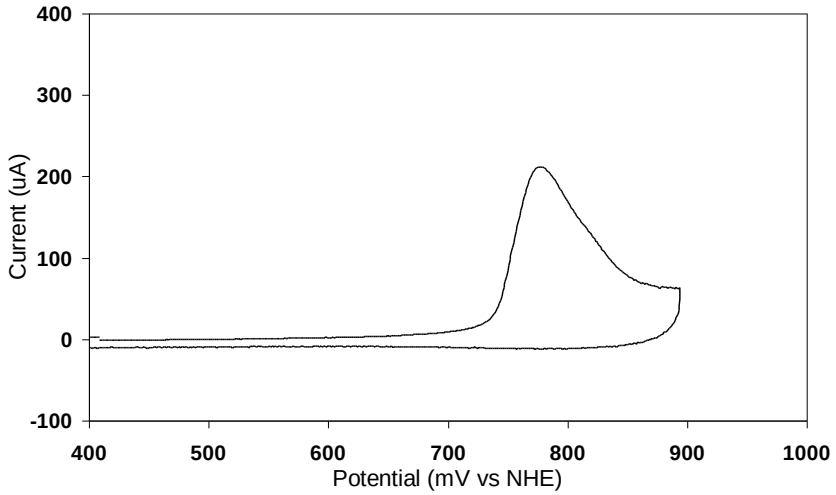

Figure 5.10. CO stripping voltammetry of Pt in 0.5M H_2SO_4; Scan rate: $10mVs^{-1}$.

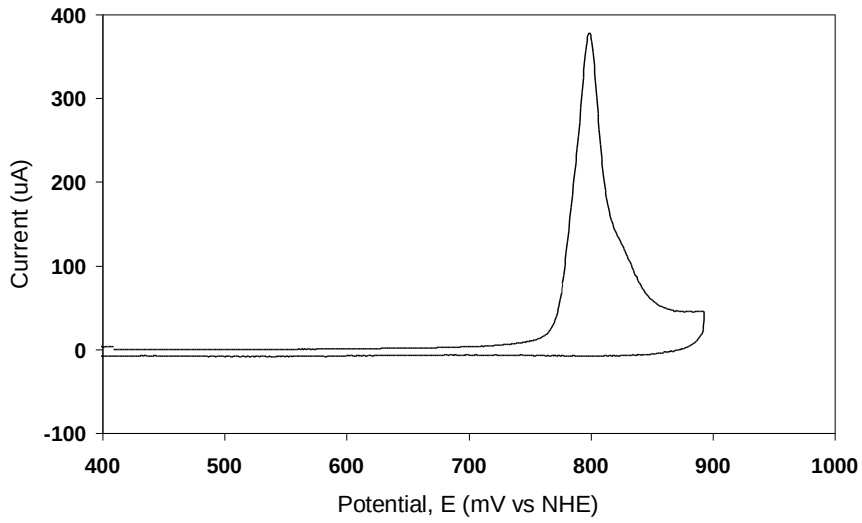

Figure 5.11. CO stripping voltammetry of Pt in 0.5M H_2SO_4; Scan rate: $10mVs^{-1}$.

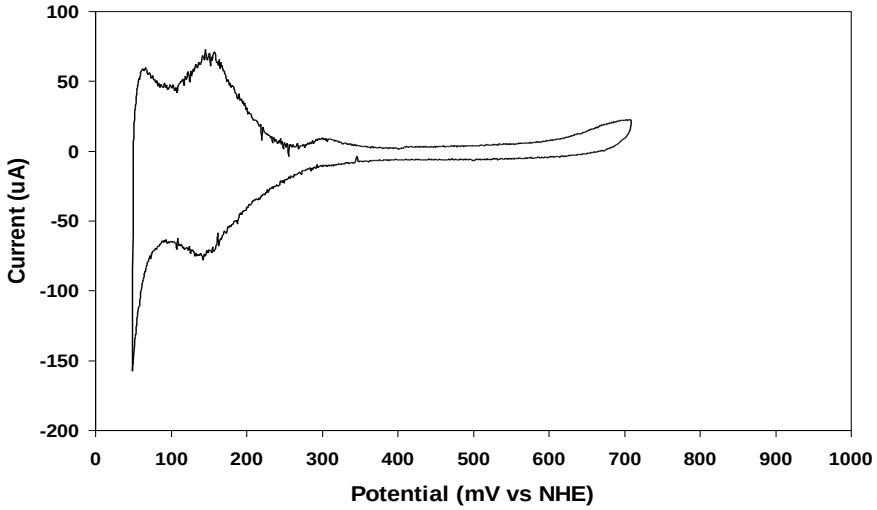

Figure 5.12. Cyclic voltammogram of Pt in 0.5M H_2SO_4; Scan rate: $10mVs^{-1}$.

CHAPTER 6

CONCLUSION AND FUTURE STUDIES

Electrochemical atomic layer deposition of catalytic active thin film of Pt, Ru, PtRu and Ru modified Pt electrodes were discussed in the chapters 2-5. In chapter 2, Pt nanofilm deposition using Cu and Pb sacrificial metals were discussed. Pt(II) and Pt(IV) precursors were also investigated for deposition. Initial Pt deposits, formed using Cu or Pb UPD sacrificial layers, were an order of magnitude thicker than expected, for a 25 cycle E-ALD deposits. Reasons for excess Pt were investigated, and appeared to how positive the OCP drifted during the exchange step. To limit the OCP, a "stop potential" was used, where once the potential exceeds the stop potential; the Pt precursor was flushed from the cell, preventing further deposition. It was, however, found that insufficient rinsing was being used, as at positive potentials, anionic Pt precursors were adsorbed to the deposit, and survived the brief rinse applied. By increasing the rinse times, complete removal of the Pt precursor was achieved, preventing the build up of Pt in excess of that resulting from replacement of the sacrificial atomic layers.

In chapter 3, PtRu nanofilm deposition was carried out using Pt(IV) and Ru(III) ions precursor ions. Pb was used as the sacrificial metal. PtRu alloys of 70/30, 82/18 and 50/50 Pt/Ru were prepared and characterized in 0.5M sulfuric acid. The catalytic activity was studied by CO adsorption and oxidation. The catalytic activities of the alloys were compared to Pt, Ru, Pt modified Ru and Ru modified Pt electrodes. 50/50 Pt/Ru electrode showed the highest activity among the alloys and other electrodes studied.

In chapter 4, Ru modified Pt electrodes were prepared and catalytic activity studied by CO electrooxidation. It was shown that the reactivity is directly proportional to the Ru coverage

on the surface. A negative potential shift of about 160mV was shown compared to pure Pt electrode.

In Chapter 5, various CO adsorption and oxidation studies carried out on the Pt electrodes prepared by E-ALD. CO adsorption helps to desorb any contaminants off the surface of Pt electrode. More prominent hydrogen adsorption and desorption waves are visible after removing the contaminants.

More studies are required to understand the stability of the alloy as well as the Ru modified Pt electrodes. Also real time testing in a fuel cell could really help understand how these electrodes behave over time.